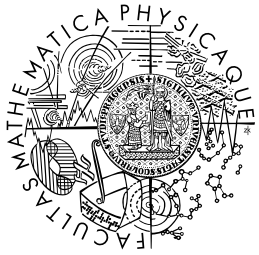

FACULTY
OF MATHEMATICS
AND PHYSICS
Charles University

MASTER THESIS

Bc. Eliška Klimešová

Multi-black-hole gravitational field

Institute of Theoretical Physics

Supervisor of the master thesis: doc. RNDr. Martin Žofka, PhD.
Study programme: Physics
Study branch: Theoretical Physics

Prague 2023

I declare that I carried out this master thesis independently, and only with the cited sources, literature and other professional sources. It has not been used to obtain another or the same degree.

I understand that my work relates to the rights and obligations under the Act No. 121/2000 Sb., the Copyright Act, as amended, in particular the fact that the Charles University has the right to conclude a license agreement on the use of this work as a school work pursuant to Section 60 subsection 1 of the Copyright Act.

In ..... date ....

Author's signature

I am very thankful to my supervisor doc. RNDr. Martin Žofka, PhD. for his active and loyal approach, shared experience and his time dedicated to our discussions. I would also like to express my gratitude to my closest family members, who always supported me during my studies.

Title: Multi-black-hole gravitational field

Author: Bc. Eliška Klimešová

Institute: Institute of Theoretical Physics

Supervisor: doc. RNDr. Martin Žofka, PhD., Institute of Theoretical Physics

Abstract: We study dynamics of an extremally charged black hole on the background of two stationary, mutually orbiting extremally charged black holes, forming thus a seed binary system. We extend the two-body perturbative solution of vacuum Einstein-Maxwell equations, known from literature, to the three body system. Restricting to slow-motion approximation and motion at a large distance, we derive the corresponding three-body Lagrangian and investigate limits of evolution of little- and large-mass black hole. Motivated by physical intuition and in order to check our results, we compare the former with solution of geodesic equation of an extremally charged test-body on identical background. Our results mainly consist of interpretation and comparison of characteristic motions.

Keywords: Majumdar-Papapetrou solution, charged black hole, perturbative solution, black-hole motion, low-velocity approximation, test-body trajectories.

Contents

Introduction

In Newtonian theory a system consisting of **extremally charged** point particles

$$|e_i| = \sqrt{4\pi G\epsilon_0} m_i \tag{1}$$

remains in static equilibrium until acted upon by any external forces. The sign in (1) can be freely flipped, provided consistency for all the source points. Viewed from a Newtonian perspective of the 17^{th} century, extremal black holes either follow straight line geodesics or stand still (which is a special case of the former, of course).

In contrast to Schwarzschild or non-extremal Reissner-Nordström black holes, there exists a static solution describing a superposition of an arbitrary finite number of extremal black holes in general relativity. This solution of the source-free, coupled Einstein-Maxwell equations was first described by S. D. Majumdar [1] and A. Papapetrou [2] independetly in 1947. As pointed out by J. B. Hartle and S. W. Hawking [3] a quarter century later, this **Majumdar-Papapetrou solution** can be extended analytically. Moreover, in a system of static electric charges of the same sign, all of the singularities of the spacetime are contained within event horizons. [3]

In the universe objects are in motion rather than remaining static. However, in dynamic systems there is much more general relativity than just "$1/r^2$" Newtonian law. It is then perhaps an astonishing discovery, that the motion of extremally charged black holes can be solved **analytically to the 2nd order in velocities**, as was first described by D. M. Eardley and R. C. Ferrell [4, 5] in 1987. Even though restricting to the adiabatic evolution (*moduli-space approximation*), this problem is solved in the full strong field regime of gravity coupled to electromagnetism.

The field degrees of freedom (associated with radiation) are not present in our approximating spacetime. We foliate the spacetime with space-like 3-dim slices instead, assuming on any slice the gravitational and electromagnetic fields are determined entirely in terms of positions of black holes and their velocities.

We aim to compare the motion of a test particle in the field of two massive black holes orbiting on a common path as per solution in [4] with the motion of a third, smaller black hole approaching the same orbiting system. Geodesics in static Majumdar-Papapetrou solution were studied in [6] so that we will perform a static limit here to compare our results. The moduli space metric of the maximally charged slowly-moving dilatonic black holes was calculated in [7]. In [8] the gravitational wave signatures of extremal black hole mergers were analytically calculated, extended by non-zero dilatonic field.

Although based on expansion in velocities, not the gravitational field, this works falls into the realm of post-Newtonian (1PN) and higher order corrections to Newtonian gravity.

The outline of the thesis is as follows. We first sum up the static situation, then proceed to the perturbed analytic solution. Though the results were already shown in [4], we recapitulate it owing to its importance in the subsequent sections. Afterwards we solve geodesic equations for both, uncharged and charged test particle. Finally we compare the latter with the motion of the third black hole.

Geometrized units

We shall make use of geometrized units system, unless explicitly stated otherwise. In geometrized units the base physical units are chosen such, that $c = 1 = G$. For SI units of

$$[\mathrm{M}^A\ \mathrm{L}^B\ \mathrm{T}^C]\ ,$$

the conversion factor from SI to geometrized units is

$$[G^A c^{C-2A}].$$

In this most likely not-peer-reviewed paper [9] we found similar results, leading to the same formula. For the reader's convenience, in Table 1 we list chosen important quantities with their dimension in geometrized units.

Quantity	Multiplication factor	SI dimension	Geometric dimension
Mass	$m_{\mathrm{geom}} = \frac{G}{c^2} \cdot m_{\mathrm{SI}}$	M	L
Time	$t_{\mathrm{geom}} = c \cdot t_{\mathrm{SI}}$	T	L
Length	$l_{\mathrm{geom}} = 1 \cdot l_{\mathrm{SI}}$	L	L
Velocity	$v_{\mathrm{geom}} = \frac{1}{c} \cdot v_{\mathrm{SI}}$	$\mathrm{L\ T^{-1}}$	1
Energy	$E_{\mathrm{geom}} = \frac{G}{c^4} \cdot E_{\mathrm{SI}}$	$\mathrm{M\ L^2\ T^{-2}}$	L
Charge	$Q_{\mathrm{geom}} = \frac{1}{c^2}\sqrt{\frac{G}{\epsilon_0}} \cdot Q_{\mathrm{SI}}$	T I	L

Table 1: List of useful conversions between SI and geometrized units system.

The physical quantities identified with a specific value are expressed as a multiple of another quantity of the same dimension. Typical example is r/M, t/M, and we scale $M = 1$.

Tensor formalism

In general relativity the physical quantities can be described by tensorial quantities. We use standard tensor index notation with indeces that are either covariant (*vectors*) or contravariant (*covectors*). Greek indices are ranging from 0 to 3, whereas Latin indices from 1 to 3. The 0-th component refers to time coordinate. Tensorial contraction is represented by repeated indeces (one label is covariant and the other contravariant), also we employ Einstein summation convention.

The signature of metric tensor is $(-,+,+,+)$, and hence the time-like vectors have negative magnitude.

List of abbreviations

BH: Black hole, M-P: the Majudmar-Papapetrou solution, R-N: the Reissner-Nordström solution, EoM: equation of motion, RHS/LHS: the right/left hand side of the equation, DoF: degree of freedom, EFE: Einstein's field equations.

Equations carried out in the thesis were solved using the software Wolfram Mathematica 13.0 and the package for tensor computer algebra, xAct 1.2.0.

1. Static spacetime

The time-independent multi-black hole solution for extremal black holes not only exists but also is very simple. Since Majumdar-Papapetrou (M-P) spacetime describes superposition of extremally charged black holes, it is convenient to start with description of a single charged Reissner-Nordström black hole, its metric and interesting properties. Then we generalize R-N metric to M-P solution (it is rather a motivation). For a rigorous derivation of M-P solution, please, visit Section 1.3.

1.1 General spacetime and extremal Reissner–Nordström solution

Reissner–Nordström (R–N) solution is very well known solution of EFE describing the spacetime containing one black hole of charge Q and mass M only. One can also directly obtain the line element for R–N solution from the line element of general spacetime which describes a rotating (Kerr parameter a)[1] electrically charged (charge Q) black hole of mass M (as seen by an observer at infinity) in a background universe with (generally non–zero) cosmological constant Λ by putting convenient parameters equal to zero. All the parameters are meant to be held fixed. This *Kerr–Newman–(anti–)de Sitter* solution reads in Boyer–Lindquist coordinates and natural units $c = 1 = G$ [10]

$$\begin{aligned} \mathrm{d}s^2 = -\frac{\Delta_r}{\Xi^2\rho^2}\left(\mathrm{d}t - a\sin^2\theta\mathrm{d}\phi\right)^2 + \frac{\rho^2}{\Delta_r}\mathrm{d}r^2 + \frac{\rho^2}{\Delta_\theta}\mathrm{d}\theta^2 + \\ + \frac{\Delta_\theta\sin^2\theta}{\Xi^2\rho^2}\left(a\mathrm{d}t - (r^2+a^2)\mathrm{d}\phi\right)^2, \end{aligned} \tag{1.1}$$

where

$$\begin{aligned} \rho^2 &= r^2 + a^2\cos^2\theta, \\ \Delta_r &= \left(r^2+a^2\right)\left(1 - \frac{1}{3}\Lambda r^2\right) - 2Mr + Q^2, \\ \Delta_\theta &= 1 + \frac{1}{3}\Lambda a^2\cos^2\theta, \\ \Xi &= 1 + \frac{1}{3}\Lambda a^2. \end{aligned} \tag{1.2}$$

Next, the event horizons of the space–time are given by $\Delta_r(r) = 0$ [10]. The event horizon represents the set of all events that can be seen by outer observers whose paths start at infinity and end at infinity. Moreover, all of the singularities included in these solutions lie within the horizons. Geometries with singularities isolated in this way are said to be black–hole solutions.

[1] $a > 0$, since we can always choose the orientation of angle ϕ in such a way, considering coordinates (r, θ, ϕ).

Now, choosing wisely $a = \Lambda = 0$ one obtains our well known Reissner–Nordström spacetime which is a static, spherically symmetric solution of Einstein-Maxwell equations[2]

$$\mathrm{d}s^2 = -\left(1 - \frac{2M}{r} + \frac{Q^2}{r^2}\right)\mathrm{d}t^2 + \frac{\mathrm{d}r^2}{\left(1 - \frac{2M}{r} + \frac{Q^2}{r^2}\right)} + r^2\mathrm{d}\Omega^2, \tag{1.3}$$

where $\mathrm{d}\Omega^2 = \mathrm{d}\theta^2 + \sin^2\theta\mathrm{d}\phi^2$ is the angular part of the metric.

Here $\Delta_r(r) = 0$ yields an equation that can be solved easily

$$\frac{1}{g_{rr}} = 0 = 1 - \frac{2M}{r} + \frac{Q^2}{r^2} \to r_\pm = M \pm \sqrt{M^2 - Q^2}. \tag{1.4}$$

Obviously, a special extremal solution $Q = M$, i.e., satisfying (1) in natural units, describes a double-degenerate horizon at $r = M$, corresponding to an extremal black hole[3]. Performing a simple limit $Q \to M$ the spacetime of extremal R–N black hole is described by

$$\mathrm{d}s^2 = -\left(1 - \frac{M}{r}\right)^2\mathrm{d}t^2 + \frac{\mathrm{d}r^2}{\left(1 - \frac{M}{r}\right)^2} + r^2\mathrm{d}\Omega_2^2 \tag{1.5}$$

with the corresponding four-potential

$$A_{RN} = \frac{Q}{R}\mathrm{d}t. \tag{1.6}$$

1.1.1 | R-N solution: pathology, asymptotics

At $r = M$ there is a coordinate singularity, which corresponds to a second-order pole in the metric. However, one can use Eddington-Finkelstein coordinates to extend the space-time to all $r > 0$. What makes extremally charged black holes so special? Let us consider a sub-extremal black hole. Looking at the (spatial) distance from a point $r = \bar{R}$ to the horizon of such a hole we obtain

$$s = \int_{r_+}^{\bar{R}} \frac{\mathrm{d}r}{\left(1 - \frac{r_+}{r}\right)\left(1 - \frac{r_-}{r}\right)} < \infty, \tag{1.7}$$

where r_+, r_- denote the inner and outer horizon, respectively. The proper distance to the horizon is thus finite whereas for the extremal black hole where the horizons coincide $r_- = r_+ = M$ one arrives at infinite spatial distance.

$$s = \int_M^{\bar{R}} \left(1 - \frac{M}{r}\right)^2 \mathrm{d}r = \infty \tag{1.8}$$

[2] $r_S = 2M$ is the Schwarzschild radius in geometrized units. In SI unit system this would be $2M \to \frac{2GM}{c^2}$ and $Q^2 \to \frac{GQ^2}{4\pi\epsilon_0 c^4}$.

[3] The case $M < Q$ would cause both $r_\pm \in \mathbb{C}$ and hence there would be no event horizons and the singularity would be naked. Thence it is convenient to use the term *extremally charged*, since it is the largest physically allowed value of charge.

However, time-like and null geodesics can reach the horizon during a finite interval of their affine parameter [11].

The horizon can be thought of as developing an infinite throat, see Figure 1.1. If we restrict the Einstein-Rosen bridge just to one side, this is what we get.

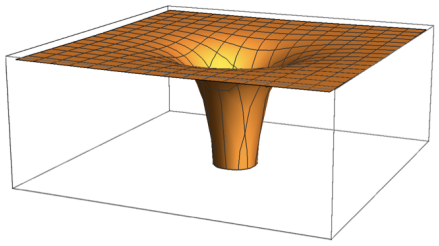

Figure 1.1: Geometry of extremal Reissner-Nordström black hole [11]

What does the geometry look like deep inside the throat? Let us take the near-horizon limit and write

$$r = r_+ + \epsilon.$$

Having $\epsilon \ll M$, the metric (1.5) reads

$$\mathrm{d}s^2 = -\frac{\epsilon^2}{r_+^2}\mathrm{d}t^2 + \frac{r_+^2}{\epsilon^2}\mathrm{d}\epsilon^2 + r_+^2\mathrm{d}\Omega_2^2. \quad (1.9)$$

One can recognize in the first two terms the Poincaré patch of 2-dim AdS spacetime, covering one half of the hyperboloid parametrizing the natural embedding of AdS in 5-dim spacetime, whilst the last term depicts a two-sphere with constant radius r_+. The near horizon geometry of R-N black hole is thus $\mathrm{AdS}_2 \times \mathrm{S}_2$, sometimes called as the *Robinson-Bertotti metric* [11], one of the calculations motivating AdS/CFT. For more information about AdS/CFT correspondence see for example the work of V. E. Hubeny [12].

Now let us have a look at the asymptotics of the R-N solution. The extremal case of R-N (1.5) can be rewritten as

$$\mathrm{d}s^2_{RN_{ex}} = -\frac{r'^2}{(r'+\Sigma)^2}\mathrm{d}t^2 + \frac{(r'+\Sigma)^2}{r'^2}\mathrm{d}r'^2 + (r'+\Sigma)^2\,\mathrm{d}\Omega^2, \quad (1.10)$$

where $r' = R - r_+$ and positions of horizons coalesce $r_+ = r_- = M = |Q| \equiv \Sigma$, singularity clearly sits at $r' = 0$ [11].

This can be reinterpreted using a harmonic function $H \equiv \frac{r'+\Sigma}{r'} = 1 + \frac{\Sigma}{r'}$ (for which $\Box H = 0$) and $r' = \sqrt{\vec{x}\cdot\vec{x}}$ as

$$\mathrm{d}s^2_{RN_{ex}} = -H^{-2}(r')\mathrm{d}t^2 + H^2(r')\mathrm{d}\vec{x}\cdot\mathrm{d}\vec{x}. \quad (1.11)$$

In the asymptotic regions ($R^2 \gg Q^2$) the metric (1.6) first goes over to the Schwarzschild one and even further it translates to a Minkovskian flat metric. M thus represents the source mass.

1.2 | Majumdar–Papapetrou solution

Now we proceed with the afore mentioned heuristic generalization of R-N to M-P spacetime, starting with the extremal R-N metric.

Motivation

The form (1.11) now admits a simple generalization to

$$\mathrm{d}s^2_{M-P} = -H^{-2}(\vec{x})\mathrm{d}t^2 + H^2(\vec{x})\mathrm{d}\vec{x}\cdot\mathrm{d}\vec{x} \tag{1.12}$$

where $\vec{x}$ is the usual Cartesian coordinate on $\mathbb{R}^3$. Then we make the following Ansatz for the gauge field corresponding to electrically charged black holes

$$A = \frac{1}{H}\mathrm{d}t.$$

The non-linear Einstein-Maxwell equations then reduce to a very simple linear condition, the Laplace equation

$$\Delta H(\vec{x}) = 0 \tag{1.13}$$

where Δ is the Laplacian on flat $\mathbb{R}^3$. With flat-spacetime asymptotic boundary conditions, (1.13) is solved by ($\vec{x}_i$ is position of the i-th black hole)

$$H(\vec{x}) = 1 + \sum_{i=1}^{n} \frac{1}{|\vec{x} - \vec{x}_i|}, \tag{1.14}$$

which is known as the Majumdar-Papapetrou solution [1, 2]. Function $H(\vec{x})$ in this section is denoted as $\psi(\vec{x})$ throughout the rest of the thesis, following the notation of [4, 5].

$$\begin{aligned} \mathrm{d}s^2 &= -\psi^{-2}\mathrm{d}t^2 + \psi^2\mathrm{d}\vec{x}\cdot\mathrm{d}\vec{x} \\ \psi(\vec{x}) &= 1 + \sum_{i=1}^{N} \frac{m_i}{|\vec{x} - \vec{x}_i|} \\ A &= \frac{1}{\psi}\mathrm{d}t. \end{aligned} \tag{1.15}$$

J. B. Hartle & S. W. Hawking showed in [3] that either the Majumdar–Papapetrou geometries contain naked singularities or correspond to systems of extremally charged black holes in equilibrium under their mutual electrostatic forces and gravitational interaction.

1.2.1 | M-P solution: asymptotics, horizons

Large distance

The Majumdar-Papapetrou (M-P) metric for the case of two equally massive black holes ($M_1 = M_2 = M$) is asymptotically ($|\vec{x}| \gg |\vec{x}_1|,\ |\vec{x}| \gg |\vec{x}_2|,\ |\vec{x}| \equiv r$)

$$\mathrm{d}s^2_{MP_{asymp.}} = -\left(1 + \frac{2M}{r}\right)^{-2} \mathrm{d}t^2 + \left(1 + \frac{2M}{r}\right)^{2} \mathrm{d}\vec{x} \cdot \mathrm{d}\vec{x} \tag{1.16}$$

which after putting $\Sigma = 2M$ and $r' = r$ becomes (1.11). Thus, the M-P metric of two black holes asymptotically behaves as the R-N metric with extremally charged source of mass $2M$.

Vicinity of the hole

If we put the two black holes into $(0, 0, \alpha)$ and $(0, 0, -\alpha)$ in Cartesian coordinates, one can write the master function as

$$\psi(\vec{x}) = 1 + \frac{m_1}{\sqrt{x^2 + y^2 + (z - \alpha^2)}} + \frac{m_2}{\sqrt{x^2 + y^2 + (z + \alpha^2)}}. \tag{1.17}$$

It seems convenient to translate this into shifted spherical coordinates

$$x = r \sin\theta \cos\phi, \qquad y = r \sin\theta \sin\phi, \qquad z - \alpha = r \cos\theta \tag{1.18}$$

and find $\psi(r, \theta, \phi)$ as

$$\psi(r, \theta, \phi) = 1 + \frac{m_1}{r} + \frac{m_2}{\sqrt{r^2 + 4\alpha r \cos\theta + 4\alpha^2}} \tag{1.19}$$

and the metric becomes

$$\mathrm{d}s^2 = -\psi(r, \theta, \phi)^{-2} \mathrm{d}t^2 + \psi(r, \theta, \phi)^2 \cdot \left(\mathrm{d}r^2 + r^2 \mathrm{d}\theta^2 + r^2 \sin^2\theta \mathrm{d}\phi^2\right). \tag{1.20}$$

This can be expanded and one recovers that the series (up to the first order) match perfectly with R-N solution. The result is that M-P geometry in the vicinity of the first black hole, i.e. $\lim_{r\to 0}$ (1.20), behaves as R-N metric with one dominating extremally charged source (sitting in the origin of shifted spherical coordinates).

Horizons

The event horizons of the holes lie at the points $\vec{x} = \vec{x}_a$. Introducing convenient coordinates into the M-P metric, that is (1.20), one can simply calculate the properties such as the surface of horizon of the first black hole S_H. Alternatively one can calculate the second black hole horizon.

$$S_H = \lim_{r\to 0} \int_0^{2\pi} \int_0^{\pi} \sqrt{g_{\theta\theta} g_{\phi\phi}} \mathrm{d}\theta \mathrm{d}\phi = \lim_{r\to 0} \int_0^{2\pi} \int_0^{\pi} \psi^2 r^2 \sin\theta \mathrm{d}\theta \mathrm{d}\phi = 4\pi m_1^2 \tag{1.21}$$

The final term corresponds to the surface of a 2-sphere with radius m_1. After a simple coordinate transformation one can see this is the null hypersufrace of the extremal R-N. Generaly, M-P metric implies that the invariant area of any 2-sphere that surrounds the origin $r = 0$ is given by

$$S(r) = 4\pi r^2 \psi^2.$$

1.2.2 | ADM mass (static)

Given a 3D manifold $\mathcal{M}$ with an asymptotically flat and positive definite metric g the ADM mass for the space $(\mathcal{M}, g)$ can be defined as [13, 14]

$$M = \frac{1}{16\pi} \lim_{\mathcal{S}^2 \to i^0} \int_{\mathcal{S}^2} g^{ij} \left(g_{ik,j} - g_{ij,k}\right) n^k \mathrm{d}^2\mathcal{A}, \tag{1.22}$$

where $\mathcal{S}^2$ is a topological 2-sphere, n^k is outward pointing unit normal vector and $\mathrm{d}^2\mathcal{A}$ is the area element. The above integral is defined for a restricted class of coordinate systems with spatial being *asymptotic Euclidean*. The metric components in such a system are required to be of the form $g_{ij} = \delta_{ij} + \mathcal{O}\left(\frac{1}{r}\right)$. We choose $x^i = \{x, y, z\}$, parameter of a 2-sphere $\mathcal{S}^2$ is the radial distance $r = \sqrt{x^2 + y^2 + z^2}$. We carry out the integral over the hypersurface $r = const.$, $t = const.$ and hence we have $n^i = \frac{\partial r}{\partial x_i} = \frac{x^i}{r}$. In stationary spacetimes the ADM mass reduces to the conserved charge associated with the time translational symmetry.

Our Majumdar-Papapetrou metric

$$\mathrm{d}s^2 = -\frac{1}{\psi^2}\mathrm{d}t^2 + \psi^2 \mathrm{d}\vec{x} \cdot \mathrm{d}\vec{x}, \qquad \psi = 1 + \sum_{a=1}^{N} \frac{m_a}{|\vec{x} - \vec{x}_a|} \tag{1.23}$$

asymptotically goes to $\eta_{\mu\nu}$, allowing us to directly use the formula for the ADM mass. We can work out the spatial partial derivatives with respect to any spatial coordinate

$$g_{ij,k} = \frac{g_{ij}}{\psi^2} \partial_k \psi^2 = -2\delta_{ij} \psi \sum_{a=1}^{N} \frac{m_a}{|\vec{r} - \vec{x}_a|^3} \left(r_k - (x_a)_k\right)$$

which can be expanded for large r

$$g_{ij,k}\Big|_{r \gg 1} = -2\delta_{ij} \frac{x_k}{r^3} \sum_{a=1}^{N} m_a + \mathcal{O}\left(\frac{1}{r^3}\right).$$

Plugging this into the formula for the ADM mass (1.22) we obtain

$$\begin{aligned} M_{ADM} &= \frac{1}{16\pi} \lim_{\mathcal{S}^2 \to i^0} \int_{\mathcal{S}^2} \left(\sum_{a=1}^{N} m_a \left[-2\delta_{ik} \frac{x^i}{r^3} + 2\delta^{ij}\delta_{ij} \frac{x_k}{r^3} \right] + \mathcal{O}\left(\frac{1}{r^3}\right) \right) \frac{x^k}{r} \mathrm{d}^2\mathcal{A} \\ &= \frac{\sum_{a=1}^{N} m_a}{16\pi} \lim_{\mathcal{S}^2 \to i^0} \int_{\mathcal{S}^2} \left(-\frac{2}{r^2} + \frac{6}{r^2} + \mathcal{O}\left(\frac{1}{r^3}\right) \right) \mathrm{d}^2\mathcal{A} \\ &= \frac{\sum_{a=1}^{N} m_a}{16\pi} \lim_{\mathcal{S}^2 \to i^0} \int_{\mathcal{S}^2} \left(\frac{4}{r^2} + \mathcal{O}\left(\frac{1}{r^3}\right) \right) \mathrm{d}^2\mathcal{A}. \end{aligned} \tag{1.24}$$

Translating into spherical coordinates $\mathrm{d}^2\mathcal{A} = r^2\mathrm{d}(\cos\theta)\mathrm{d}\phi$ we finally obtain

$$M_{ADM} = \frac{\sum_{a=1}^{N} m_a}{16\pi} \lim_{\mathcal{S}^2 \to i^0} \int_0^{2\pi} \int_{-1}^{1} \left(\frac{4}{r^2} + \mathcal{O}\left(\frac{1}{r^3}\right) \right) r^2 \mathrm{d}(\cos\theta)\mathrm{d}\phi = \sum_{a=1}^{N} m_a. \quad (1.25)$$

The ADM mass of Majumdar-Papapetrou spacetime is, as expected, just a sum of the partial masses of the extremally charged bodies. We will compare this with the value calculated for a perturbed system in Section 3.1.3.

1.3 | Rigorous derivation of M-P

Let us derive somewhat more rigorously the Majumdar-Papapetrou solution. M-P spacetime is a vacuum solution to coupled Einstein-Maxwell partial differential equations of the second order. We first proceed with general background-space metric h_{ij} and in the last stage we assume it to be flat. It is a generalisation of [15], where they have chosen Cartesian coordinates already at the beginning. We also turn Cartesian, however in the second part only. The beginning of procedure freely follows [16]. To regularize the singularities during calculation we choose to smudge extremal black holes to a charge-dust with a given distribution, as done in [4, 5]. Charged-dust Einstein-Maxwell equations read

$$G_{\mu\nu} = 8\pi T_{\mu\nu}, \quad (1.26)$$

$$F^{\mu\nu}{}_{;\nu} = 8\pi J^{\mu}, \quad (1.27)$$

where $G_{\mu\nu}, F^{\mu\nu}$ denote Einstein and Maxwell tensor, respectively. The total energy-momentum (en-mom) tensor of a charged dust $T_{\mu\nu}$ is given by the sum of Maxwell en-mom tensor and the matter en-mom tensor with four-velocity u^{μ}. Let ρ be a smooth distribution of pressureless dust with charge-to-mass ratio unity.

$$T_{\mu\nu} = \frac{1}{4\pi}\left(F_{\mu\alpha}F_{\nu}{}^{\alpha} - \frac{1}{4} g_{\mu\nu} F_{\alpha\beta}F^{\alpha\beta} \right) + \rho u_{\mu} u_{\nu} \quad (1.28)$$

The four-current is four-velocity multiplied by charge density σ

$$J^{\mu} = \sigma u^{\mu}. \quad (1.29)$$

Let us assume a static spacetime and an Ansatz for conformastatic metric [17]

$$\mathrm{d}s^2 = -Q^2\mathrm{d}t^2 + \frac{1}{Q^2} h_{ij}\mathrm{d}x^i\mathrm{d}x^j, \quad (1.30)$$

with the background metric h_{ij} and master function Q depend on spatial coordinates x^i only. Let us further assume an electrostatic form of four-potential, four-current and also we have four-velocity of time-like particle satisfying normalization $u_{\mu}u^{\mu} = -1$:

$$A_{\alpha} = A_0(x_i)\delta^0_{\alpha}, \quad J^{\alpha} = \frac{\sigma(x^i)}{Q(x^i)}\delta^{\alpha}_0, \quad u^{\alpha} = \frac{1}{Q(x^i)}\delta^{\alpha}_0. \quad (1.31)$$

If we use the definition of Maxwell tensor $F_{\mu\nu} = \partial_\mu A_\nu - \partial_\nu A_\mu$, we see that (1.27) includes only one non-trivial equation ($h = \det(h_{ij})$, h^{ij} is inverse of h_{ij})

$$\frac{1}{\sqrt{h}}\partial_i\left(\sqrt{h}\frac{h^{ij}}{Q^2}\partial_j A_0\right) = \frac{4\pi\sigma}{Q^3} \tag{1.32}$$

Now we are left with *EFE* (Einstein field equations). We can calculate the components of Einstein tensor.

$$\begin{aligned} G_{00} &= 2Q^3\Delta_{(h)}Q - 3Q^2(\nabla_{(h)}Q)\cdot(\nabla_{(h)}Q) + \frac{1}{2}Q^4 R_{(h)} \\ G_{0i} &= 0 \\ G_{ij} &= R_{(h)ij} - \frac{2}{Q^2}\partial_i Q\partial_j Q + h_{ij}\left(\frac{1}{Q^2}(\nabla_{(h)}Q)\cdot(\nabla_{(h)}Q) - \frac{1}{2}R_{(h)}\right) \end{aligned} \tag{1.33}$$

Here $\nabla_{(h)},\ \Delta_{(h)},\ R_{(h)ij},\ R_{(h)}$ denote the gradient, Laplace operator, Ricci tensor and Ricci scalar associated with the background space metric h_{ij}. En-mom tensor is given as follows.

$$\begin{aligned} T_{00} &= \frac{1}{8\pi}Q^2(\nabla_{(h)}A_0)\cdot(\nabla_{(h)}A_0) + \rho Q^2 \\ T_{0i} &= 0 \\ T_{ij} &= \frac{1}{4\pi}\left(-\frac{1}{Q^2}\partial_i A_0\partial_j A_0 + \frac{1}{2}\frac{1}{Q^2}h_{ij}(\nabla_{(h)}A_0)\cdot(\nabla_{(h)}A_0)\right) \end{aligned} \tag{1.34}$$

Now we are allowed to put down an explicit form of *EFE*, giving us only seven non-trivial equations.

Furthermore, we assume the background space is Euclidean in Cartesian coordinates; $h_{ij} = \delta_{ij}$. Equation for $G_{00},\ G_{ij}$ become (now the operators ∇, Δ operate on flat space)

$$-3\nabla Q\cdot\nabla Q + 2Q\Delta Q = \nabla A_0\cdot\nabla A_0 + 8\pi\rho \tag{1.35}$$

$$-2\nabla_i Q\nabla_j Q + \delta_{ij}\nabla Q\cdot\nabla Q = -2\nabla_i A_0\nabla_j A_0 + \delta_{ij}\nabla A_0\cdot\nabla A_0 \tag{1.36}$$

Spatial-spatial part $G_{ij} = 8\pi T_{ij}$

Now we contract (1.36) with δ^{ij}, use $\delta_{ij}\delta^{ij} = 3$ and obtain

$$\nabla Q\cdot\nabla Q = \nabla A_0\cdot\nabla A_0 \tag{1.37}$$

which we can substitute back into (1.36) and obtain

$$\nabla_i Q\nabla_j Q = \nabla_i A_0\nabla_j A_0 \tag{1.38}$$

and that we integrate (with additive integration constant equal to zero)

$$A_0 = \alpha Q,\ \alpha^2 = 1. \tag{1.39}$$

Time-time part $G_0 = 8\pi T_{00}$

Now one can substitute A_0 (1.39) into (1.35), hence one eliminates A_0 and gets equation in terms of Q only. Then we use a somewhat artificial identity

$$Q\Delta Q = 2\nabla Q \cdot \nabla Q - Q^3 \Delta \left(\frac{1}{Q}\right)$$

and we obtain an equation of Poisson type

$$\Delta \left(\frac{1}{Q}\right) + 4\pi\rho \frac{1}{Q^3} = 0. \tag{1.40}$$

Maxwell equation $F^{0\nu}{}_{;\nu} = 4\pi J^0$

Equation $F^{0\nu}{}_{;\nu} = 4\pi J^0$ is the Gauss law for M-P coordinate system. Here we substitute for A_0 from (1.39) into Maxwell equation (1.32) and we arrive at

$$\Delta \left(\frac{1}{Q}\right) + \frac{4\pi\sigma}{\alpha} \left(\frac{1}{Q^3}\right) = 0. \tag{1.41}$$

Comparing the resulting equations (1.40) and (1.41) we obtain the relation between σ and ρ

$$\sigma = \alpha\rho \tag{1.42}$$

This relation (1.42) is the characterisation of Majumdar-Papapetrou class of static solution of Einstein-Maxwell-(extremally)-charged-dust equations [16].

Master function ψ

To determine the black hole solution we need the matter distribution to be singular. Fortunately, this can be done without any difficulties and it was known to Majumdar and Papapetrou already [5]. The geometry of a spacetime with an uncharged mass looks as a well deepening as the mass increases, similar to Figure 1.1. For a maximally charged matter the bottom of the well falls down and the throat keeps lenghtening. As the distribution becomes a δ-function (singularity) the throat is infinitely long [5], depicted in Figure 1.1[4].

The black hole limit means that smooth distribution of pressureless extremally charged dust ρ is allowed to turn into a sum of point-like sources, mathematically expressed as

$$\rho\psi^3 \to \sum_a m_a \delta^3(\vec{x} - \vec{x}_a),$$

where a goes over the black holes and we denoted

$$\psi \equiv 1/Q.$$

[4]Due to our limited opportunities only a finite part of the well is plotted, the reader is encouraged to extrapolate the infinite remainder in his/her mind.

All of the infinities will, out of the blue, cancel out, leaving us with working *regularization* (and hence with no need of further *renormalization*). Our equation to solve is now Poisson's equation

$$\Delta\psi = -4\pi \sum_a m_a \delta^{(3)}(\vec{x} - \vec{x}_a). \tag{1.43}$$

One can see ψ has just turned into Green's function for 3D Laplace operator. General prescription for the equation and its solution is well known

$$\Delta G(\vec{x}, \vec{x}') = \delta^{(3)}(\vec{x} - \vec{x}')$$

$$G(\vec{x}, \vec{x}') = -\frac{1}{4\pi} \frac{1}{|\vec{x} - \vec{x}'|}.$$

The Laplace equation is linear, and hence the full solution to our equation (1.43) is clearly given by superposition of individual solutions

$$\psi = 1 + \sum_a \frac{m_a}{|\vec{x} - \vec{x}_a|}. \tag{1.44}$$

The solution is normalized to unity on the boundary, the metric is thus asymptotically flat ($\lim_{x\to\infty} \psi = 1$ trivially solves the Laplace equation). Thus the resulting form of metric is the desired Majumdar-Papapetrou static solution

$$\begin{aligned} \mathrm{d}s^2 &= -\frac{1}{\psi^2}\mathrm{d}t^2 + \psi^2 \mathrm{d}\vec{x} \cdot \mathrm{d}\vec{x} \\ A &= \frac{1}{\psi}\mathrm{d}t. \end{aligned} \tag{1.45}$$

2. Perturbed spacetime

2.1 | Analytic form of metric

We have already met the static solution, called the Majumdar-Papapetrou solution for a set of extremally charged static black holes (1.45). We aim to describe a more realistic situation with mutual motion, since not much of the universe is really static. We achieve this by giving our black holes non-zero initial velocities. One can easily see that such perturbation causes a lot of non-trivial physics in our space-time. While in the static case the electrostatic repulsion cancelled exactly with gravito-static interaction, now we need to take into account different electro-dynamic and general-relativistic processes.

This undoubtedly very complex problem is still in the full strong-field regime of gravity (even though restricting to slow motion). Regarding this, it is quite amazing that such a solution can be found analytically within the framework of general relativity to the lowest order in the velocity perturbation.

Regarding the metric, only the terms quadratic in first-order perturbation of fields can survive through $O(v^2)$. In addition to that, all the first-order perturbations even under the time reversal vanish. Thus, there is no perturbation in g_{tt}, g_{ij} and A_t. The general analytic form of perturbed spacetime is then [5]

$$\begin{aligned} \mathrm{d}s^2 &= -\psi^{-2}\mathrm{d}t^2 + 2\vec{N}\cdot\mathrm{d}\vec{x}\;\mathrm{d}t + \psi^2\mathrm{d}\vec{x}\;\cdot\mathrm{d}\vec{x} \\ A &= -\left(1-\frac{1}{\psi}\right)\mathrm{d}t + \vec{A}\cdot\mathrm{d}\vec{x}, \end{aligned} \tag{2.1}$$

where the perturbation is expressed using two first-order three-tensorial quantities $\vec{N}$, $\vec{A}$ on the $t = const.$ spacetime slice. Instead of the original form (2.1) we further use $A_0 = 1/\psi$ for the time component of the 4-potential, i.e. normalisation to unity at infinity. Subtracting unity yields an equivalent form, i.e. leaves the equations of motion unchanged. We write the Lagrangian to second order in these perturbative quantities and velocity $\vec{v}$.

2.1.1 | Slow-motion approximation

Let us begin with the salient feature of slow-motion approximation. Within the framework of general relativity a number of effects is connected with charged, massive and moving bodies; namely gravitational and electromagnetic radiation, magnetic and frame-dragging (gravitomagnetic) forces, etc. Regarding radiation we are left with an infinite number of field degrees of freedom (DoF).

Imposing the *low-velocity condition*, circumstances begin to turn in our favor. The radiation is a consequence of the finite speed of propagation of field disturbances. If we neglect radiation, then the fields are entirely determined by initial positions and velocities and the speed of propagating information can be treated

as infinite, compared to v. Moreover, the retarded time then merges with standard time coordinate and we can neglect, so to say, the phase shift proportional to $\frac{r}{c}$. As is well known, black holes have only three DoF. An infinite number of radiation DoF is thus truncated to a **finite number** of black hole DoF within slow-motion approximation.

Our approach is based on coming through a sequence of static configurations within a quasistatic motion. The system thus pursues a path in moduli space, such an approach is called *moduli space approximation* [4, 5]. The velocities are small $v \ll 1$ (or $v \ll c$ in SI units) and we find the corrections to Newtonian gravity to the order of v^2 (or v^2/c^2 in SI units), which falls into the realm of post-Newtonian corrections (1PN). While velocities are small the gravitational field is still quite strong so we cannot provide a limit $c \to \infty$, terms of type GM/c^2 are finite and nonzero. As stated above, we work in full strong-field regime of gravitation. Note, that the finiteness of the last term provides a finite limitation to the separation of two extremal R-N holes $r \geq \frac{GM}{c^2}$.

Looking at a snapshot of the system at a constant time, the gravitational interaction and electrostatic repulsion cancel exactly, no matter the positions. The only remainder will be magnetic and gravito-magnetic (sometimes being referred to as frame-dragging) interactions. Let us have two slowly moving ($v \ll 1$) charges q separated by distance r. Then a simple calculation makes an estimate of the ratio of magnetic force to electric force exerted on the second charge by the first one (let us work in SI units for a second)

$$|\vec{F}_B| = q|(\vec{v} \times \vec{B})| = \frac{\mu_0}{4\pi}\frac{q^2v^2}{r^2}, \quad |\vec{F}_E| = k_e\frac{q^2}{r^2}$$

$$\frac{F_B}{F_E} = \frac{v^2}{c^2}.$$

Magnetic interactions are of the order v^2, hence they influence motion in our approximation and give rise to electric currents, affecting charges.

How about the other forces[1]? In the low velocity limit of extremal BH the gravitational reaction interactions scale as v^5, the electromagnetism reaction forces (currents) scale as v^3 [18] and frame-dragging effects remain small enough as long as the velocities are small [5]. The gravitational waves (GW) emitted by the slowly rotating system are of the order v^5 [4, 5]. So far so good, everything can be neglected as $\mathcal{O}(v^3)$. A query could arise since in case of coalescence the GW can be even of order v^2 [8]. However, we do not study such a case here, having a stationary, mutually orbiting system instead and our situation is safe.

[1]We take the word "force" with a grain of salt, especially regarding gravity.

2.2 | Approximate action

We keep perturbations through up to the second order, since we are interested in first-order field equations. We start with the prescription for total exact action in general relativity and derive the perturbed action, which is to be varied to obtain the right Einstein-Maxwell equations.

2.2.1 | Total exact action

The total action is given by a sum of four pieces, that is gravity, Maxwell fields, action from current and from matter.

$$S = S_{\text{gravity}} + S_{\text{EM-fields}} + S_{\text{current}} + S_{\text{matter}}. \tag{2.2}$$

These are to be evaluated as

$$S = \int \mathrm{d}^4x\sqrt{-g}\cdot\left(\frac{R}{16\pi} - \frac{F^2}{16\pi} + A_\mu\rho u^\mu - \rho\right). \tag{2.3}$$

The determinant of perturbed metric (2.1) is

$$\sqrt{-g} = \psi^2\sqrt{1+\vec{N}\cdot\vec{N}}.$$

Action from Maxwell fields

For electromagnetic field we have

$$S_{\text{EM}} = -\frac{1}{8\pi}\int_{\mathcal{M}} F\wedge F^* = -\frac{1}{16\pi}\int \mathrm{d}t\ \mathrm{d}^3x\ \sqrt{-g}F_{\mu\nu}F^{\mu\nu}, \tag{2.4}$$

where $\mathcal{M}$ denotes in general Lorentzian manifold. $F^{\mu\nu}$ has the following "Hodge-like" structure

$$F^{\mu\nu} = \begin{pmatrix} 0 & -G_1 & -G_2 & -G_3 \\ G_1 & 0 & H_3 & -H_2 \\ G_1 & -H_3 & 0 & H_1 \\ G_3 & H_2 & -H_1 & 0 \end{pmatrix},$$

where we introduced the following functions for brevity

$$\begin{aligned} \vec{G} &\equiv \frac{1}{\psi^2(1+\vec{N}^2)}\left(\psi^2\partial_t\vec{A} + \nabla\psi + \vec{N}\times(\nabla\times\vec{A})\right) \\ \vec{H} &\equiv \frac{1}{\psi^4(1+\vec{N}^2)}\vec{N}\times\left(\nabla\psi + \psi^2\partial_t\vec{A} + \vec{N}\times(\nabla\times\vec{A})\right) + (\nabla\times\vec{A})(1+\vec{N}^2) \\ &= \frac{\vec{N}\times\vec{G}}{\psi^2} + (\nabla\times\vec{A})(1+\vec{N}^2). \end{aligned} \tag{2.5}$$

The Maxwellian field $F^2 \equiv F_{\mu\nu}F^{\mu\nu}$ reads

$$\begin{aligned} F^2 = 2\frac{\left[\vec{N}\times\left(\nabla\psi+\psi^2\partial_t\vec{A}+\vec{N}\times(\nabla\times\vec{A})\right)+(\nabla\times\vec{A})(1+\vec{N}^2)\right]\cdot\left(\nabla\times\vec{A}\right)}{\psi^4(1+\vec{N}^2)} \\ -2\frac{\left(\psi^2\partial_t\vec{A}+\nabla\psi+\vec{N}\times(\nabla\times\vec{A})\right)\cdot\left(\psi^2\partial_t\vec{A}+\nabla\psi\right)}{\psi^4(1+\vec{N}^2)} \\ \equiv 2\left\{\vec{H}\cdot(\nabla\times\vec{A})-\psi^{-2}\vec{G}\cdot\left(\psi^2\partial_t\vec{A}+\nabla\psi\right)\right\} \end{aligned} \tag{2.6}$$

Note, that each time derivative brings another order of v

$$\vec{A}\sim v,\quad \vec{N}\sim v,\quad \partial_t\vec{A}\equiv\dot{\vec{A}}\sim v^2$$

simply because $\partial_t Q(x^i) = (\partial_j Q)\cdot(\mathrm{d}x^i/\mathrm{d}t) = (\partial_j Q)\cdot v$ for any quantity.
Now, let us drop $\mathcal{O}(v^3)$ in F^2. Identites that we used during derivation of the action from Maxwell fields are written in chronological order of usage here.

$$\vec{N}\times(\nabla\times\vec{A})\cdot(\nabla\psi) = -(\nabla\times\vec{A})\cdot\left(\vec{N}\times(\nabla\psi)\right) \tag{2.7}$$

$$\nabla\times(\psi\vec{N}) = \psi\nabla\times\vec{N}+(\nabla\psi)\times\vec{N} \qquad \textit{(product rule)} \tag{2.8}$$

$$\rightarrow \vec{N}\times(\nabla\psi) = -(\nabla\psi)\times\vec{N} = \psi(\nabla\times\vec{N})-\nabla\times(\psi\vec{N}) \tag{2.9}$$

$$\nabla\times\left(\psi^2\vec{N}\right) = \psi^2\nabla\times\vec{N}+\underbrace{\left(\nabla\left(\psi^2\right)\right)}_{2\psi(\nabla\psi)\times\vec{N}}\times\vec{N} \tag{2.10}$$

$$\rightarrow -(\nabla\psi)\times\vec{N} = \frac{1}{2\psi}\left(\psi^2\nabla\times\vec{N}-\nabla\times\left(\psi^2\vec{N}\right)\right) \tag{2.11}$$

$$|\nabla\times(\psi N)|^2 = \nabla\times(\psi N)\cdot\left(\frac{1}{\psi}(\nabla\times(\psi^2 N))-(\nabla\psi)\times N\right) \tag{2.12}$$

Then we use this

$$\begin{aligned} &(\nabla\times(\psi N))\cdot[(\nabla\psi)\times N] = \\ &= \overbrace{\frac{1}{\psi^2}|\nabla\times(\psi^2 N)|^2-\frac{1}{\psi}(\nabla\times(\psi N))\cdot(\nabla\times(\psi^2 N))-\frac{1}{\psi}\nabla\times(\psi^2 N)\cdot[(\nabla\psi)\times N]}^{\text{“clever zero”}} \\ &\qquad +(\nabla\times(\psi N))\cdot[(\nabla\psi)\times N]. \end{aligned} \tag{2.13}$$

Another useful identity is

$$\begin{aligned} &-\frac{1}{\psi}(\nabla\times(\psi N))\cdot(\nabla\times(\psi^2 N)-(\nabla\times A)\cdot(\nabla\times(\psi N)) = \\ &= -\frac{1}{\psi}(\nabla\times(A+\psi N))\cdot(\nabla\times(\psi^2 N))+(\nabla\times A)\cdot((\nabla\psi)\times N). \end{aligned} \tag{2.14}$$

Combining the preceding identities one can obtain this identity

$$-\frac{1}{\psi}\left(\nabla\times(\psi^2 N)\right)\cdot((\nabla\psi)\times N)+(\nabla\times(\psi N))\cdot((\nabla\psi)\times N) = -\left|(\nabla\psi)\times N\right|^2. \tag{2.15}$$

Then, after tedious operations we arrive at the resulting action from Maxwell fields (to the order $O(v^2)$). Using the Taylor expansion we have $1/\sqrt{1+N^2} \doteq 1 - \frac{1}{2}N^2$. The only contribution containing N^2 from expansion of denominator originates in $(\nabla\psi)^2$, which is the only term $\mathcal{O}(v^0)$, the rest is neglected as $\vec{N}^2 \cdot \mathcal{O}(v) = \mathcal{O}(v^3)$.
We can integrate by parts one of the ongoing expressions, the first term on the RHS vanishes due to the asymptotical flatness

$$\frac{1}{4\pi}\dot{\vec{A}}\cdot(\nabla\psi) = \cancelto{0}{\frac{\left(\vec{A}\cdot(\nabla\psi)\right)^{\cdot}}{4\pi}} - \frac{1}{4\pi}\vec{A}\cdot(\nabla\dot{\psi}) \tag{2.16}$$

After quite a lot of manipulations we arrive at

$$\begin{aligned} S_{\mathrm{EM}} = \int \mathrm{d}t\ \mathrm{d}^3x\ \Bigg(& -\frac{1}{8\pi}\frac{\left|\vec{A}+\psi\vec{N}\right|^2}{\psi^2} + \frac{1}{4\pi}\frac{[\nabla\times(\vec{A}+\psi\vec{N})]\cdot[\nabla\times(\psi^2\vec{N})]}{\psi^3} \\ & -\frac{3}{32\pi}\frac{\left|\nabla\times(\psi^2\vec{N})\right|^2}{\psi^4} - \frac{1}{4\pi}\vec{A}\cdot(\nabla\dot{\psi}) \\ & +\frac{1}{32\pi}|\nabla\times\vec{N}|^2 - \frac{1}{16\pi}\frac{[\nabla\times\psi^2\vec{N}].[\nabla\times\vec{N}]}{\psi^2} \\ & +\frac{1}{8\pi}\frac{(\nabla\psi)^2}{\psi^2}\left(1-\frac{1}{2}\vec{N}\cdot\vec{N}\right)\Bigg). \end{aligned} \tag{2.17}$$

From now on, the terms highlighted in "blue" match exactly with the terms in [5]. The remaining terms are expected to cancel with other parts of action or be vanishing hidden Gauss-divergences.

Action from current

We begin with

$$S_{\mathrm{current}} = \int \mathrm{d}t\ \mathrm{d}^3x\ \sqrt{-g}\rho A_\mu U^\mu, \tag{2.18}$$

where we have the four-velocity $u^\mu = \frac{\mathrm{d}t}{\mathrm{d}\tau}(1, v^i) \equiv \gamma(1, v^i)$ and normalization for time-like object $g_{\mu\nu}u^\mu u^\nu = -1$. Now we have

$$-1 = \gamma^2\left(-\frac{1}{\psi^2} + \psi^2 v^2 + 2\vec{N}\cdot\vec{v}\right)$$

and hence

$$\gamma \doteq \psi + \frac{\psi^3}{2}(\psi^2 v^2 + 2\vec{N}\cdot\vec{v}).$$

Then we use Taylor expansion to the leading order $\sqrt{1+\vec{N}\cdot\vec{N}} \doteq 1 + \frac{1}{2}\vec{N}\cdot\vec{N}$.

$$\begin{aligned} S_{\mathrm{current}} &= \int \mathrm{d}t\ \mathrm{d}^3x\sqrt{-g}A_\mu\rho\frac{\mathrm{d}x^\mu}{\mathrm{d}\tau} = \\ &= \int \mathrm{d}t\ \mathrm{d}^3x\ \rho\psi^2\left(\psi + \frac{\psi^3}{2}(\psi^2v^2 + 2\vec{N}\cdot\vec{v})\right)\left(1+\frac{1}{2}N^2\right)\left(-1+\frac{1}{\psi}+\vec{A}\cdot\vec{v}\right) \\ &= \int \mathrm{d}t\ \mathrm{d}^3x\ \left(\rho\psi^2 - \rho\psi^3 + \vec{A}\cdot\vec{v}\rho\psi^3 + \frac{1}{2}\rho\psi^2\left[\left(\vec{N}+\vec{v}\psi^2\right)\right]^2(1-\psi)\right). \end{aligned} \tag{2.19}$$

Action from matter

$$S_{\text{matter}} = \int \mathrm{d}t\ \mathrm{d}^3x\ \left(-\rho\psi^2 - \frac{1}{2}\rho\psi^2\vec{N}^2\right) \tag{2.20}$$

Einstein gravitational action

Einstein (or Einstein-Hilbert) action reads

$$\begin{aligned}
S_{\text{grav}} = {} & \frac{1}{16\pi}\int \mathrm{d}t\ \mathrm{d}^3x\ \left(1+\frac{1}{2}\vec{N}\cdot\vec{N}\right)\times(-1)\Bigg(\\
& -\frac{2}{\psi}\left[3\,\ddot{\psi}\psi^4 + 6\,\dot{\psi}^2\psi^3 - \Delta\psi\right] \\
& + 2\left[3\psi\dot{\psi}\left(\nabla\cdot\vec{N}\right) + \psi\left(\dot{\vec{N}}\cdot\nabla\psi\right) + \psi^2\left(\nabla\cdot\dot{\vec{N}}\right) + 4\psi\left(\vec{N}\cdot\nabla\dot{\psi}\right) + 2\dot{\psi}\left(\vec{N}\cdot\nabla\psi\right)\right] \\
& + \frac{1}{2\psi^2}\Bigg[24\dot{\psi}^2\psi^4N^2 + 12\psi^5\left(\ddot{\psi}N^2 + \dot{\psi}\left(\vec{N}\cdot\dot{\vec{N}}\right)\right) \\
& + \psi^2\Big((\nabla\times\vec{N}).(\nabla\times\vec{N}) + \Delta(\vec{N}.\vec{N}) - 2\left(\Delta\vec{N}\right).\vec{N} - 4(\nabla\times(\nabla\times\vec{N})).\vec{N} \\
& - 2(\nabla\cdot\vec{N})^2\Big) - 4\psi\Bigg(\left(\vec{N}\cdot\nabla\psi\right)\left(\nabla\cdot\vec{N}\right) + \vec{N}\cdot(\nabla\nabla\psi)\cdot\vec{N}\Bigg) \\
& + 4\left(2\left(\vec{N}\cdot\nabla\psi\right)^2 + \left(\vec{N}\times\nabla\psi\right)^2 - 2N^2\left(\nabla\psi\right)^2\right)\Bigg]\Bigg).
\end{aligned} \tag{2.21}$$

$\sim v^4 \sim 0$

We drop the 4th line due to the order of approximation. In the first line we can use

$$\ddot{\psi}\psi^3 = (\dot{\psi}\psi^3\dot{)} - 3\psi^2\dot{\psi}^2. \tag{2.22}$$

By S_{grav_i} we denote the i-th line of Einstein action. The first line of Einstein action (combined with other actions) produces the right term matching with [5], highlighted again in "blue"

$$S_{\text{grav}_1} = \int \mathrm{d}t\ \mathrm{d}^3x\ \left[-\frac{3}{8\pi}\dot{\psi}^2\psi^2 - (1+\frac{1}{2}N^2)\frac{1}{8\pi}\frac{\Delta\psi}{\psi}\right]. \tag{2.23}$$

For the second line we use the following identity, where after integration LHS vanishes

$$\begin{aligned}
\nabla\cdot\left(\psi^2\vec{N}\right)\dot{} &= \psi^2\nabla\cdot\dot{\vec{N}} + \dot{\vec{N}}\cdot\nabla\psi^2 + (\psi^2\dot{)}\nabla\cdot\vec{N} + \vec{N}\cdot\nabla(\psi^2\dot{)} \\
&= \psi^2\nabla\cdot\dot{\vec{N}} + \left(\dot{\vec{N}}\cdot\nabla\psi\right)2\psi + 2\psi\dot{\psi}\nabla\cdot\vec{N} + 2\vec{N}\cdot\left(\psi\nabla\dot{\psi} + \dot{\psi}\nabla\psi\right)
\end{aligned} \tag{2.24}$$

and hence we arrive at

$$S_{\text{grav}_2} = \int \mathrm{d}t\ \mathrm{d}^3x\ \Big[-\frac{1}{8\pi}\psi\dot{\psi}\nabla\cdot\vec{N} - \frac{1}{4\pi}\psi\vec{N}\cdot\nabla\dot{\psi} + \frac{1}{8\pi}\psi\dot{\vec{N}}\cdot\nabla\psi\Big]. \tag{2.25}$$

Finally, we use that $\dot{\vec{N}} \cdot (\psi \nabla \psi) = \frac{1}{2} \dot{\vec{N}} \cdot \nabla \psi^2$ which after integration by parts with respect to the time gives only $-\frac{1}{2} \vec{N} \cdot \nabla (\dot{\psi^2})$. The "black" terms on RHS cancel and the only nonzero remainder is

$$S_{\text{grav}_2} = \int \mathrm{d}t \; \mathrm{d}^3x \left[-\frac{1}{4\pi} \psi \vec{N} \cdot \nabla \dot{\psi} \right]. \tag{2.26}$$

2.2.2 | Total approximate action

The total action was separated into several parts with respect to their origin, i.e., current, matter, electromagnetic and gravitational action.

$$S_{\text{total}} = S_{\text{current}} + S_{\text{matter}} + S_{\text{EM}} + S_{\text{grav}_1} + S_{\text{grav}_2} + S_{\text{grav}_{4,5}} \tag{2.27}$$

In what follows, we treat all of the terms in (2.28) as if under the sum to see explicit cancellations, being able to track down the origin of terms according to the LHS. The cancelling counterparts are crossed out in the same graphic manner.

$$\begin{aligned}
S_{\text{current}} &= \int \mathrm{d}t \; \mathrm{d}^3x \left(\cancel{\rho\psi^2} - \rho\psi^3 + \vec{A} \cdot \vec{v} \rho \psi^3 + \left[\cancel{\frac{1}{2} N^2 \rho \psi^2} + \psi \vec{N} \cdot \vec{v} \rho \psi^3 + \frac{1}{2} v^2 \psi^6 \rho \right] \right. \\
&\qquad \left. - \psi \left[\frac{1}{2} N^2 \rho \psi^2 + \psi \vec{N} \cdot \vec{v} \rho \psi^3 + \frac{1}{2} v^2 \psi^6 \rho \right] \right) \\
S_{\text{matter}} &= \int \mathrm{d}t \; \mathrm{d}^3x \left(-\cancel{\rho\psi^2} - \cancel{\frac{1}{2} \rho \psi^2 N^2} \right) \\
S_{\text{EM}} &= \int \mathrm{d}t \; \mathrm{d}^3x \left(-\frac{1}{8\pi} \frac{\left| \vec{A} + \psi \vec{N} \right|^2}{\psi^2} + \frac{1}{4\pi} \frac{[\nabla \times (\vec{A} + \psi \vec{N})] \cdot [\nabla \times (\psi^2 \vec{N})]}{\psi^3} \right. \\
&\qquad - \frac{3}{32\pi} \frac{\left| \nabla \times (\psi^2 \vec{N}) \right|^2}{\psi^4} - \frac{1}{4\pi} \vec{A} \cdot (\nabla \dot{\psi}) \\
&\qquad + \cancel{\frac{1}{32\pi} |\nabla \times \vec{N}|^2} - \frac{1}{16\pi} \frac{[\nabla \times \psi^2 \vec{N}] . [\nabla \times \vec{N}]}{\psi^2} \\
&\qquad \left. + \frac{1}{8\pi} \frac{(\nabla \psi)^2}{\psi^2} \left(\cancel{1} - \frac{1}{2} \vec{N} \cdot \vec{N} \right) \right) \\
S_{\text{grav}_1} &= \int \mathrm{d}t \; \mathrm{d}^3x \left[-\frac{3}{8\pi} \dot{\psi}^2 \psi^2 - (\cancel{1} + \frac{1}{2} \vec{N} \cdot \vec{N}) \frac{1}{8\pi} \frac{\Delta \psi}{\psi} \right] \\
S_{\text{grav}_2} &= \int \mathrm{d}t \; \mathrm{d}^3x \left[-\frac{1}{4\pi} \psi \vec{N} \cdot \nabla \dot{\psi} \right] \\
S_{\text{grav}_{4,5}} &= \int \mathrm{d}t \; \mathrm{d}^3x \left[-\frac{1}{32\pi} \left(\cancel{(\nabla \times \vec{N}) . (\nabla \times \vec{N})} + \cancel{\Delta (\vec{N} . \vec{N})} - 2 \left(\Delta \vec{N} \right) . \vec{N} \right. \right. \\
&\qquad \left. - 4 (\nabla \times (\nabla \times \vec{N})) . \vec{N} - 2 (\nabla \cdot \vec{N})^2 \right) \\
&\qquad + \frac{1}{8\pi} \frac{1}{\psi} \left(\left(\vec{N} \cdot \nabla \psi \right) \left(\nabla \cdot \vec{N} \right) + \vec{N} \cdot (\nabla \nabla \psi) \cdot \vec{N} \right) \\
&\qquad \left. + \frac{1}{8\pi} \frac{1}{\psi^2} \left(\vec{N} \times \nabla \psi \right)^2 \right]
\end{aligned} \tag{2.28}$$

The "violet" 1 and -1 from S_{EM} and S_{grav_1} cancelled, since

$$\frac{\Delta\psi}{\psi} = \nabla\cdot\frac{\nabla\psi}{\psi} - \nabla\psi\frac{-1}{\psi^2}\nabla\psi = \nabla\cdot\frac{\nabla\psi}{\psi} + \frac{(\nabla\psi)^2}{\psi^2}, \tag{2.29}$$

where after integration the divergence vanishes.
The "red" crossed term $\Delta(\vec{N}\cdot\vec{N})$ vanishes after the integration, since

$$\Delta f = \nabla^2 f = \nabla\cdot(\nabla f),$$

following the preceding argument. Note the structure of the terms, namely in Einstein action there appears in each term twice ∇, twice $\vec{N}$ and ψ with the same exponent in both numerator and denominator. One could also use

$\nabla\times(\nabla\times\vec{N}) = \nabla(\nabla\cdot\vec{N}) - \Delta\vec{N}$ in $S_{\mathrm{grav}_{4,5}}$.

To summarize this, the action can be written as a sum of the "blue" part which is the right one to be derived [5] and the remaining terms.

$$\begin{aligned} S_{\mathrm{approx}} = \int \mathrm{d}^4x \Bigg(& -\frac{3}{8\pi}\dot{\psi}^2\psi^2 - \rho\psi^3 + \frac{\rho v^2\psi^6}{2} + (\vec{A}+\psi\vec{N})\cdot\left(\rho\psi^3 - \frac{(\nabla\psi)^{\cdot}}{4\pi}\right) \\ & + \frac{1}{8\pi}\frac{\left|\vec{A}+\psi\vec{N}\right|^2}{\psi^2} + \frac{1}{4\pi}\frac{[\nabla\times(\vec{A}+\psi\vec{N})]\cdot[\nabla\times(\psi^2\vec{N})]}{\psi^3} \\ & - \frac{3}{32\pi}\frac{\left|\nabla\times(\psi^2\vec{N})\right|^2}{\psi^4}\Bigg) + S_{\mathrm{rest}} \end{aligned} \tag{2.30}$$

The remainder reads

$$\begin{aligned} S_{\mathrm{rest}} = & -\psi\left[\frac{1}{2}N^2\rho\psi^2 + \psi\vec{N}\cdot\vec{v}\rho\psi^3 + \frac{1}{2}v^2\psi^6\rho\right] \\ & - \frac{1}{16\pi}\frac{[\nabla\times(\psi^2\vec{N})].[\nabla\times\vec{N}]}{\psi^2} \\ & - \frac{1}{16\pi}\left(\vec{N}\cdot\vec{N}\right)\frac{(\nabla\psi)^2}{\psi^2} - \frac{1}{16\pi}\left(\vec{N}\cdot\vec{N}\right)\frac{\Delta\psi}{\psi} \\ & - \frac{1}{32\pi}\Big(-2\left(\Delta\vec{N}\right).\vec{N} - 4(\nabla\times(\nabla\times\vec{c})).\vec{N} - 2(\nabla\cdot\vec{N})^2\Big) \\ & + \frac{1}{8\pi}\frac{1}{\psi}\left(\left(\vec{N}\cdot\nabla\psi\right)\left(\nabla\cdot\vec{N}\right) + \vec{N}\cdot(\nabla\nabla\psi)\cdot\vec{N}\right) \\ & + \frac{1}{8\pi}\frac{1}{\psi^2}\left(\vec{N}\times\nabla\psi\right)^2. \end{aligned} \tag{2.31}$$

In accordance with [5], we expect these terms to cancel and vanish.

2.2.3 | Variation of action

The approximate action is to be varied with respect to fields $\vec{N}$ and $\vec{A}$ (first order quantities) to obtain equations for the metric. The mass distribution ρ doesn't vary freely, it is rather regulated to provide us with the matter conservation during other variations. The field perturbations are fully determined in terms of the perturbations of matter $\rho\psi^3, \vec{v}$ by constraint equations to the order of $\mathcal{O}(v^2)$ in perturbed Einstein-Maxwell equations. We shall use the following linear combinations

$$\begin{aligned} \vec{P} &= \vec{A} + \psi\vec{N} \\ \vec{Q} &= \psi^2\vec{N} \end{aligned} \tag{2.32}$$

using which the first order field equations take the form [4]

$$\begin{aligned} \nabla \times \left(\frac{\nabla \times \vec{P}}{\psi^2} - \frac{\nabla \times \vec{Q}}{\psi^3} \right) &= \nabla \times \left(\nabla \times \vec{K} \right) \\ \nabla \times \left(\frac{\nabla \times \vec{P}}{\psi^3} - \frac{3\nabla \times \vec{Q}}{4\psi^4} \right) &= 0. \end{aligned} \tag{2.33}$$

The vector operators operate on flat $\mathbb{R}^3$ with Cartesian-like coordinates, we denote

$$\vec{K} = -4\pi\nabla^{-2}(\rho\psi^3\vec{v}) \tag{2.34}$$

Rather symbolic meaning of ∇^{-2} should be clear during following manipulations, we will not need to perform the operation explicitly. Note, that equations (2.33) are linear combinations of the first order approximations of Ampere's law and super-momentum constraint, which are now our initial value equations

$$F^{\iota j}{}_{;\iota} = 4\pi J^j$$

$$G^{0i} = 8\pi T^{0i}.$$

On the other hand, Gauss's law and the zeroth-order Hamiltonian constraint

$$F^{i0}{}_{;i} = 4\pi J^0$$

$$G^{00} = 8\pi T^{00}$$

are satisfied (to the order we need) by $\phi = \frac{1}{\psi}$ and the Majumdar-Papapetrou spacetime $\mathrm{d}s^2 = -\psi^{-2}\mathrm{d}t^2 + \psi^2\mathrm{d}\vec{x}\cdot\mathrm{d}\vec{x}$.

The solution to (2.33) in its full generality is [4]

$$\begin{aligned} \nabla \times \vec{P} &= -3\psi^2\nabla \times \vec{K} - 2\nabla\chi - 3\psi^2\nabla\xi \\ \nabla \times \vec{Q} &= -4\psi^3\nabla \times \vec{K} - 4\psi\nabla\chi + 4\chi\nabla\psi - 4\psi^3\nabla\xi, \end{aligned} \tag{2.35}$$

where the "integration constants" ξ, χ can be determined taking the divergence, $\nabla\cdot$ (2.35). However, in the black hole limit contribution of these scalar functions to the effective action vanishes. We still need to solve equations for $\vec{P}$ and $\vec{Q}$. The charge conservation equation is

$$\nabla \cdot (\rho\psi^3\vec{v}) + \partial_t(\rho\psi^3) = 0. \tag{2.36}$$

We also have the Laplace equation

$$\Delta\psi = -4\pi\rho\psi^3. \tag{2.37}$$

We take the time derivative of (2.37), then we substitute from the charge conservation (2.36) and finally substitute in the definition of $\vec{K}$

$$\dot{\psi} = -4\pi\partial_t\nabla^{-2}(\rho\psi^3) = 4\pi\nabla^{-2}(\nabla\cdot(\rho\psi^2\vec{v})) = -\nabla\cdot\vec{K}. \tag{2.38}$$

Using this we can adjust the right hand side of the first equation of (2.33)

$$\nabla\times\left(\nabla\times\vec{K}\right) = \nabla(\nabla\cdot\vec{K}) - \Delta\vec{K} = 4\pi\nabla\left(\partial_t\nabla^{-2}(\rho\psi^3)\right) + 4\pi\Delta\left(\nabla^{-2}(\rho\psi^2\vec{v})\right)$$

and obtain[2]

$$\nabla\times\left(\nabla\times\vec{K}\right) = -\nabla\dot{\psi} + 4\pi\rho\psi^3\vec{v}. \tag{2.39}$$

In the black hole limit we have

$$\rho\psi^3 \to \sum_a m_a\delta^{(3)}(\vec{x}-\vec{x}_a)$$

and we are looking for Green's function of Laplace operator. From (1.43) we obtain the black hole limit of $\vec{K}$, where a labels the black hole, $r_a = |\vec{x}-\vec{x}_a|$ and $\vec{v}_a = \frac{\mathrm{d}\vec{x}_a}{\mathrm{d}t}$

$$\vec{K} = \sum_a \frac{m_a}{r_a}\vec{v}_a. \tag{2.40}$$

[2]In [4] one curl in equation (2.39) is missing.

3. Geodesics

One of the main goals of this thesis is to study the motion of test particles on the background of two maximally charged black holes stationary orbiting on a common circular orbit as per solution in [5]. Orbiting distance is determined by their masses [19]. Existence of such solution is a salient feature of general relativity framework, we comment on this below.

In the preceding chapters we introduced equations to solve (2.35), obtained by varying the approximate action.

In this chapter we solve them, obtain the metric and proceed with geodesic equation. We thereby investigate the geodesic motion of test particles with different charge-to-mass ratio κ. As we shall see, such motions depend crucially on the value of κ. Charged test particles are affected by both electro-magnetic force and gravitational interaction, while the uncharged test particles are affected by the latter only. We concentrate ourselves on maximally charged test particles, we aim to compare their motion with motion of the third black hole. Three black hole system will be studied in the next chapter.

Two orbiting black holes

One may naturally wonder about the existence of solution containing two extremal black holes on a common circular path. In Newtonian situation the forces of extremally charged bodies exerted on each other cancel exactly $\vec{F}_e = -\vec{F}_g$, in motion all of them act as free bodies. Turning into general relativity we have to take into account various effects, such as relativistic mass $m_{\text{rel}} = \gamma m_0$, spacetime curvature or gravitational waves.

Existence of mutually orbiting binary system of two equally massive extremally charged holes was already shown in [4, 5]. We generalized this for an arbitrary ratio of their masses in [19], the boundary allowed values of orbiting radius in center of mass system are $r_{\text{circ}(m_1=m_2)} = \frac{\sqrt{3}-1}{2} \approx 0.366$ and $r_{\text{circ}(m_1 \gg m_2)} = \frac{1}{2}$.

It may seem counterintuitive, why the extremally charged black holes can mutually orbit. Even just the argument based on special relativistic observations, namely mass increasing with velocity, provides us with an answer. Later we will calculate the Lorentz-like γ-factor explicitly. The gravitational interaction is therefore a bit stronger than electrostatic repulsion (magnitude of which remains unchanged throughout the evolution).

3.1 | Lagrangian density

We shall make use of Lagrange formalism of mechanics. The dynamics of the gravito-electro-magnetic system is managed by the appropriate Lagrangian density $\mathcal{L}$, scalar function of particle's coordinate and velocity. There are several

equivalent[1] definitions of Lagrangian density, we shall choose the following one

$$\mathcal{L} = \frac{1}{2} g_{\mu\nu} \dot{x}^\mu \dot{x}^\nu + \kappa \dot{x}^\mu A_\mu. \tag{3.1}$$

The charge-to-mass ratio of test particle $\kappa \in \{-1, 0, 1\}$ describes a particle of opposite-sign extremal charge, no charge and same-sign extremal charge respectively. Correspondence means with respect to the sign of charge of orbiting system. The choice of κ has far-reaching consequences already in the leading order, i.e. electrostatic approximation.

Let us find out an explicit form of $g_{\mu\nu}$.

3.1.1 | Metric as a solution of Poisson equation

Let us begin with finding the perturbed metric. Our framework is 3+1 splitting of spacetime. The field equations we want to obtain will be the initial value equations for tensorial quantities $\vec{N}$, $\vec{A}$ on the initial 3-dim spacelike ($t = const.$) hypersurface. One can vary the approximate action (2.30) with respect to the fields $\vec{N}$ and $\vec{A}$ and obtain equations (2.33). These are solved by (3.2), we are halfway through the way to our metric.

$$\begin{aligned} \nabla \times \vec{P} &= -3\psi^2 \nabla \times \vec{K} \\ \nabla \times \vec{Q} &= -4\psi^3 \nabla \times \vec{K} \end{aligned} \tag{3.2}$$

As said before, the scalar functions, integration "constants", do not contribute into effective action after performing the black hole limit, hence we dropped them. Once we solve (3.2), the metric and four-current functions $\vec{N}$, $\vec{A}$ can be easily obtained from $\vec{P}$, $\vec{Q}$ by solving almost trivial algebraic equations (2.32). Schematically written procedure is as follows

$$S_{\text{approx}} \;\rightarrow\; \vec{P}, \vec{Q} \;\xrightarrow{\vec{K}}\; \vec{A}, \vec{N} \;\rightarrow\; g_{\mu\nu}.$$

Solving equations

Each vector field can be written as a sum of divergence-free and curl-free part

$$\vec{V} = \nabla \times \vec{\alpha} + \vec{\beta},$$

moreover, fixing the gauge

$$\nabla \cdot \vec{\alpha} = 0$$

allows the Poisson equation for α

$$\Delta \vec{\alpha} = \vec{f},$$

which we can solve by method of Green's function of Poisson's equation. We write our fields $\vec{P}$, $\vec{Q}$ in this way and substitute into (3.2). Then, after substituting (2.40), that is

$$\vec{K} = \sum_a \frac{m_a}{r_a} \vec{v}_a,$$

[1] They yield the same equations of motion.

into our system of equations (3.2) we obtain rather general solution

$$\begin{aligned}\vec{P}(\vec{x}) &= \frac{3}{4\pi}\int \frac{\psi^2(\vec{r'})}{|\vec{x}-\vec{r'}|^3}\left(\vec{x}-\vec{r'}\right)\times\left(\nabla'\times\vec{K}(\vec{r'})\right)\mathrm{d}V' \\ \vec{Q}(\vec{x}) &= \frac{1}{\pi}\int \frac{\psi^3(\vec{r'})}{|\vec{x}-\vec{r'}|^3}\left(\vec{x}-\vec{r'}\right)\times\left(\nabla'\times\vec{K}(\vec{r'})\right)\mathrm{d}V'.\end{aligned} \tag{3.3}$$

Given the positions of black holes, what are these fields? Let us use

$$\nabla'\times\vec{K}(\vec{r'}) = \sum_{a=1}^{2} m_a\vec{v}_a\times\frac{\vec{r'}-\vec{x}_a}{|\vec{r'}-\vec{x}_a|^3} \tag{3.4}$$

and apply the well known vector identity

$$\vec{a}\times(\vec{b}\times\vec{c}) = \vec{b}(\vec{a}\cdot\vec{c}) - \vec{c}(\vec{a}\cdot\vec{b}).$$

Finally we arrive at the explicit form of $\vec{P}$ and $\vec{Q}$, which holds generally for any perturbation, provided the slow-motion limit.

$$\begin{aligned}\vec{P}(\vec{x}) = \frac{3}{4\pi}\sum_{a=1}^{2} m_a\Bigg[&\vec{v}_a\int\psi^2(\vec{r'})\frac{\left(\vec{x}-\vec{r'}\right)\cdot\left(\vec{r'}-\vec{x}_a\right)}{|\vec{x}-\vec{r'}|^3|\vec{r'}-\vec{x}_a|^3}\mathrm{d}V' \\ &-\int\psi^2(\vec{r'})\left(\vec{v}_a\cdot\frac{\left(\vec{x}-\vec{r'}\right)}{|\vec{x}-\vec{r'}|^3}\right)\frac{\left(\vec{r'}-\vec{x}_a\right)}{|\vec{r'}-\vec{x}_a|^3}\mathrm{d}V'\Bigg]\end{aligned} \tag{3.5}$$

$$\begin{aligned}\vec{Q}(\vec{x}) = \frac{1}{\pi}\sum_{a=1}^{2} m_a\Bigg[&\vec{v}_a\int\psi^3(\vec{r'})\frac{\left(\vec{x}-\vec{r'}\right)\cdot\left(\vec{r'}-\vec{x}_a\right)}{|\vec{x}-\vec{r'}|^3|\vec{r'}-\vec{x}_a|^3}\mathrm{d}V' \\ &-\int\psi^3(\vec{r'})\left(\vec{v}_a\cdot\frac{\left(\vec{x}-\vec{r'}\right)}{|\vec{x}-\vec{r'}|^3}\right)\frac{\left(\vec{r'}-\vec{x}_a\right)}{|\vec{r'}-\vec{x}_a|^3}\mathrm{d}V'\Bigg]\end{aligned} \tag{3.6}$$

3.1.2 | Fate of the perturbation

We have gone through somewhat tedious procedure up to now to obtain an explicit integral expression for $\vec{P}$, $\vec{Q}$. Equations (3.5) and (3.6) provide us with a fully general prescription for perturbation, restricted to low velocities only. No limitation on position of particle has been done till now. Let us now move on to its particular form for the field of an extremally charged binary stationary orbiting on circular path, i.e. substitute for the known $\vec{x}_1, \vec{x}_2$.

The second line of $\vec{Q}$ vanishes...

Let us begin with the function $\vec{Q}$, since it contains all of the terms in $\vec{P}$. Once we have $\vec{Q}$ we get result for $\vec{P}$ for free. We start with the 2nd line of $\vec{Q}$ in (3.6),

which looks easier to calculate and also could provide a tool to evaluate the 1st line. The 2nd line reads

$$\vec{Q}_{\text{line 2}}(\vec{x}) = \frac{1}{\pi}\sum_{a=1}^{2} m_a \left[-\int \psi^3(\vec{r'}) \left(\vec{v}_a \cdot \frac{\left(\vec{x}-\vec{r'}\right)}{|\vec{x}-\vec{r'}|^3} \right) \frac{\left(\vec{r'}-\vec{x}_a\right)}{|\vec{r'}-\vec{x}_a|^3} \mathrm{d}V' \right]. \tag{3.7}$$

At first, let us split the integration region into regions Γ and Λ (and also Ω which contributes negligibly). A very detailed description of this procedure can be found in Chapter 4.3. Figure 4.3 provides a brief sketch of our approach. The main point now is that we arrived at a couple of integrals that do not always allow us to solve them analytically. The remedy for this issue is separation of the integration domain and the individual integrals can be solved analytically (although we will use approximation).

From now on, integral with separated integral domains we will denote by bar $\bar{\vec{Q}}$ and with corresponding subscript (Γ or Λ). Let us first have a look at the vicinity of the origin, the region Γ.

$$\bar{\vec{Q}}_{\text{line 2 }\Gamma} = -\frac{1}{\pi}\sum_{a=1}^{2} m_a \int \left(1 + \frac{m_1}{|\vec{r'}-\vec{x}_1|} + \frac{m_2}{|\vec{r'}-\vec{x}_2|}\right)^3 \left(\vec{v}_a \cdot \frac{\vec{x}}{x^3}\right) \frac{\vec{r'}-\vec{x}_a}{|\vec{r'}-\vec{x}_a|^3} \mathrm{d}^3 r' \tag{3.8}$$

We denote

$$\psi\left(\vec{r'}, \vec{x}_1, \vec{x}_2\right) = \left(1 + \frac{m}{|\vec{r'}-\vec{x}_1|} + \frac{m}{|\vec{r'}-\vec{x}_2|}\right).$$

Now let us write out the sum and use

$$m_1 = m_2 \equiv m. \tag{3.9}$$

$$\begin{aligned} \bar{\vec{Q}}_{\text{line 2 }\Gamma} = -\frac{m}{\pi} \int \psi(\vec{r'}, \vec{x}_1, \vec{x}_2)^3 \Bigg[& \left(\vec{v}_1 \cdot \frac{\vec{x}}{x^3}\right) \frac{\vec{r'}-\vec{x}_1}{|\vec{r'}-\vec{x}_1|^3} \\ & + \left(\vec{v}_2 \cdot \frac{\vec{x}}{x^3}\right) \frac{\vec{r'}-\vec{x}_2}{|\vec{r'}-\vec{x}_2|^3} \Bigg] \mathrm{d}^3 r' \end{aligned} \tag{3.10}$$

Subsequently, imposing the physical setting-conditions considering the two hole system is spinning around the origin

$$\vec{x}_2 = -\vec{x}_1, \qquad \vec{v}_2 = -\vec{v}_1. \tag{3.11}$$

our function reads

$$\bar{\vec{Q}}_{\text{line 2 }\Gamma} = -\frac{m}{\pi}\left(\vec{v}_1 \cdot \frac{\vec{x}}{x^3}\right) \int \psi\left(\vec{r'}, \vec{x}_1, -\vec{x}_1\right)^3 \left[\frac{\vec{r'}-\vec{x}_1}{|\vec{r'}-\vec{x}_1|^3} - \frac{\vec{r'}+\vec{x}_1}{|\vec{r'}+\vec{x}_1|^3} \right] \mathrm{d}^3 r'. \tag{3.12}$$

The two terms under the bracket look perhaps similar, hence one wonders whether they could cancel. Let us transform the integration variable in the integral associated with the term in bracket $\frac{\vec{r'}-\vec{x}_1}{|\vec{r'}-\vec{x}_1|^3}$ in (3.12)

$$\vec{r'} \to -\vec{r'}$$

and keep the original variable in the integral associated with $-\frac{\vec{r}'+\vec{x}_1}{|\vec{r}'+\vec{x}_1|^3}$. Notice, that $\psi(\vec{r}', \vec{x}_1, -\vec{x}_1)$ does not change under such transformation. Accordingly, the sum becomes

$$\begin{aligned}\vec{\bar{Q}}_{\text{line 2 }\Gamma} = &-\frac{m}{\pi}\left(\vec{v}_1 \cdot \frac{\vec{x}}{x^3}\right) \times \\ &\times \left[\int \left(1 + \frac{m}{|-\vec{r}'-\vec{x}_1|} + \frac{m}{|-\vec{r}'+\vec{x}_1|}\right)^3 \frac{-\vec{r}'-\vec{x}_1}{|-\vec{r}'-\vec{x}_1|^3}(-\mathrm{d}^3 r') \right. \\ &\left. - \int \left(1 + \frac{m}{|\vec{r}'-\vec{x}_1|} + \frac{m}{|\vec{r}'+\vec{x}_1|}\right)^3 \frac{\vec{r}'+\vec{x}_1}{|\vec{r}'+\vec{x}_1|^3}\mathrm{d}^3 r'\right]\end{aligned} \tag{3.13}$$

This altogether means, that

$$\vec{\bar{Q}}_{\text{line 2 }\Gamma} = 0. \tag{3.14}$$

Within Λ we have a slightly different approximation.

$$\vec{\bar{Q}}_{\text{line 2 }\Lambda} = -\frac{1}{\pi}\sum_{a=1}^{2} m_a \int \left(1 + \frac{m_1}{|\vec{r}'|} + \frac{m_2}{|\vec{r}'|}\right)^3 \left(\vec{v}_a \cdot \frac{\vec{x}-\vec{r}'}{|\vec{x}-\vec{r}'|^3}\frac{\vec{r}'}{|\vec{r}'|^3}\right)\mathrm{d}^3 r' \tag{3.15}$$

We put $m_1 = m_2 \equiv m$ again and write the sum out.

$$\vec{\bar{Q}}_{\text{line 2 }\Lambda} = -\frac{1}{\pi} m \int \frac{\vec{r}'}{|\vec{r}'|^3}\left(1 + \frac{2m}{|\vec{r}'|}\right)^3 \left[(\vec{v}_1 + \vec{v}_2) \cdot \frac{\vec{x}-\vec{r}'}{|\vec{x}-\vec{r}'|^3}\right]\mathrm{d}^3 r' \tag{3.16}$$

After we substitute our motion (3.11), i.e., $\vec{v}_2 = -\vec{v}_1$ into the last formula, it is obviously zero

$$\vec{\bar{Q}}_{\text{line 2 }\Lambda} = 0. \tag{3.17}$$

The first line of $\vec{Q}$ vanishes, too.

Looking closer at the first line, using the above trick with $\vec{r} \to -\vec{r}$ we can follow the procedure of the second line. We further omit the argument of ψ, the meaning should be clear.

$$\begin{aligned}\vec{\bar{Q}}_{\text{line 1 }\Gamma} &= \frac{m}{\pi}\sum_{a=1}^{2}\vec{v}_a \int \psi^3 \frac{\vec{x}}{x^3}\cdot\frac{\vec{r}'-\vec{x}_a}{|\vec{r}'-\vec{x}_a|^3}\mathrm{d}^3 r' \\ &= \frac{m}{\pi}\vec{v}_1\left[\int \psi^3 \frac{\vec{x}}{x^3}\cdot\frac{\vec{r}'-\vec{x}_1}{|\vec{r}'-\vec{x}_1|^3}\mathrm{d}^3 r' - \int \psi^3 \frac{\vec{x}}{x^3}\cdot\frac{\vec{r}'+\vec{x}_1}{|\vec{r}'+\vec{x}_1|^3}\mathrm{d}^3 r'\right] \\ &= \frac{m}{\pi}\vec{v}_1\left[-\int \psi^3 \frac{\vec{x}}{x^3}\cdot\frac{-\vec{r}'-\vec{x}_1}{|-\vec{r}'-\vec{x}_1|^3}\mathrm{d}^3 r' - \int \psi^3 \frac{\vec{x}}{x^3}\cdot\frac{\vec{r}'+\vec{x}_1}{|\vec{r}'+\vec{x}_1|^3}\mathrm{d}^3 r'\right] \\ \vec{\bar{Q}}_{\text{line 1 }\Gamma} &= 0\end{aligned} \tag{3.18}$$

In the region Γ the entire perturbation vanishes.

Finally, the region Λ. (Maybe a sign of repetitive pattern can be noted...)

$$\begin{aligned}\vec{\bar{Q}}_{\text{line 1 }\Lambda} &= \frac{m}{\pi}\sum_{a=1}^{2}\vec{v}_a\int\psi^3\frac{\vec{x}-\vec{r}'}{|\vec{x}-\vec{r}'|^3}\cdot\frac{\vec{r}'-\vec{x}_a}{|\vec{r}'-\vec{x}_a|^3}\mathrm{d}^3r' \\ &= \frac{m}{\pi}\vec{v}_1\left(\int\psi^3\frac{\vec{x}-\vec{r}'}{|\vec{x}-\vec{r}'|^3}\cdot\frac{\vec{r}'}{|\vec{r}'|^3}\mathrm{d}^3r' - \int\psi^3\frac{\vec{x}-\vec{r}'}{|\vec{x}-\vec{r}'|^3}\cdot\frac{\vec{r}'}{|\vec{r}'|^3}\mathrm{d}^3r'\right) \qquad (3.19)\\ \vec{\bar{Q}}_{\text{line 1 }\Lambda} &= 0\end{aligned}$$

We have determined $\vec{Q}$ completely; this function vanishes identically

$$\vec{\bar{Q}} = 0.$$

All of the integrals contained in $\vec{Q}$ are contained in $\vec{P}$ as well. As stated before, we are done, because $\vec{P}$ differs from $\vec{Q}$ only in factor $\psi^3 \to \psi^2$, where ψ does not change under the transformations we carried out and the numerical prefactor $\frac{1}{\pi} \to \frac{3}{4\pi}$ does not affect any crucial point of our calculation. The terms involved in $\vec{\bar{P}}$ cancel in the same way as in case of $\vec{\bar{Q}}$. Finally we conclude

$$\vec{P} \doteq \vec{\bar{P}}(\vec{x}) = 0 = \vec{\bar{Q}}(\vec{x}) \doteq \vec{Q}.$$

substituting into (2.32) yields vanishing analytic perturbation of metric and four-potential

$$\vec{N} = 0 = \vec{A}. \qquad (3.20)$$

The only difference in perturbed metric we arrived at is that now $\psi(\vec{x}, \vec{x}_1(t), \vec{x}_2(t))$, the master function is a function of time and the functions $\vec{x}_1(t), \vec{x}_2(t)$ are given, since we have circular motion. The diagonal form of metric surprisingly remains.

3.1.3 | Step aside: ADM mass with motion

Does the ADM mass in perturbed space-time differ from the ADM mass calculated of the static solution for N black holes from Section 1.2.2 ADM mass (static)? Considering our black hole binary system with two extremal black holes on a mutual circular orbit, the preceding section revealed that perturbation identically vanishes. Consequently, the metric (3.22) remains, except the fact that all black hole positions, included in $\psi(\vec{x}, \vec{x}_1(t), \vec{x}_2(t))$, are now functions of time. Throughout the calculation of the ADM mass neither time derivatives nor time integration occurred and hence the ADM mass is the same for both perturbed and static binary system

$$M_{ADM} = \sum_{a=1}^{2} m_a. \qquad (3.21)$$

3.2 | Equation of geodesic

Once we found the perturbed metric we can proceed with solving equation of geodesic, that describes motion of test-particles on the background of two orbiting black holes. We can study the motion of an uncharged particle which we will call geodesic, or a charged one which will be dubbed as electrogeodesic for obvious reason.

The perturbation vanished and the only consequence in metric is the time dependence of positions of black holes $\vec{x}_1(t),\ \vec{x}_2(t)$. Our spacetime is

$$\begin{aligned} g_{\mu\nu} &= \mathrm{diag}(-\psi^{-2},\ \psi^2,\ \psi^2,\ \psi^2) \\ A &= \frac{1}{\psi}\mathrm{d}t, \end{aligned} \tag{3.22}$$

where the master function ψ is

$$\psi = \psi(\vec{x}, \vec{x}_1(t), \vec{x}_2(t)) = 1 + \frac{M}{|\vec{x} - \vec{x}_1(t)|} + \frac{M}{|\vec{x} - \vec{x}_2(t)|}. \tag{3.23}$$

During calculations we scale the problem such a way that $M = 1$. We chose the Lagrangian density following [10], it reads

$$\mathcal{L} = \frac{1}{2} g_{\mu\nu}\dot{x}^\mu \dot{x}^\nu + \kappa \dot{x}^\mu A_\mu. \tag{3.24}$$

Here κ is the charge-to-mass ratio of the studied test particle, x^μ is the position and $\dot{x}^\mu = \dfrac{\mathrm{d}x^\mu}{\mathrm{d}\tau}$ is its total derivative with respect to an affine parameter. Having a time-like particle we can identify the affine parameter τ with proper time of our particle and hence $\dot{x}^\mu$ becomes a four-velocity of the particle u^μ. For the time-like particle, i.e. moving slower than light, we have normalization

$$g_{\alpha\beta} u^\alpha u^\beta = -1. \tag{3.25}$$

The first term of (3.24) measures the invariant distance along a path, so our parametrisation with the proper time should lead to the simplest form of equations of motion.

By inserting our spacetime (3.22) into $\mathcal{L}$ (3.24) we obtain

$$\mathcal{L} = \frac{1}{2}\left(-\psi^{-2}\dot{t}^2 + \psi^2\left(\dot{x}^2 + \dot{y}^2 + \dot{z}^2\right)\right) + \kappa\dot{t}\frac{1}{\psi}. \tag{3.26}$$

Our equations of motion are the well known Euler-Lagrange equations of the second kind

$$\frac{\mathrm{d}}{\mathrm{d}\tau}\left(\frac{\partial\mathcal{L}}{\partial\dot{x}^\alpha}\right) = \frac{\partial\mathcal{L}}{\partial x^\alpha}. \tag{3.27}$$

Note, that equations (3.27) are equivalent to traditional form of electrogeodesic equation with the source on right hand side

$$\frac{\mathrm{D}u^\mu}{\mathrm{d}\tau} \equiv \frac{\mathrm{d}u^\mu}{\mathrm{d}\tau} + \Gamma^\mu_{\alpha\beta} u^\alpha u^\beta = \kappa F^\mu{}_\nu u^\nu. \tag{3.28}$$

Christoffel's symbols are defined in the traditional way. The source term in (3.28) corresponds to electromagnetic interaction [20]. This can be seen easily after a few somewhat simple algebraic manipulations with (3.27).

Let us stick to Lagrangian for now. Derivative with respect to affine parameter is denoted as $\dot{x}^\mu$. Taking the derivatives we obtain

$$\begin{aligned}\frac{\partial \mathcal{L}}{\partial \dot{x}^\alpha} &= g_{\alpha\beta}\dot{x}^\beta + \kappa A_\alpha = \left(-\frac{\dot{t}}{\psi^2} + \frac{\kappa}{\psi},\ \psi^2\dot{x},\ \psi^2\dot{y},\ \psi^2\dot{z}\right) \\ \frac{\mathrm{d}}{\mathrm{d}\tau}\frac{\partial \mathcal{L}}{\partial \dot{x}^\alpha} &= g_{\alpha\beta}\ddot{x}^\beta + g_{\alpha\beta,\gamma}\dot{x}^\beta\ \dot{x}^\gamma + \kappa A_{\alpha,\beta}\dot{x}^\beta\end{aligned} \tag{3.29}$$

$$\begin{aligned}\frac{\mathrm{d}}{\mathrm{d}\tau}\frac{\partial \mathcal{L}}{\partial \dot{x}^i} &= \psi^2\ddot{x}^i + 2\psi\dot{x}^i\left(\dot{x}^\alpha\psi_{,\alpha}\right) \\ \frac{\mathrm{d}}{\mathrm{d}\tau}\frac{\partial \mathcal{L}}{\partial \dot{t}} &= -\frac{1}{\psi^2}\ddot{t} + 2\frac{\dot{t}}{\psi^3}\left(\dot{x}^\alpha\psi_{,\alpha}\right) - \frac{\kappa}{\psi^2}\left(\dot{x}^\alpha\psi_{,\alpha}\right)\end{aligned} \tag{3.30}$$

$$\begin{aligned}\frac{\partial \mathcal{L}}{\partial x^\alpha} &= \frac{1}{2}g_{\mu\nu,\alpha}\dot{x}^\mu\dot{x}^\nu + \kappa\dot{x}^\mu A_{\mu,\alpha} \\ &= \frac{1}{2}\left(g_{00,\alpha}\dot{t}\dot{t} + g_{ij,\alpha}\dot{x}^i\dot{x}^j\right) + \kappa\dot{t}A_{0,\alpha} \\ &= \psi_{,\alpha}\left(\frac{1}{\psi^3}\dot{t}^2 + \psi\left(\dot{x}^2+\dot{y}^2+\dot{z}^2\right) - \kappa\dot{t}\frac{1}{\psi^2}\right).\end{aligned} \tag{3.31}$$

The derivatives of our master function read

$$\begin{aligned}\psi_{,i} &= -\frac{M\left(x_i - x_{1i}(t)\right)}{|\vec{x}-\vec{x}_1(t)|^3} - \frac{M\left(x_i - x_{2i}(t)\right)}{|\vec{x}-\vec{x}_2(t)|^3} \\ \psi_{,0} &= \frac{M\left(\vec{x}-\vec{x}_1(t)\right)\cdot\partial_t\vec{x}_1(t)}{|\vec{x}-\vec{x}_1(t)|^3} + \frac{M\left(\vec{x}-\vec{x}_2(t)\right)\cdot\partial_t\vec{x}_2(t)}{|\vec{x}-\vec{x}_2(t)|^3},\end{aligned} \tag{3.32}$$

where the derivative with respect to coordinate time is denoted by explicit partial derivative sign. Hence we obtain equations of motion with two independent structures, so to say time and spatial part.

$$\begin{aligned}\alpha = 0: \qquad & -\frac{1}{\psi^2}\ddot{t} + 2\frac{\dot{t}}{\psi^3}\left(\dot{x}^\alpha\psi_{,\alpha}\right) - \frac{\kappa}{\psi^2}\left(\dot{x}^\alpha\psi_{,\alpha}\right) \\ & = \psi_{,0}\left(\frac{1}{\psi^3}\dot{t}^2 + \psi\left(\dot{x}^2+\dot{y}^2+\dot{z}^2\right) - \kappa\dot{t}\frac{1}{\psi^2}\right)\end{aligned} \tag{3.33}$$

$$\begin{aligned}\alpha = i: \qquad & \psi^2\ddot{x}^i + 2\psi\dot{x}^i\left(\dot{x}^\alpha\psi_{,\alpha}\right) \\ & = \psi_{,i}\left(\frac{1}{\psi^3}\dot{t}^2 + \psi\left(\dot{x}^2+\dot{y}^2+\dot{z}^2\right) - \kappa\dot{t}\frac{1}{\psi^2}\right)\end{aligned} \tag{3.34}$$

3.2.1 | Static solution

First, let us choose a static solution $x^\mu = (t, x_0, y_0, z_0)$ with spatial coordinates independent of time. From geodesic equation we have the following equations.

Time component $\alpha = 0$

$$\alpha = 0 : \qquad -\frac{1}{\psi^2}\ddot{t} + \frac{2\dot{t}^2}{\psi^3}\psi_{,0} = \psi_{,0}\frac{\dot{t}^2}{\psi^3} \tag{3.35}$$

$$\ddot{t} - \frac{\dot{t}^2}{\psi}\psi_{,0} = 0 \tag{3.36}$$

$$\left[\ln \dot{t}\right]^{\cdot} = \left[\ln \psi\left(t(\tau)\right)\right]^{\cdot} \tag{3.37}$$

Integrating both sides with respect to τ, the result is

$$\dot{t} = C\ \psi(t(\tau)), \tag{3.38}$$

where $C = \ln C_0$ is the integration constant. We must have $\dot{t}^2 = \ddot{t}\psi/\psi_{,0} \geq 0$. Substituting $\psi_{,0} = 0$ we obtain simplified solution for unperturbed M-P binary, (3.36) then yields $\ddot{t} = 0$. This "static result" agrees with [6].

Spatial components $\alpha = i$

$$\alpha = i : \qquad 0 = \psi_{,i}\left(\frac{\dot{t}^2}{\psi^3} - \kappa\dot{t}\frac{1}{\psi^2}\right) \tag{3.39}$$

From definition provided $\psi_{,i} \neq 0$ we have

$$\dot{t} = \kappa\ \psi(t(\tau)) \tag{3.40}$$

The equations for $\alpha \in \{0, 1, 2, 3\}$ must be satisfied at the same time. Hence, comparing the preceding result (3.38) with (3.40) we obtain following condition for the integration constant

$$C = \kappa. \tag{3.41}$$

Solving the equation (3.40) we obtain the result in integral form

$$t = \kappa \int \psi(t(\tau))\mathrm{d}\tau. \tag{3.42}$$

In case of original static Majumdar-Papapetrou black-hole solution $\psi(\not{t}, x, y, z)$ this becomes $x^0 = t = \psi\tau$. The "static result" again agrees with [6].

We still long for a condition on κ. We expect one, since the set of extremal black holes should intuitively provide a static solution for an extremally charged particle only ($\kappa = 1$). For a particle with $\kappa \neq 1$ one would expect non-existence of such static solution, since the forces exerted on the particle would not cancel at all.

The only unused, however useful, equation is the normalisation (3.25). From $u_\mu u^\mu = -1$ one can see that for static solution with $u^i = u_i = 0$ we necessarily have

$$u^0 = \dot{t} = \psi(t(\tau)). \tag{3.43}$$

Comparing (3.43) to (3.40) fixes a value of κ, as we expected

$$\kappa = 1. \tag{3.44}$$

Interpreting the last equality, extremality is the necessary condition for a particle to be able to remain static in the field of two[2] extremal black holes in motion. Putting our results all together, our solution is thus following

$$x^\mu = \left(\int \psi \, \mathrm{d}\tau, x_0, y_0, z_0 \right). \tag{3.45}$$

We also studied geodesic equation from the other side, by which we mean $\dot{u}^\mu + \Gamma^\mu{}_{\alpha\beta} u^\alpha u^\beta = \kappa F^\mu{}_\alpha u^\alpha$. Result is that the Taylor expansion of $\ddot{x}^i$ as a function of time and evaluated at the initial moment is proportional to $(1 - \kappa)$ and hence all of the higher order terms such as acceleration vanish for extremal particle. For the detailed description, please, visit Appendix B: Taylor expansion of geodesic equation.

3.2.2 | Charged vs. uncharged particle

One would like to compare the motion of a charged particle and an uncharged particle. Charge is imprinted in electro-geodesic equations, determined by value of κ in (3.24). If the sign of charges (of black holes and particle) is the same, e.g., everything is positively extremally charged, we have charge-to-mass ratio $\kappa = 1$. Conversely, $\kappa = -1$ describes extremally charged test particle, charged oppositely than the system of black holes. Finally, $\kappa = 0$ describes a particle with no electric charge, only gravity acting upon it.

In a flat space the electrostatic potential for a particle placed at $\vec{r}_0$ is exactly $\phi(\vec{r}) = \frac{q}{|\vec{r} - \vec{r}_0|}$. Giving the charge a small velocity, that is $\vec{r}_0 = \vec{r}_0(t)$, then the scalar potential is approximately $\phi(\vec{r}) \approx \frac{q}{|\vec{r} - \vec{r}_0(t)|}$ and the vector potential is close to $\vec{A}(\vec{r}) \approx \frac{q\vec{v}_0}{|\vec{r} - \vec{r}_0(t)|}$ with $\vec{v}_0 = \frac{\mathrm{d}\vec{r}_0}{\mathrm{d}t}$. These are also approximate solutions to Maxwell equations. Hence, we expect the 0th order approximation (the leading order) to follow the laws of electrostatics. Dynamical corrections to the motion are of a higher order. In Figure 3.1 and Figure 3.3 we observe that electrostatics determines crucially the character of motion.

Also the time-scale of motion is affected by κ, although as a consequence of electrostatics. The particle with $\kappa = -1$, being pulled by approximately twice the gravitational force, travels about twice faster than that of no charge $\kappa = 0$, studied numerically in several cases. And hence the travelled distance of $\kappa = -1$ is around twice the distance of $\kappa = 0$, which follows our basic physical intuition. This can best be seen from Figure 3.1.

[2] Or more holes, in principle.

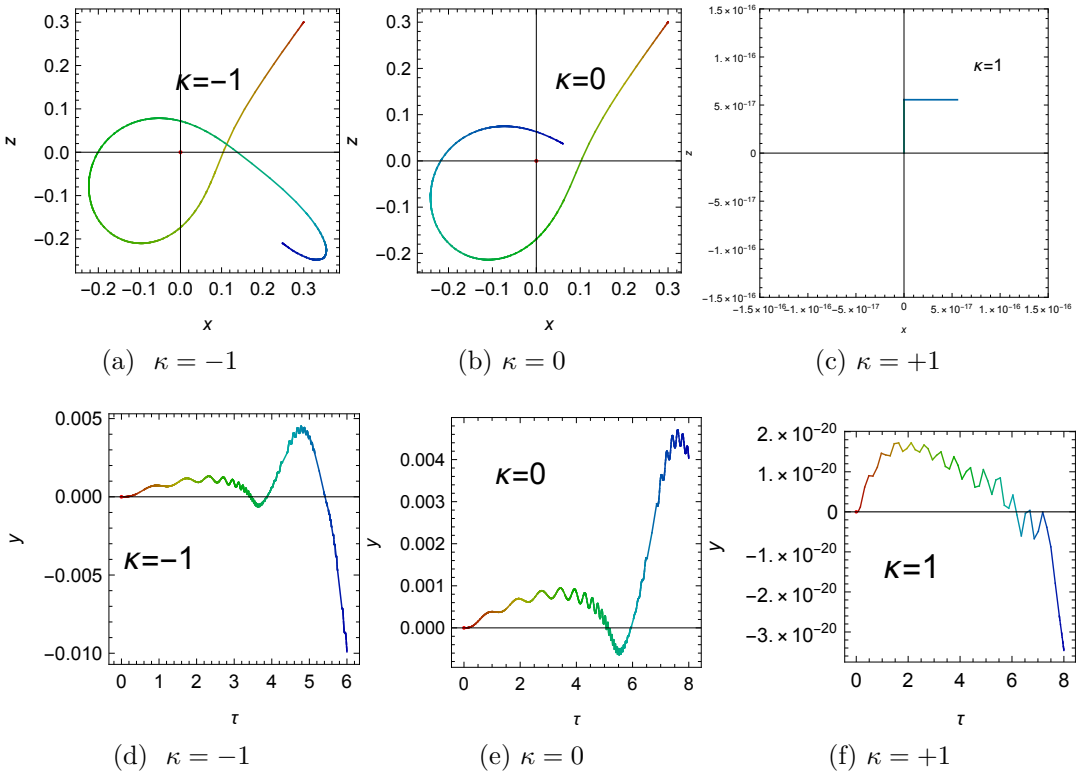

(a) $\kappa = -1$ (b) $\kappa = 0$ (c) $\kappa = +1$

(d) $\kappa = -1$ (e) $\kappa = 0$ (f) $\kappa = +1$

Figure 3.1: Comparing electrostatics. Initial conditions of particle: $\vec{x}(t_0) = (0.3, 0, 0.3)$, $\dot{\vec{x}}(t_0) = (0, 0, 0)$. On one hand, during the given time interval an uncharged particle $\kappa = 0$ travelled about half the distance than that of opposite charge $\kappa = -1$. On the other hand, $\kappa = \{0, -1\}$ are both attracted, as expected. Notice the small range of wavy y-perturbations, each wave corresponds to one approach of the nearer BH. Both motions resolve into uniform rectilinear motion in late times. The motion starts at "red" and ends up at "blue", the color encodes the passing of time. We shifted the position of $\kappa = 1$ into the origin to arrive at better numerical resolution. $\kappa = 1$ stands still, fluctuations of velocity on the scale 10^{-20} are caused by numerical noise only; this scale is closely related to numerical precision which we set.

3.2.3 | Important classes of motions

Between the infinite number of initial conditions there is a set of those reflecting some characteristics of the system. For us this will be, e.g., standing on the z-axis, the motion along the z-axis or motion in the $z = 0$ plane.

Standing still on the z-axis

We expect static solution on the z-axis to exist, since from physical point of view the z-axis is, roughly said, axis of symmetry of gravito-electro-magnetic interactions.

However, this is not the only allowed static position. We found out analytically that $\kappa = 1$ particle **can stand still** wherever wished. The calculations are carried out in Appendix B: Taylor expansion of geodesic equation. This conjecture was

also confirmed numerically. See Figure 3.1, (c) and (f) describe particle with $\kappa = 1$ and the velocity is one the scale of numerical noise 10^{-20}. For further details about these issues, please, visit Appendix C: Magic of numerics, where we sketch the process we went through with the most interesting points.

Motion along the z-axis, origin

The motion along z-axis is described in Figure 3.2, where $z_0 \neq 0$, $\dot{z}_0 \neq 0$. Particle with $\kappa = 1$ just flies through the origin and escapes to infinity. The $\kappa = 0$ and $\kappa = -1$ particles act naturally as harmonic oscillators.

What if we put the particle in z_0 with zero initial velocity? $\kappa = (0, -1)$ particles are pulled towards the system and, as one would expect, turn into harmonic oscillators with turnarounds at the initial points, satisfying the energy conservation.

In origin all of the particles with $\kappa = (-1, 0, 1)$ can stand still, the origin thus stands out from the whole space.

Equatorial plane

The equatorial plane can give us a good insight concerning what really happens. Considering $\kappa = (0, -1)$ particles, it is clear that due to the gravitational and electrostatic interaction, respectively, no matter the initial position of a static particle, it is at first pulled towards the gravitating charged system of black holes.

Forces acting upon extremally charged particle $\kappa = 1$ are cancelled exactly in the electrostatic order and the remainder is of the order $\mathcal{O}(v^2)$, hence the resulting force is perhaps weak, although still present. Let us compare the motion in Figure 3.3.

Vicinity of the black holes

The Newtonian prescription for gravitational interaction is

$$F_g = \kappa \frac{m_1 m_2}{r^2} = \kappa \frac{m_{01} m_{02}}{r^2} \gamma^2. \tag{3.46}$$

From normalisation of four-velocity we find an approximate value of Lorentz-like γ-factor

$$\gamma^2 \doteq \psi^2 \left(1 + \psi^4 v^2 + 2\psi^2 \vec{N} \cdot \vec{v}\right) \tag{3.47}$$

We have $\vec{N} = 0$, also $v^2 = \dot{r}^2 + r^2\dot{\phi}^2 = \left(\frac{r_{21}}{2}\right)^2 \doteq 0.033$ with $r = r_{21} = const.$, we fix $\dot{\phi} \equiv \omega = 1$. Obviously, γ-factor increases considerably in the vicinity of each hole only (regarding ψ dependence). Matching expectations, the moving $\kappa = 1$ particles show signs of attraction in Figure 3.2 (c).

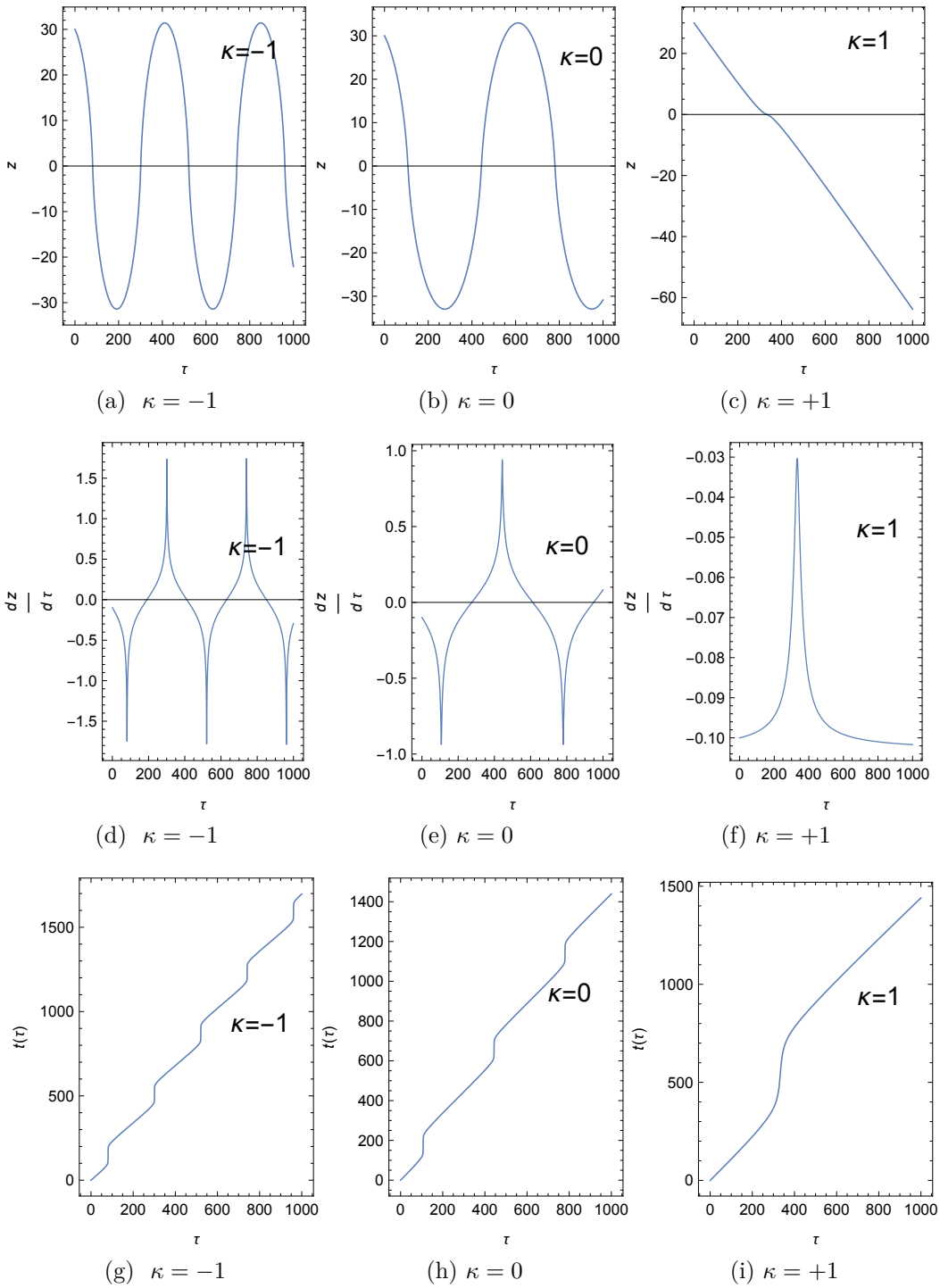

(a) $\kappa = -1$ (b) $\kappa = 0$ (c) $\kappa = +1$

(d) $\kappa = -1$ (e) $\kappa = 0$ (f) $\kappa = +1$

(g) $\kappa = -1$ (h) $\kappa = 0$ (i) $\kappa = +1$

Figure 3.2: **Motion along z-axis**: positions, velocities, coordinate time as functions of the particle's proper time. Initial conditions of particle: $z(t_0) = 30$, $\dot{z}(t_0) = -0.1$. Black holes orbit in $z = 0$ plane. Again, in (a) $\kappa = -1$ took a longer path than $\kappa = 0$ in (b). $\kappa = (0, -1)$ keep oscillating, satisfying the conservation of energy, $\kappa = 1$ flies through origin to infinity along z-axis.

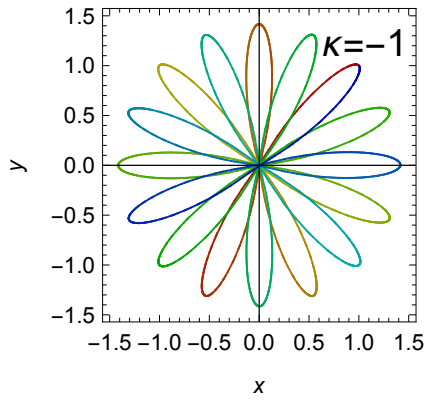

(a) Electrostatic order of forces slows the motion down.
$\vec{F}_\Sigma = \vec{F}_E + \vec{F}_g \doteq 2\vec{F}_g$

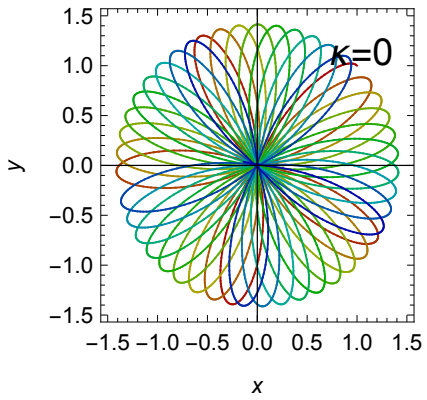

(b) Only gravitational interaction acting.
$\vec{F}_\Sigma = \vec{F}_g$

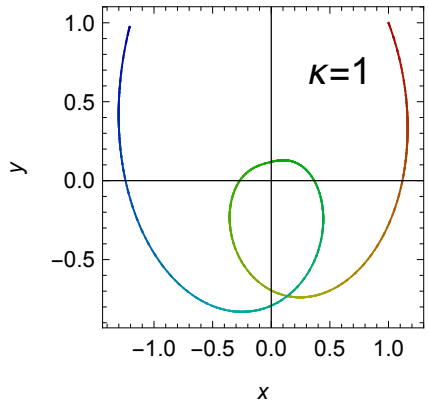

(c) Sum of interactions is of higher order, resulting force is weak compared with (a), (b) and (d).
$\vec{F}_\Sigma = \vec{F}_g - \vec{F}_E = \mathcal{O}(v^2)$

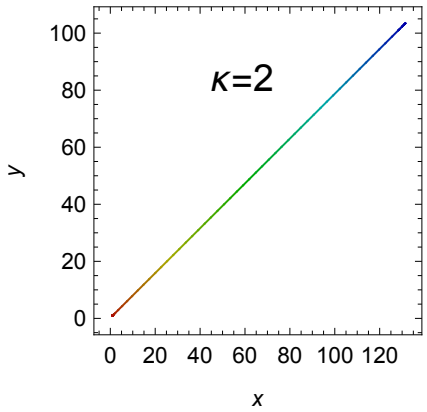

(d) Particle is strongly repelled already in the electrostatic order.
$\vec{F}_\Sigma = \vec{F}_g - 2\vec{F}_E \doteq -\vec{F}_g$

Figure 3.3: **Equatorial plane**. Comparing motion of un/charged test particles in the field of two extremal black holes orbiting in $x-y$ plane with diameter $r_{\text{circ}} = \frac{\sqrt{3}-1}{2}$. Particle's initial conditions: $\vec{x}(t_0) = (1, 1, 0)$, $\dot{\vec{x}}(t_0) = (-0.05, 0.05, 0)$. We have $\vec{F}_\Sigma = \vec{F}_G - \kappa\vec{F}_E$ which denotes electrostatic order of total force, where $\vec{F}_g$ is the gravitational "force" on unit mass, $\vec{F}_E$ electrostatic force on unit charge, $\kappa = \frac{q}{m}$. We can assume that $\vec{F}_g \doteq \vec{F}_E$ in geometrized units (clarifying the equalities below plots).

4. Three black hole Lagrangian

In this chapter we shall make use of Euler-Lagrange equations of the 2nd kind, having the Lagrangian control the motion of our system. The two-body Lagrangian is derived in Section 4.2. A detailed calculation of the three-body Lagrangian is somewhat longer. In Section 4.3, we only outline the main points of the tedious procedure here, the whole calculation is carried out in Appendix A: Calculation of three-body Lagrangian.

We foliate the spacetime with equal-time space-like slices and assume that on any given slice the electromagnetic and gravitational fields are fully determined in terms of positions and velocities of black holes, instead of being independent degrees of freedom (DoF) of Lagrangian density. We can take steps in this way, since there are no field DoF associated with radiation in slow-motion approximation. The initial value equations of general relativity and electromagnetism in slow-motion approximation provide the relation between the black holes and fields.

The resulting formula prescribes an effective action that reduces the problem to classical mechanics of point particles with the dynamics being managed by the effective Lagrangian.

We first sum up basic information about motion of two extremal black holes and derive the Lagrangian. Then we investigate the motion of **three black holes**, one of the main goals of this thesis. Even though the binary systems are not trivial, they are still relatively simple, compared to general three-body problem.

The general three-body motion is far from having a general closed-form solution and thus some restrictions are inevitable. We assume the **restricted three body problem**, where a black hole moves under the influence of two black holes at a large distance and all of the black holes have charge-to-mass ratio unity with non-zero mass. Moreover, we require that the two black holes orbit around origin at a constant radius, determined by the two black hole Lagrangian. Hence we assume we can neglect the back-reaction of the oncoming black hole on the orbiting circular binary.

Restriction to slow motion approximation allows the analytical prescription for perturbation of spacetime-metric with the fields $\vec{N}, \vec{A}$. This approximation for two black holes remains valid within wide range of motion satisfying [5]

$$r \gg v_\infty^2 M, \tag{4.1}$$

where $v_\infty \ll 1$ is the initial relative velocity of the two black holes, r their distance and M is the mass of each.

Condition for the restricted three body problem is the same. We find Lagrangian of the third black hole moving in the field of the orbiting binary as a (not necessarily small) perturbation of the two-body Lagrangian, assuming large distance from the binary. The charged binary asymptotically behaves like R-N black hole. The condition (4.1) is then naturally fulfilled (r denotes the distance of the third black hole from center of mass of the binary).

Although restricting to the slow-motion limit, we still work in the **full strong-field regime** of gravitation coupled to electromagnetism. The analytical solv-

ability of the problem is perhaps amazing.

4.1 Multi black hole Lagrangian

Substituting (3.2) into the action S_{approx} (2.30) and performing the black hole limit (while keeping terms up through $O(v^2)$) one obtains that action approaches a finite limit S_{eff}. This effective action manages the motion of n extremally charged non-rotating black holes in slow motion approximation and can be written as a sum of two pieces [4, 5]

$$S_{\text{eff}} = \int \mathrm{d}t \left(L_{\text{free}} + L_{\text{int}}\right). \tag{4.2}$$

The foliation of space-time is now obviously useful, since it allows us to write S_{eff} in such a simple form. General prescription for the Lagrangian in black hole limit is given by a sum of free and interacting part, which read (the Latin indices label the black holes) [4, 5]

$$\begin{aligned} L_{\text{free}} &= \frac{1}{2}\sum_a m_a v_a^2 - \sum_a m_a \\ L_{\text{int}} &= \frac{3}{8\pi}\int \psi^2 \sum_{b\neq c} \frac{m_b m_c}{(r_b r_c)^3}\left[\frac{1}{2}|\vec{v}_b - \vec{v}_c|^2(\vec{r}_v\cdot\vec{r}_c) - (\vec{v}_b\times\vec{v}_c)\cdot(\vec{r}_b\times\vec{r}_c)\right]\mathrm{d}^3x, \end{aligned} \tag{4.3}$$

where

$$\vec{r}_a = \vec{x} - \vec{x}_a, \quad \vec{v}_a = \frac{\mathrm{d}}{\mathrm{d}t}\vec{x}_a, \quad \psi^2 = 1 + 2\sum_d \frac{m_d}{r_d} + \sum_{d,e}\frac{m_d m_e}{r_d r_e}.$$

According to polynomial dependence of L_{int} on masses m_i the Lagrangian describes only interactions through up to four bodies.

4.2 Two-body Lagrangian

In this section we derive the Lagrangian for two black holes. Their motion was previously studied [4, 5], extended to arbitrary black-hole masses in [19] and coupling with dilatonic fields was added in [8]. We verify here the calculation of Lagrangian and sum up the main results.

Derivation

Let us first denote

$$\begin{aligned} M &= m_1 + m_2 \\ \mu &= \frac{1}{m_1} + \frac{1}{m_2} \\ \vec{r} &= \vec{x}_1 - \vec{x}_2 \\ \vec{v} &= \frac{\mathrm{d}\vec{r}}{\mathrm{d}t} = \vec{v}_1 - \vec{v}_2 \\ \vec{V} &= \frac{m_1\vec{v}_1 + m_2\vec{v}_2}{M}. \end{aligned}$$

One can express the free part as

$$\begin{aligned} L_{\text{free}} &= -M + \frac{1}{2}m_1 v_1^2 + \frac{1}{2}m_2 v_2^2, \\ &= -M + \frac{1}{2}\left(\frac{m_1^2 + m_1 m_2}{M}v_1^2 + \frac{m_2^2 + m_1 m_2}{M}v_2^2\right) + \left(\frac{m_1 m_2}{M} - \mu\right)\vec{v}_1 \cdot \vec{v}_2 \\ &= -M + \frac{1}{2}\left(\frac{m_1^2 v_1^2 + m_2 v_2^2 + 2m_1 m_2 \vec{v}_1 \cdot \vec{v}_2}{M}\right) + \frac{1}{2}\mu\left(v_1^2 + v_2^2 - 2\vec{v}_1 \cdot \vec{v}_2\right) \\ &= -M + \frac{1}{2}M\vec{V} \cdot \vec{V} + \frac{1}{2}\mu\vec{v} \cdot \vec{v}, \end{aligned} \tag{4.4}$$

which coincides with [5]. For the interaction part we have

$$\begin{aligned} L_{\text{int}} = \frac{3}{8\pi}\int \Bigg(&\underbrace{1}_{I_1} + \underbrace{\frac{2m_1}{r_1}}_{I_2} + \underbrace{\frac{2m_2}{r_2}}_{I_2'} + \underbrace{\frac{m_1^2}{r_1^2}}_{I_3} + \underbrace{\frac{m_2^2}{r_2^2}}_{I_3'} + \underbrace{\frac{2m_1 m_2}{r_1 r_2}}_{I_4} \Bigg) \times \\ &\times 2\frac{1}{2}\vec{v} \cdot \vec{v}\frac{\vec{r}_1 \cdot \vec{r}_2}{(r_1 r_2)^3} m_1 m_2 \ \ \mathrm{d}^3x, \end{aligned} \tag{4.5}$$

where the explicitly written 2 in the second line comes from the symmetry in indices $\{b, c\} = \{1, 2\}$. We transform the coordinate using the shift vector $\vec{r} \equiv \vec{x}_2 - \vec{x}_1$ and calculate particular integrals

$$\vec{x} - \vec{x}_1 = \vec{y}, \quad \vec{x} - \vec{x}_2 = \vec{y} - \vec{r}.$$

$$\begin{aligned} I_1 &= \int \frac{\vec{r}_1 \cdot \vec{r}_2}{(r_1 r_2)^3}\mathrm{d}^3x = \int \frac{(\vec{x} - \vec{x}_1) \cdot (\vec{x} - \vec{x}_2)}{|\vec{x} - \vec{x}_1|^3 |\vec{x} - \vec{x}_2|^3}\mathrm{d}^3x = \int \frac{\vec{y} \cdot (\vec{y} - \vec{r})}{y^3|\vec{y} - \vec{r}|^3}\mathrm{d}^3y = \\ &= \int_0^{2\pi}\mathrm{d}\phi \int_{-1}^{1}\left(\int_0^{\infty} \frac{y^2\left(y^2 - yr\cos\theta\right)}{y^3\left(y^2 + r^2 - 2yr\cos\theta\right)^{\frac{3}{2}}}\mathrm{d}y\right)\mathrm{d}(\cos\theta) = \\ &= 2\pi\int_{-1}^{1}\left(\int_0^{\infty} \frac{y - r\cos\theta}{\left(y^2 + r^2 - 2yr\cos\theta\right)^{\frac{3}{2}}}\mathrm{d}y\right)\mathrm{d}(\cos\theta) = \\ &= -2\pi\int_{-1}^{1}\frac{1}{\sqrt{r^2 + y^2 - 2yr\cos\theta}}\Bigg|_{y=0}^{y=\infty}\mathrm{d}(\cos\theta) = \\ &= 2\pi\int_{-1}^{1}\frac{1}{r}\mathrm{d}(\cos\theta) = \frac{4\pi}{r}, \end{aligned} \tag{4.6}$$

The second integral is, using the same substitution,

$$\begin{aligned} I_2 &= 2m_1 \int \frac{\vec{r}_1 \cdot \vec{r}_2}{r_1^4 r_2^3} \mathrm{d}^3x = 2m_1 \int \frac{(\vec{y}-\vec{r})\cdot\vec{y}}{|\vec{y}-\vec{r}|^4 y^3} \mathrm{d}^3y = \\ &= 4\pi m_1 \int_{-1}^{1} \left(\int_0^\infty \frac{y - r\cos\theta}{\left(y^2 + r^2 - 2yr\cos\theta\right)^2} \mathrm{d}y \right) \mathrm{d}(\cos\theta) = \\ &= 4\pi m_1 \int_{-1}^{1} \left(-\frac{1}{2}\right) \frac{1}{r^2 + y^2 - 2yr\cos\theta} \Big|_{y=0}^{y=\infty} \mathrm{d}(\cos\theta) = \\ &= \frac{2\pi m_1}{r^2} \int_{-1}^{1} \mathrm{d}(\cos\theta) = \frac{4\pi m_1}{r^2}. \end{aligned} \tag{4.7}$$

If we exchange the indices $\{1, 2\}$ this result will remain valid, except the mass term in the numerator and hence a sum of the counterparts becomes

$$I_2 + I_2' = \frac{4\pi M}{r^2}.$$

Then we have

$$\begin{aligned} I_3 &= m_1^2 \int \frac{\vec{r}_1 \cdot \vec{r}_2}{r_1^5 r_2^3} \mathrm{d}^3x = m_1^2 \int \frac{\vec{y}\cdot(\vec{y}-\vec{r})}{y^3 |\vec{y}-\vec{r}|^5} \mathrm{d}^3y = \\ &= 2\pi m_1^2 \int_{-1}^{1} \left(\int_0^\infty \frac{y - r\cos\theta}{\left(y^2 - 2yr + r^2\right)^{5/2}} \mathrm{d}y \right) \mathrm{d}(\cos\theta) = \\ &= -2\pi m_1^2 \int_{-1}^{1} \frac{1}{3\sqrt{r^2 - 2ry\cos(\theta) + y^2}^3} \Bigg|_{y=0}^{y=\infty} \mathrm{d}(\cos\theta) = \\ &= \frac{2\pi m_1^2}{3} \int_{-1}^{1} \frac{1}{r^3} \mathrm{d}(\cos\theta) = \frac{4\pi m_1^2}{3r^3}, \end{aligned} \tag{4.8}$$

which is, again, symmetric under $\{1 \leftrightarrow 2\}$ exchange, except the mass term and summing the counterparts gives

$$I_3 + I_3' = \frac{4\pi}{3} \frac{m_1^2 + m_2^2}{r^3} = \frac{4\pi}{3} \frac{M^2 - 2\mu M}{r^3}.$$

Now if we use $\mu M = m_1 m_2$ for the constant factor in the integral (4.5), we arrive at the desired formula.

Thus, the other integrals, that is I_4 and also the last term of (4.3), must vanish. Let us have a coordinate system such, that the two black holes are placed symmetrically with respect to the origin, $\vec{x}_1 = -\vec{x_2} =: -\vec{L}$. This setting is

depicted in Figure 4.1, and one can integrate

$$\begin{aligned} I_4 &= \int \frac{\vec{r_1}\cdot\vec{r_2}}{(r_1 r_2)^4}\ \mathrm{d}^3x = \\ &= \int \frac{(\vec{x}-\vec{x_1})\cdot(\vec{x}-\vec{x_2})}{|\vec{x}-\vec{x_1}|^4|\vec{x}-\vec{x_2}|^4}\ \mathrm{d}^3x = \\ &= \int \frac{(\vec{x}+\vec{L})\cdot(\vec{x}-\vec{L})}{|\vec{x}+\vec{L}|^4|\vec{x}-\vec{L}|^4}\ \mathrm{d}^3x = \\ &= \int \frac{x^2-L^2}{(x^2+L^2+2\vec{x}\cdot\vec{L})^2(x^2+L^2-2\vec{x}\cdot\vec{L})^2}\ \mathrm{d}^3x = \\ &= \int \frac{x^2-L^2}{\left((x^2+L^2)^2-4(\vec{x}\cdot\vec{L})^2\right)^2}\ \mathrm{d}^3x = \\ &= \int_0^\pi\int_0^\infty \frac{x^2-L^2}{\left((x^2+L^2)^2-4x^2L^2\sin^2\theta\right)^2} 2\pi x^2 \mathrm{d}x\ \sin\theta \mathrm{d}\theta. \end{aligned} \tag{4.9}$$

After the definite integration with respect to x one obtains 0 for $x \to 0$, while for $x \to \infty$ one has $-\frac{i\pi^2 e^{i\theta}\left(\frac{1}{\sqrt{e^{-2i\theta}}}-\sqrt{e^{2i\theta}}\right)}{4\left(-1+e^{2i\theta}\right)^2 L^3}$, which, after the definite integration with respect to θ also vanishes. Note, that θ measures the deviation of $\vec{x}$ from the axis z, while the angle between $\vec{x}$ and $\vec{L}$ is $(\pi/2-\theta)$, which produces sine in the very last denominator.

Another vanishing integral is of the type

$$\int \frac{\vec{r_1}\times\vec{r_2}}{(r_1 r_2)^n}\ \mathrm{d}^3x$$

for n natural. Following the geometrical insight one can easily see it vanishes, as described in the caption for Figure[1] 4.1. The last term in (4.3) vanishes upon the integration over a symmetric integration domain.
Thus, we arrive at the final formula in full accordance with [4, 5]

$$\begin{aligned} L_{\mathrm{2B}} &= L_{\mathrm{free}} + L_{\mathrm{int}} \\ L_{\mathrm{free}} &= -M + \frac{1}{2}M\vec{V}\cdot\vec{V} + \frac{1}{2}\mu\vec{v}\cdot\vec{v} \\ L_{\mathrm{int}} &= \frac{3}{2}\mu M\vec{v}\cdot\vec{v}\left(\frac{1}{r}+\frac{M}{r^2}+\frac{M^2-2\mu M}{3r^3}\right), \end{aligned} \tag{4.10}$$

We sum up the features of two body motion, beginning with impact parameter. Let the two holes approach from infinity with initial speed $v_\infty \ll 1$ and with an impact parameter b. Impact parameter describes the perpendicular distance of projectile and target at infinite distance. There are two classes of solutions separated by the critical value b_{crit}, which solves [19]

$$-\frac{4}{3}b^6 + 9M^2b^4 - 36\mu M^3b^2 - 36\mu^2M^4 = 0 \tag{4.11}$$

[1]We use the *arrow notation*, where the dot in circle depicts a tip of an arrow pointing out of a paper, while the inscribd cross denotes the end of the arrow, heading towards the paper.

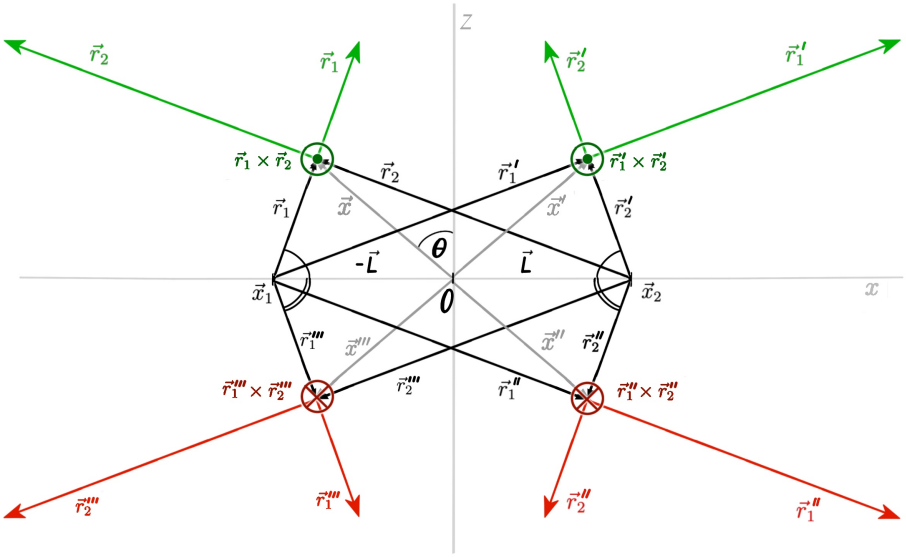

Figure 4.1: About the vanishing integral $\int \frac{\vec{r}_1 \times \vec{r}_2}{(r_1 r_2)^n} \, \mathrm{d}^3 x$ for n natural. We describe the axially symmetric system by a single plane, with "angular dimension" suppressed. The two black holes are placed symmetrically with respect to the origin, θ describes the deviation of $\vec{x}$ from z-axis. One can see that each point of the upper hemisphere $\vec{r}_1 \times \vec{r}_2$ defined by the actual position $\vec{x}$ of the integration has its counterpart in the lower hemisphere. Contributions of these two points, placed symmetrically with respect to x-axis, cancel out exactly within integration over a symmetric domain and we end up with zero.

where μ is the reduced mass. For general ratio of masses the solution is rather long and uninformative algebraic Cardano-type expression, which can be found in [19], eq. (2.50). For two equally massive black holes $m_1 = m_2$ the solution becomes [5, 8, 19]

$$b_{\text{crit}} = \sqrt{3 + \frac{3}{2}\sqrt{3}} M \doteq 2.366 M. \tag{4.12}$$

The critical value separates two classes of motion, coalescence and scattering. See Figure 4.2 with representatives of these motions. In between there is a critical circular orbit, on which the two black holes can orbit steadily (within our approximation)[2]. Two limits of critical circular radius (two equally massive BHs and BH + test particle) correspond with other works [5] and the well know value for the test particle

$$r_{\text{equal-mass}} = \frac{\sqrt{3}-1}{2}, \qquad r_{\text{test-particle}} = \frac{1}{2}. \tag{4.13}$$

This critical radius was found to be not only a critical path that the holes can inspiral to, but also a path of two maximally charged black holes, mutually orbiting at a constant distance. This system will form the background for evolution in the thesis. According to its importance, we mention again, that such a

[2]There are gravitational waves of the order $\Delta E_{rad} \sim v_\infty^5 M$ [5], which we do not take into account in our order of approximation.

situation is allowed in relativistic approach only, not in Newtonian physics, where the bodies would move along straight lines.

Moreover, the circular velocity of orbiting holes $\dot{\phi}$ is for two equal black holes proportional to the initial angular momentum L (which is preserved)

$$\dot{\phi} = \frac{8(\sqrt{3}-1)}{3(\sqrt{3}+1)} L. \tag{4.14}$$

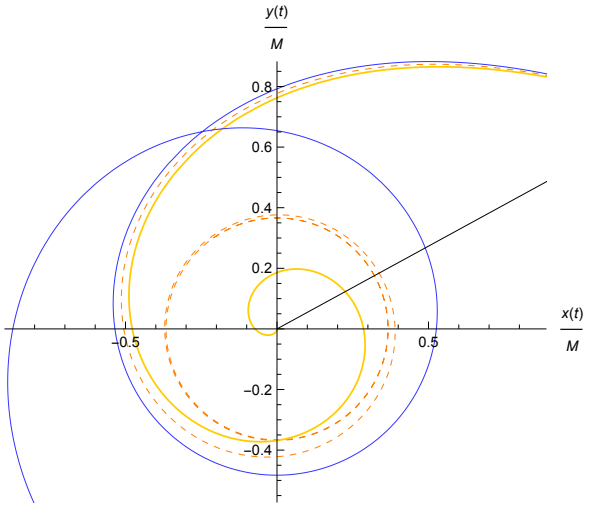

Figure 4.2: Trajectories of two black holes in center of mass coordinates for equal mass black holes and various values of impact parameter. The dashed "red" line corresponds to critical case $b_{crit} \doteq 2.366 \times M$, "orange" coalescing line to $b = 0.99 \times b_{crit}$, "blue" scattering line to $b = 1.01 \times b_{crit}$ and the "black" straight line to head-on collision with $b = 0$. The initial conditions are $\phi_0 = 0.5$, $r_0 = 1.5$, the same for all of the cases.

4.3 Three-body Lagrangian

We begin with a general integral prescription, including our restrictions and known paths $\vec{x}_1, \vec{x}_2$. In contrast to the preceding two-body case, the situation we experience here is quite a bit more complicated, since the integrals in Lagrangian do not seem to provide us with any analytical solution[3].

The subsequent calculation is rather tedious, the detailed calculation can be found in Appendix A: Calculation of three-body Lagrangian. In this section we sketch the procedure of calculation in one example and reproduce the result only.

[3]Unfortunately, not even after hours and hours of looking for the right variable system and inventing a list of creative analytical mechanisms.

Separating Lagrangian

We will separate the whole Lagrangian into two parts; the two-body Lagrangian independent of $\vec{x}_3$ and the remainders. The two-body formula for $L_{2\mathrm{B}}$ is already known from previous sections and the rest will be thought of as a perturbation (depending on $\vec{x}_3$). We shall denote it suggestively as "perturbation". Since the positions of black holes often appear subtracted from $\vec{x}$, we denote

$$\vec{r}_a = \vec{x} - \vec{x}_a,$$

where $\vec{x}$ is position in spacetime and $\vec{x}_a$ is position of the a-th black hole, $a \in \{1, 2, 3\}$. The Lagrangian then reads

$$L_{3B} = L_{2B}(r_1, r_2, \cancel{r_3}) + \text{perturbation}(r_1, r_2, r_3) \tag{4.15}$$

where $L_{2\mathrm{B}}$ is known and we have to calculate the perturbation

$$\begin{aligned}
\text{perturbation} \equiv -\frac{3}{8\pi}\int\Bigg(&\frac{2m_3\left(\frac{m_1}{r_1}+\frac{m_2}{r_2}+1\right)\left(\frac{m_1 m_2\ \vec{r}_1\cdot\vec{r}_2|\vec{v}_1-\vec{v}_2|^2}{r_1^3 r_2^3}\right)}{r_3}\\
&+\frac{m_3^2\left(\frac{m_1 m_2\ \vec{r}_1\cdot\vec{r}_2|\vec{v}_1-\vec{v}_2|^2}{r_1^3 r_2^3}\right)}{r_3^2}\\
&+\frac{\frac{m_1 m_3\ \vec{r}_1\cdot\vec{r}_3|\vec{v}_1-\vec{v}_3|^2\left(\frac{m_1}{r_1}+\frac{m_2}{r_2}+1\right)^2}{r_1^3}+\frac{m_2 m_3\ \vec{r}_2\cdot\vec{r}_3|\vec{v}_2-\vec{v}_3|^2\left(\frac{m_1}{r_1}+\frac{m_2}{r_2}+1\right)^2}{r_2^3}}{r_3^3}\\
&+\frac{\frac{2m_1 m_3^2\ \vec{r}_1\cdot\vec{r}_3|\vec{v}_1-\vec{v}_3|^2\left(\frac{m_1}{r_1}+\frac{m_2}{r_2}+1\right)}{r_1^3}+\frac{2m_2 m_3^2\ \vec{r}_2\cdot\vec{r}_3|\vec{v}_2-\vec{v}_3|^2\left(\frac{m_1}{r_1}+\frac{m_2}{r_2}+1\right)}{r_2^3}}{r_3^4}\\
&+\frac{\frac{m_1 m_3^3\ \vec{r}_1\cdot\vec{r}_3|\vec{v}_1-\vec{v}_3|^2}{r_1^3}+\frac{m_2 m_3^3\ \vec{r}_2\cdot\vec{r}_3|\vec{v}_2-\vec{v}_3|^2}{r_2^3}}{r_3^5}\Bigg)\mathrm{d}^3x
\end{aligned} \tag{4.16}$$

From now on we denote the i-th line of (4.16) as "pert(i)".

Integration strategy

Looking at the Lagrangian (4.16) for some time, one convinces herself to use the afore mentioned restrictions rather than chase an apparently non-existent analytical solution. A very small subset of integrals in (4.16) can be solved analytically by the preceding techniques, if the denominator is a monomial of the form $r_i^m r_j^n$, instead of $r_i^m r_j^n r_k^o$, for which we need an approximation.

Our physical setting is such, that the two extremally charged massive black holes (interacting with each other and creating gravito-electro-magnetic field around) are near the origin and the third black hole, extremally charged as well, approaches from *infinity*. We shall definitely make use of this restriction when choosing the regions of integration.

The integration domains are chosen so that each domain covers the area of dominant contribution, within each of which we can use a convenient approximation, allowing us to evaluate it analytically. Regions are depicted in Figure 4.3 and analytically defined by

$$r_{21} \ll \Gamma \ll x_3 \ll \Lambda.$$

Here $\vec{r}_{21}$ is the distance between the two orbiting black holes, Γ, Λ are the radii of the corresponding regions and $\vec{x}_3$ is the distance of the 3rd black hole from origin. Furthermore, there are regions that contribute negligibly to our integral. This is namely the white region Ω in Figure 4.3. Let us show that we can neglect its contribution in good conscience.

In Ω, i.e. very far from origin, one has

$$|\vec{r}_2| \approx |\vec{r}_1| \approx |\vec{r}_3| \approx |\vec{x}|$$

Looking at lines of (4.16), after substituting the last "approximative equality" one can see, that the weakest decrease is on the 3rd line, falling as

$$\int \frac{\mathrm{d}^3 x}{x^4} \sim \frac{1}{x}\Big|_{x=\Omega},$$

which vanishes as we approach infinity with Ω. The other terms of perturbation Lagrangian fall off even faster (and vanish), hence one need not worry about the region Ω. Performing the final limit of radial parameter $\Lambda \to \infty$ also effectively includes even the furthest regions and according to this discussion, extending the integration domain to infinity does not bring any contributions that could blow-up and hence is safe[4]. Now we calculate one of the integrals as an example, leaving the rest to Appendix A: Calculation of three-body Lagrangian.

Example: 1st line of the perturbation

As an example of tedious work involved in calculation of "perturbation" we perform the calculation of one integral from the 1st line of Lagrangian (4.16). The rest of procedure can be found in the Appendix Appendix A: Calculation of three-body Lagrangian. Velocities are, of course, independent of positions.

$$-\frac{8\pi}{3} \cdot \mathrm{pert}(1) = 2m_1 m_2 m_3 \left|\vec{v}_1 - \vec{v}_2\right|^2 \int \left(\frac{m_1}{r_1} + \frac{m_2}{r_2} + 1\right) \frac{\vec{r}_1 \cdot \vec{r}_2}{r_1^3 r_2^3} \frac{1}{r_3} \, \mathrm{d}^3 x. \quad (4.17)$$

The unity from parenthesis on the right hand side gives

$$I_1 = \int \frac{\vec{r}_1 \cdot \vec{r}_2}{r_1^3 r_2^3} \frac{1}{r_3} \, \mathrm{d}^3 x \; \equiv I_{1\Gamma} + I_{1\Lambda}.$$

This integral cannot be analytically solved in general. We use the restrictions stated above and separate the space–time region into several domains, see Figure 4.3.

[4]Moreover, for us it will be very desirable, since after such a limit contributions caused by finiteness of integration area Λ ultimately drop out.

The shifts we use in later calculations, for example centering our integration coordinate system at $\vec{x}_2$ instead of the origin, might seem inaccurate at the first sight. However, our condition $r_{21} \ll \Gamma \ll x_3 \ll \Lambda$ and the initial distance of the 3rd black hole from the system of two black holes allows us to shift integration region by a small distance (small with respect to the actual size of the region, at least two orders) with consequences of negligible order.

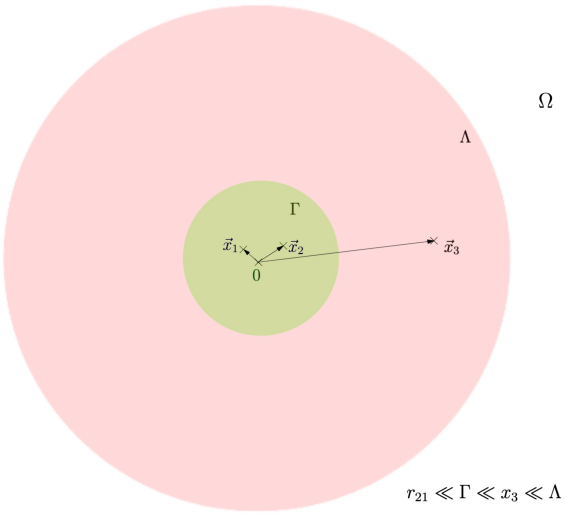

Figure 4.3: Sketch of splitting the integration domain into three parts, each of which either contributes significantly to our integral (Γ - small sphere, Λ - larger spherical shell) or contributes negligibly (remaining Ω region). We define the regions by the condition $r_{21} \ll \Gamma \ll x_3 \ll \Lambda$. In each of these regions the individual integrals simplify significantly.

In the first area Γ contribution of the part $\frac{\vec{r}_1 \cdot \vec{r}_2}{r_1^3 r_2^3}$ dominates, we have $|\vec{x}| \ll |\vec{x}_3|$, and hence $r_3 = |\vec{x} - \vec{x}_3| \approx |\vec{x}_3| = \text{const}$, which can be factored out of the integral. Since we split the integral into independent parts, coordinates can be chosen differently in each integral. After we introduce the shift of coordinates

$$\vec{r}_2 = \vec{x} - \vec{x}_2 = \vec{y}, \quad \vec{r}_1 = \vec{x} - \vec{x}_1 = \vec{y} + \vec{x}_2 - \vec{x}_1 \equiv \vec{y} - \vec{r}_{21} \tag{4.18}$$

it is convenient to use locally spherical coordinates in a similar way to what we did when integrating L_{2B}, i.e., θ measures the angle between $\vec{y}$ & $\vec{r}_{12}$, where $\vec{r}_{12} = \vec{x}_2 - \vec{x}_1$ is the relative position shift vector. One should proceed carefully since integration with respect to $\vec{y}$ in region Γ is not over a sphere centered at

origin; however, as stated above, the difference is negligible.

$$
\begin{aligned}
I_{1\Gamma} &= \int_\Gamma \frac{\vec{r}_1\cdot\vec{r}_2}{r_1^3 r_2^3}\frac{1}{r_3}\,\mathrm{d}^3x \doteq \frac{1}{x_3}\int_\Gamma \frac{\vec{r}_1\cdot\vec{r}_2}{r_1^3 r_2^3}\,\mathrm{d}^3x = \\
&= \frac{1}{x_3}\int_0^{2\pi}\mathrm{d}\phi\int_{-1}^{1}\mathrm{d}(\cos\theta)\left[\frac{-1}{\sqrt{y^2+r_{12}^2-2yr_{12}\cos\theta}}\right]_{y=0}^{y=\Gamma} = \\
&= \frac{2\pi}{x_3}\int_{-1}^{1}\mathrm{d}(\cos\theta)\left[\frac{-1}{\sqrt{\Gamma^2+r_{12}^2-2\Gamma r_{12}\cos\theta}}+\frac{1}{r_{12}}\right] = \\
&= \frac{2\pi}{x_3}\left[\frac{1}{\Gamma r_{12}\frac{1}{\Gamma-r_{12}}}-\frac{1}{\Gamma r_{12}\frac{1}{\Gamma+r_{12}}}+\frac{2}{r_{12}}\right] = \\
&= \frac{4\pi}{x_3}\left[\frac{1}{r_{12}}-\frac{1}{\Gamma}\right]
\end{aligned}
\tag{4.19}
$$

Notice, that we could use $r_{12} \ll \Gamma$ and drop the blue term, however, it will cancel exactly with its counterpart later. Since in Λ we have $x_1, x_2 \ll x$, one can write in this region

$$r_1 = |\vec{x}-\vec{x}_1| \approx r_2 = |\vec{x}-\vec{x}_2| \approx |\vec{x}|.$$

In the second line we introduce locally spherical coordinates, that describe a spherical shell with radial coordinate $y \in [\Gamma, \Lambda]$. In the last step we perform the limit $\Lambda \to \infty$ and hence we cover the entire rest of space–time region.

$$
\begin{aligned}
I_{1\Lambda} &= \int_\Lambda \frac{\vec{r}_1\cdot\vec{r}_2}{r_1^3 r_2^3}\frac{1}{r_3}\,\mathrm{d}^3x \doteq \int_\Lambda \frac{\vec{x}\cdot\vec{x}}{x^6}\frac{1}{|\vec{x}-\vec{x}_3|}\,\mathrm{d}^3x = \int_\Lambda \frac{\mathrm{d}^3x}{x^4|\vec{x}-\vec{x}_3|} = \\
&= \int_0^{2\pi}\mathrm{d}\phi\int_\Gamma^\Lambda \mathrm{d}x\int_{-1}^{1}\mathrm{d}(\cos\theta)\frac{1}{x^2\sqrt{x^2+x_3^2-2xx_3\cos\theta}} = \\
&= -\frac{2\pi}{x_3}\int_\Gamma^\Lambda \mathrm{d}x\frac{1}{x^3}\left[\sqrt{x^2+x_3^2-2xx_3\cos\theta}\right]_{\cos\theta=-1}^{\cos\theta=1} = \\
&= +\frac{2\pi}{x_3}\int_\Gamma^\Lambda \frac{|x+x_3|-|x-x_3|}{x^3} = \\
&= \frac{2\pi}{x_3}2\int_\Gamma^{x_3}\frac{1}{x^2}\mathrm{d}x + \frac{2\pi}{x_3}2x_3\int_{x_3}^{\Lambda}\frac{1}{x^3}\mathrm{d}x = \\
&= -\frac{4\pi}{x_3}\left[\frac{1}{x}\right]_\Gamma^{x_3} - 2\pi\left[\frac{1}{x^2}\right]_{x_3}^{\Lambda} = \\
&= \left(-\frac{4\pi}{x_3^2}+\frac{4\pi}{x_3\Gamma}\right) - 2\pi\left(\cancelto{0}{\frac{1}{\Lambda^2}}-\frac{1}{x_3^2}\right)
\end{aligned}
\tag{4.20}
$$

The "blue" counterterms in $I_{1\Gamma}$ and $I_{1\Lambda}$ cancel exactly and I_1 gives

$$I_1 = \frac{4\pi}{x_3 r_{12}} - \frac{2\pi}{x_3^2}.$$

Overall perturbation

After carrying out the rather lengthy calculation, see Appendix A: Calculation of three-body Lagrangian, we arrived at Lagrangian of the 3rd black hole. Having the Lagrangian at hand we can proceed with equations of motion. The worrisome term with $1/x_3^2\Gamma$, the only surviving term containing Γ, need not concern us since later we will dispose of it during the 1st and 2nd order approximation. It is in high demand that our choice of the actual size of the integration domain does not affect the results.

$$
\begin{aligned}
&L_{BH3}(x_{3x}, x_{3y}, x_{3z}, v_{3x}, v_{3y}, v_{3z}) \equiv \text{perturbation} = \\
&\quad = \sum_{i=1}^{5} \text{pert(i)} = \\
&\quad = -\frac{3}{2} m_1 m_2 m_3 \left|\vec{v}_1 - \vec{v}_2\right|^2 \left(\frac{2}{x_3} \frac{1}{r_{12}} + \frac{1}{x_3^2} + \right. \\
&\qquad\qquad \left. + (m_1 + m_2) \left[\frac{1}{x_3} \frac{1}{r_{21}^2} - \frac{1}{x_3^3} \right] \right) \\
&\qquad - \frac{3}{2} m_3^2 m_1 m_2 |\vec{v}_1 - \vec{v}_2|^2 \left(\frac{1}{x_3^2} \frac{1}{r_{12}} \right) \\
&\qquad - \frac{3}{2} m_1 m_3 \left|\vec{v}_1 - \vec{v}_3\right|^2 \left(\frac{1}{r_{31}} + \frac{m_1}{r_{31}^2} + \frac{m_2}{x_3^2} + \frac{1}{3} \frac{m_1^2}{r_{31}^3} + \frac{2}{3} \frac{m_1 m_2}{x_3^3} \right. \\
&\qquad\qquad \left. + m_2^2 \left(-\frac{1}{r_{21}} \frac{x_{3z}}{x_3^3} + \frac{1}{3} \frac{1}{x_3^3} \right) \right) \\
&\qquad - \frac{3}{2} m_2 m_3 \left|\vec{v}_2 - \vec{v}_3\right|^2 \left(\frac{1}{r_{32}} + \frac{m_2}{r_{32}^2} + \frac{m_1}{x_3^2} + \frac{1}{3} \frac{m_2^2}{r_{32}^3} + \frac{2}{3} \frac{m_1 m_2}{x_3^3} \right. \\
&\qquad\qquad \left. + m_1^2 \left(+\frac{1}{r_{21}} \frac{x_{3z}}{x_3^3} + \frac{1}{3} \frac{1}{x_3^3} \right) \right) \\
&\qquad - \frac{3}{2} m_3^2 \left(\frac{m_1 |\vec{v}_1 - \vec{v}_3|^2}{r_{13}^2} + \frac{m_2 |\vec{v}_2 - \vec{v}_3|^2}{r_{23}^2} \right) \\
&\qquad - \frac{3}{2} m_3^2 m_1 m_2 \left(|\vec{v}_1 - \vec{v}_3|^2 + |\vec{v}_2 - \vec{v}_3|^2 \right) \cdot \left(\frac{-1}{4} \frac{1}{x_3^2 \Gamma} \right) \\
&\qquad - \frac{m_3^3}{2} \left(\frac{m_1 |\vec{v}_1 - \vec{v}_3|^2}{r_{31}^3} + \frac{m_2 |\vec{v}_2 - \vec{v}_3|^2}{r_{32}^3} \right)
\end{aligned}
\tag{4.21}
$$

4.4 | Equation of motion: 3rd BH

We will state properly which approximations take place there to obtain the 1st and 2nd order Lagrangian. In addition to that, in each order of Lagrangian we comment on its asymptotical freedom and compare with physical expectations. The resulting plots with comments close down each section.

Setting the scene

Our current physical setting is such that the binary rotates near the origin as the third black hole approaches from large distance.

$$\begin{aligned}
&\vec{x}_2 = -\vec{x}_1 \\
&\vec{v}_1 = -\vec{v}_2 \equiv \vec{v}, \quad 1 \gg v,\ 1 \gg v_3 \\
&|\vec{v}_1 - \vec{v}_2|^2 = 4v^2, \\
&|\vec{v}_1 - \vec{v}_3|^2 + |\vec{v}_2 - \vec{v}_3|^2 = 2\left(v^2 + v_3^2\right) \\
&|\vec{v}_1 - \vec{v}_3|^2 - |\vec{v}_2 - \vec{v}_3|^2 = -4\vec{v}\cdot\vec{v}_3 \\
&r_{21} = |\vec{x}_2 - \vec{x}_1| = const. = r_{\text{circ}} \\
&x_3 \gg r_{21}
\end{aligned} \tag{4.22}$$

In this context, velocity is a time derivative of the position with respect to the coordinate time

$$\vec{v_i} = \frac{\mathrm{d}\vec{x}_i}{\mathrm{d}t}.$$

Unlike in section about geodesics, now the only time we use is the coordinate one. The constant distance of two rotating black holes of equal mass is [19]

$$r_{21} \equiv r = \frac{\sqrt{3}-1}{2} \approx 0.366$$

For the approximation we use our preceding conditions, namely

$$\begin{aligned}
&r_{21} \ll \Gamma,\ r_{21} \ll x_3 \\
&x_3 \gg x_1, x_2 \implies r_{31} \approx x_3 \approx r_{32} \\
&(m_1 = m_2 \equiv m \gg m_3)
\end{aligned} \tag{4.23}$$

The last condition regarding m_3 will be discussed later. It is useful condition for comparing the black hole behavior with motion of test particle.

4.4.1 | First-order approximation

Let us proceed with the first order approximation of our Lagrangian. That is, we keep the largest terms only. The interaction part of perturbation is then

$$L_{BH3C1} = -\frac{3}{2}m_1m_2m_3\left|\vec{v}_1-\vec{v}_2\right|^2\left(\frac{2}{x_3}\frac{1}{r_{12}}+(m_1+m_2)\left[\frac{1}{x_3}\frac{1}{r_{21}^2}\right]\right) - \frac{3}{2}m_1m_3\left|\vec{v}_1-\vec{v}_3\right|^2\left(\frac{1}{r_{31}}\right)-\frac{3}{2}m_2m_3\left|\vec{v}_2-\vec{v}_3\right|^2\left(\frac{1}{r_{32}}\right).$$

Now we add the free part of Lagrangian, too. Having the above conditions (4.22) and (4.23) at hand, the full Lagrangian finally reads[5]

$$L_{BH3C1F} = L_{BH3C1} + L_{3Free} = L_{BH3C1} + \frac{1}{2}m_3v_3^2 - m_3$$

$$L_{BH3C1F} = -\frac{3}{2}m_3\left(-\frac{v_3^2}{3}+\frac{2}{3}+8m^2v^2\left[\frac{1}{x_3r}+\frac{m}{x_3r^2}\right]+\frac{2m}{x_3}\left[v^2+v_3^2\right]\right) \tag{4.24}$$

The Lagrangian (4.24) gives rise to the equations of motion (EOM) which are three Euler–Lagrange equations of the 2nd kind

$$\frac{\mathrm{d}}{\mathrm{d}t}\frac{\partial L}{\partial v_{3i}} = \frac{\partial L}{\partial x_{3i}}, \quad i=1,2,3.$$

Also the Lagrangian (4.24) controls asymptotically free motion

$$\lim_{x_3\to\infty}\nabla_{\vec{v}_3}L_{BH3C1} = m_3\vec{v}_3.$$

The asymptotical freedom manifests itself as a straight path at late times in Figure 4.4. It is an expected result, consistent with the limiting Newtonian situation, which we used to check our results.

Moreover, the whole Lagrangian is proportional to m_3 (no other m_3 occurs). We can thus conclude that, to the leading order, the limit of small or large black hole does not affect the motion qualitatively.

[5]Legend to the subscript: BH3 – the third black hole, C – circular, 1 – the first order, F – full, including free terms.

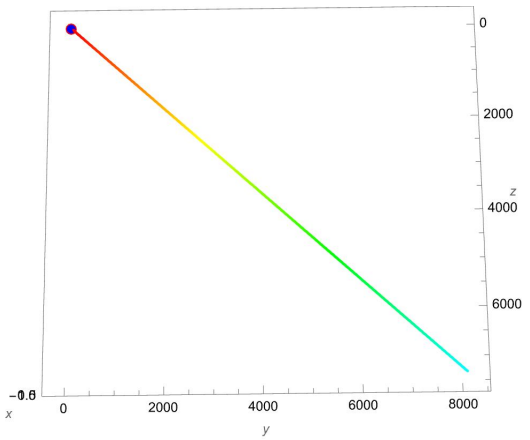

(a) Whole trajectory of the third black hole

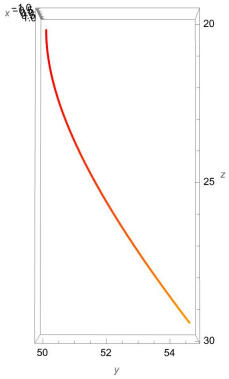

(b) Beginning of the trajectory

Figure 4.4: First order approximation, using the Lagrangian (4.24). The trajectory of the 3rd black hole starts at "red", finishes at "cyan", the color shows the passing of time. System of two mutually rotating holes is located in the vicinity of origin. Initial conditions: $\vec{x}_3(t_0) = (0, 50, 20)$, $\vec{v}_3(t_0) = (0, 0, 0.05)$.

4.4.2 | Second-order approximation

In the second-order approximation we impose (4.23) again. Then we simply count the "order of smallness" of each term with respect to the largest term (of the same structure) in (4.24). To begin with, each $\frac{1}{x_3} \ll \frac{1}{r}$ brings one order of smallness.

$$\begin{aligned} L_{BH3C2} = &-\frac{3}{2} m_1 m_2 m_3 \left|\vec{v}_1 - \vec{v}_2\right|^2 \left(\frac{2}{x_3}\frac{1}{r_{12}} + \frac{1}{x_3^2} + \right. \\ &\left. + (m_1 + m_2) \left[\frac{1}{x_3}\frac{1}{r_{21}^2}\right] \right) \\ &- \frac{3}{2} m_3^2 m_1 m_2 |\vec{v}_1 - \vec{v}_2|^2 \left(\frac{1}{x_3^2}\frac{1}{r_{12}}\right) \\ &- \frac{3}{2} m_1 m_3 \left|\vec{v}_1 - \vec{v}_3\right|^2 \left(\frac{1}{r_{31}} + \frac{m_1}{r_{31}^2} + \frac{m_2}{x_3^2} - m_2^2 \frac{1}{r_{21}}\frac{x_{3z}}{x_3^3} \right) \\ &- \frac{3}{2} m_2 m_3 \left|\vec{v}_2 - \vec{v}_3\right|^2 \left(\frac{1}{r_{32}} + \frac{m_2}{r_{32}^2} + \frac{m_1}{x_3^2} + m_1^2 \frac{1}{r_{21}}\frac{x_{3z}}{x_3^3} \right) \\ &- \frac{3}{2} m_3^2 \left(\frac{m_1 |\vec{v}_1 - \vec{v}_3|^2}{r_{13}^2} + \frac{m_2 |\vec{v}_2 - \vec{v}_3|^2}{r_{23}^2} \right) \end{aligned} \tag{4.25}$$

In addition, we could impose $m_3 \ll m_1 = m_2 \equiv m$, which would bring another order of smallness, further simplifying the Lagrangian. Despite this tempting option, let us first proceed with general m_3, thereupon the Lagrangian controls the motion of a black hole of any m_3, which is amazing. We will compare behavior of the limits $m_3 \ll m$ and $m_3 \gg m$.

Using trivial algebraic manipulations and conditions (4.23), one can convert

Lagrangian into the following form ($r \equiv r_{21} = const.$). The full Lagrangian[6] is again the sum of free and interaction part.

$$L_{BH3C2F} = L_{BH3C2} + L_{3Free} = L_{BH3C2} + \frac{1}{2}m_3 v_3^2 - m_3$$

$$\begin{aligned} L_{BH3C2F1} = -\frac{3}{2}m_3\Bigg(&- \frac{v_3^2}{3} + \frac{2}{3} + 4m^2v^2\left[\frac{1}{x_3^2} + \frac{2}{x_3 r} + \frac{2m}{x_3 r^2} + \frac{m_3}{x_3^2 r}\right] + \\ &+ \left[\frac{1}{x_3} + \frac{2m}{x_3^2} + \frac{m_3}{x_3^2}\right] 2m\left[v^2 + v_3^2\right] + \frac{m^3}{r}\frac{x_{3z}}{x_3^3}\left(4\vec{v}\cdot\vec{v}_3\right)\Bigg). \end{aligned} \tag{4.26}$$

So far the rotation of our binary system around the origin did not manifest itself in our Lagrangian. Now such a possible term appeared. x_{3z} is a projection of $\vec{x}_3$ onto the rotating axis $\vec{r}_{21}$, which connects the two holes. Furthermore, velocity $\vec{v} = \vec{v}_1 = -\vec{v}_2$ rotates in the same manner as $\vec{r}_{21}$, although the phase is shifted by one quarter period. We use trivial goniometric operations to obtain a simple-shaped term.

$$x_{3z} = \vec{x}_3 \cdot \frac{\vec{r}_{21}}{r_{21}} = x_3\cos(\omega t)$$

$$\vec{v}\cdot\vec{v}_3 = vv_3\cos\left(\omega t - \frac{\pi}{2}\right) = vv_3\sin(\omega t)$$

$$\frac{x_{3z}}{x_3^3}(\vec{v}\cdot\vec{v}_3) = \frac{vv_3}{x_3^2}\sin(\omega t)\cos(\omega t) = \frac{vv_3}{x_3^2}\frac{1}{2}\sin(2\omega t)$$

$$\frac{4m^3}{r}\frac{x_{3z}}{x_3^3}(\vec{v}\cdot\vec{v}_3) = \frac{2m^3}{r}\frac{vv_3}{x_3^2}\sin(2\omega t)$$

The coordinate system we just transformed into is rotating. Our Cartesian-like z-axis is now given by $\vec{z} = \vec{r}_{21}$. That requires a bit of comment on interpretation of the following plots. Planes characterised by $z = const.$ in plots are orbiting with frequency ω rather than static.

Substituting the above into Lagrangian we arrive at

$$\begin{aligned} L_{BH3C2F2} = -\frac{3}{2}m_3\Bigg(&- \frac{v_3^2}{3} + \frac{2}{3} + 4m^2v^2\left[\frac{1}{x_3^2} + \frac{2}{x_3 r} + \frac{2m}{x_3 r^2} + \frac{m_3}{x_3^2 r}\right] + \\ &+ \left[\frac{1}{x_3} + \frac{2m}{x_3^2} + \frac{m_3}{x_3^2}\right] 2m\left[v^2 + v_3^2\right] + \frac{2m^3}{r}\frac{vv_3}{x_3^2}\sin(2\omega t)\Bigg). \end{aligned} \tag{4.27}$$

The Lagrangian L_{BH3C2F} describes asymptotically free motion. The straightness of the path at later times in figures, again, agrees with this observation, matching our expectation based on Newtonian physics.

$$\lim_{x_3\to\infty}\frac{\partial L_{BH3C2F}}{\partial {v_3}^i} = m_3 v_3^i$$

[6]Legend to the subscript: BH3-3rd black hole, C-circular, 2-2nd order, F-full and includes free terms, 1-the first written form.

4.5 | Comparison of results

Comparing 1st and 2nd order approximation

The 1st order Lagrangian allows a black hole of low-mass, compared to that of the binary. We will study numerically the deviation of solutions of equations of motion associated with the 1st and 2nd order Lagrangian.

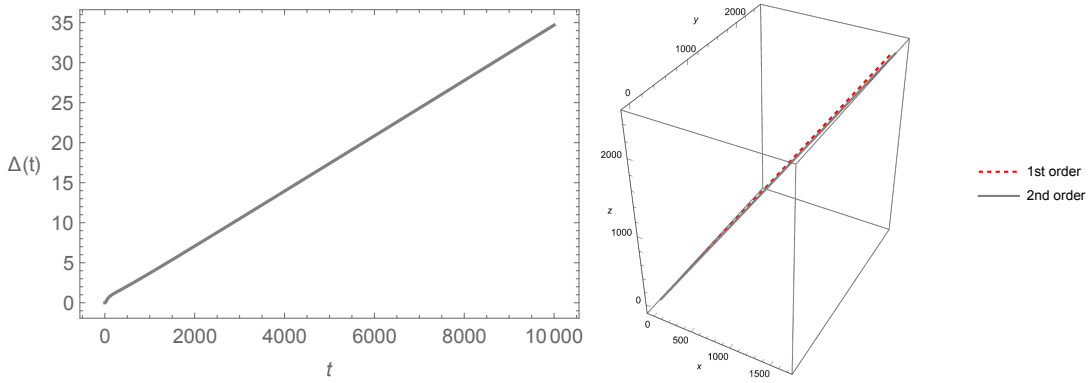

(a) Δ is deviation of the 1st and 2nd order solution (b) Both solutions in one plot.

Figure 4.5: Comparison of plots, numerical solution to the EoMs associated with the 1st and 2nd order Lagrangian of the 3rd black hole, $m_3 \ll m$. System of two rotating black holes is located in the vicinity of origin. Initial conditions: $\vec{x}_3(t_0) = (10, 10, 10)$, $\vec{v}_3(t_0) = (-0.05, 0, 0)$. Deviation is a distance between the two solutions at each time, $\Delta = \sqrt{\delta x^2 + \delta y^2 + \delta z^2}$.

Comparing mass limits in the 2nd order

The 2nd order Lagrangian allows not only the limit of a small hole, but also the limit of large black hole! This result is worth the effort. The dependence on m_3 is more complicated than just proportionality. We can separate motions of the third black hole into two classes, representing the two limits. The first, $m_3 \ll m$, results in scattering and the second, $m_3 \gg m$, results in coalescence. The particular value of m_3 is entirely our choice. Limit of large black hole brings an interesting behavior. The limit of a small black hole is convenient for later comparison with motion of an extremally charged test particle.

– Collinear initial velocity and position

We show the difference between $m_3 \gg m$ and $m_3 \ll m$ black hole in the second-order. The case of collinear initial velocity and position (small velocity heading away from origin) reveals a surprising difference between the two limits. The **low-mass** black hole $m_3 \lesssim 30m$ is ***repelled***, while the interaction between

a **very heavy** black hole and orbiting binary causes they are ***attracted*** towards each other[7].

Let us compare both paths at Figure 4.6. In Figure 4.7 one can see the radial measure of the black hole from origin. Figure 4.8 shows velocities of the hole in x-direction, there is one-to-one correspondence with the paths of Figure 4.7.

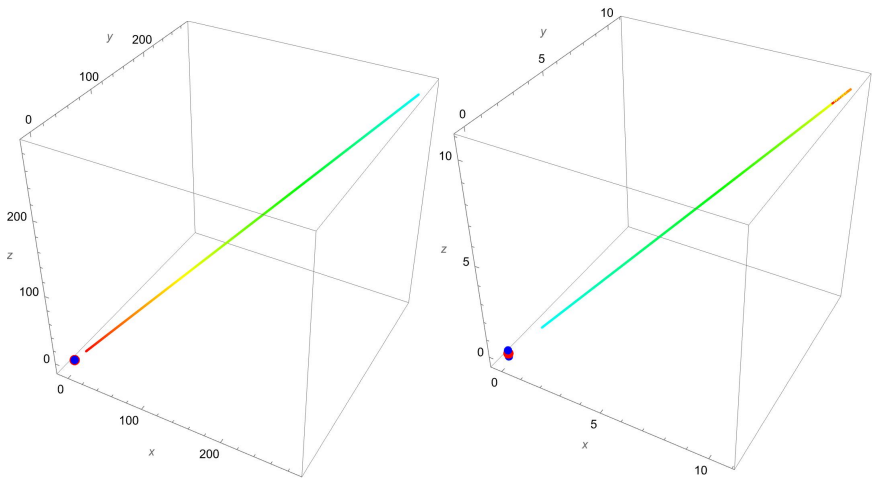

(a) $0.01m = m_3 \ll m$, escapes (b) $500m = m_3 \gg m$, dragged back

Figure 4.6: Comparison of two mass limits (heavy and light). Motion of the 3rd black hole associated with the 2nd order Lagrangian. System of two black holes $m_1 = m_2 \equiv m$ orbits in the vicinity of origin. Initial conditions $\vec{x}_3(t_0) = (10, 10, 10)$, $\vec{v}_3(t_0) = (0.05, 0.05, 0.05)$. While the small black hole escapes, the heavy one recedes for some time, then reaches the turning point and flies back towards the binary.

[7]Considering Newton's Third Law: Action & Reaction, there is no need of specifying which object is being attracted and which actually attracts. Let us understand attracting of m_3 and the binary in this way throughout this chapter.

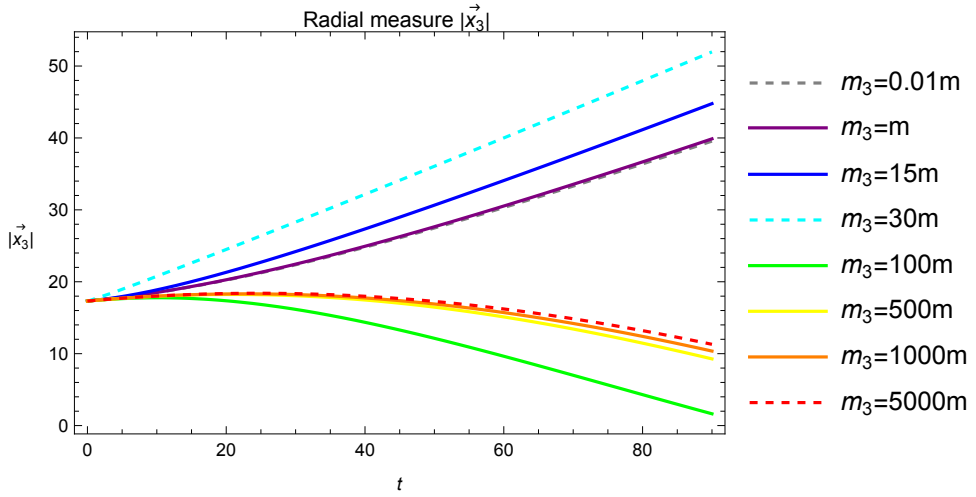

Figure 4.7: Comparison of radial measure of the 3rd BH from origin $|\vec{x}_3| = \sqrt{x_{3_x}^2 + x_{3_y}^2 + x_{3_z}^2}$ for various m_3, m is the mass of each orbiting BH. Initial conditions $\vec{x}_3(t_0) = (10, 10, 10)$, $\vec{v}_3(t_0) = (0.05, 0.05, 0.05)$. Corresponding velocities are at Figure 4.8. $m_3 = m$ is the case of three equally massive BHs.

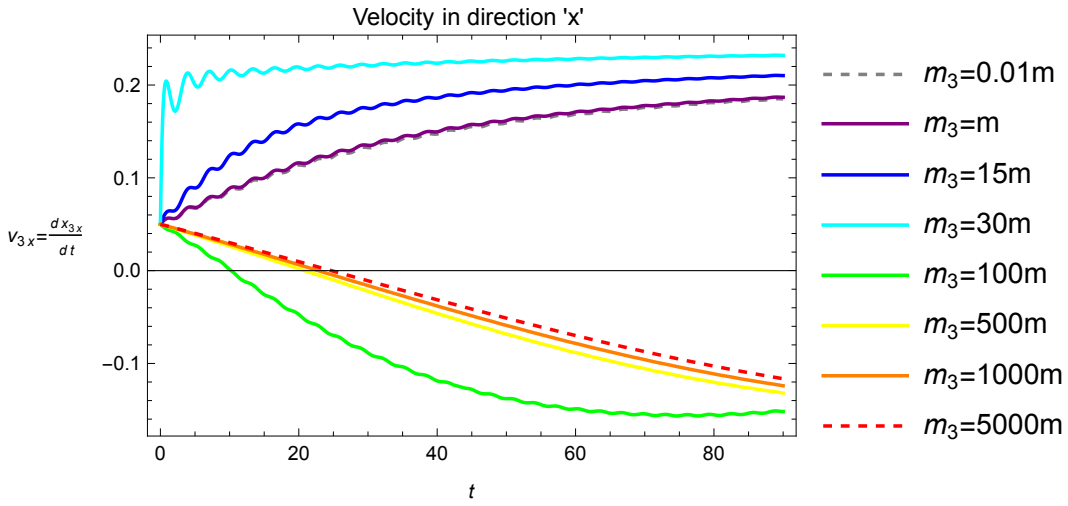

Figure 4.8: Comparison of velocity in x-direction of the 3rd BH various m_3, initial conditions: $\vec{x}_3(t_0) = (10, 10, 10)$, $\vec{v}_3(t_0) = (0.05, 0.05, 0.05)$. For this init. conditions the directions are equivalent, we chose x. Corresponds to radial measures in Figure 4.7. The smaller holes show signs of wavy-like behavior.

z-axis

As one would expect according to the preceding discussion, the small black hole escapes with ease, while the large one attracts the binary, see Figure 4.9.

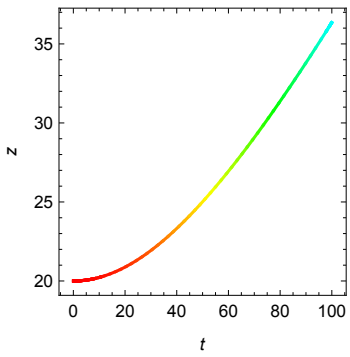

(a) $m_3 \ll m$ BH is repelled.

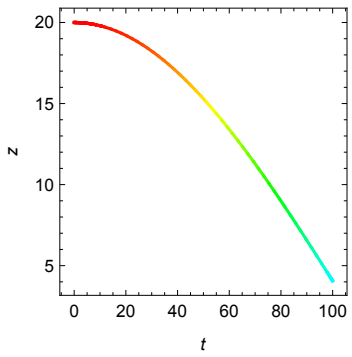

(b) $m_3 \gg m$ is attracted (and attracting, too).

Figure 4.9: Comparing evolution of the low- and large-mass black hole on z-axis. System of two rotating black holes $m_1 = m_2 = m$ is located in the vicinity of origin. Initial conditions: $\vec{x}_3(t_0) = (0, 0, 20)$, $\vec{v}_3(t_0) = (0, 0, 0)$.

$z = 0$ plane

Another case of evolution within $z = 0$ plane is shown in Figure 4.10.

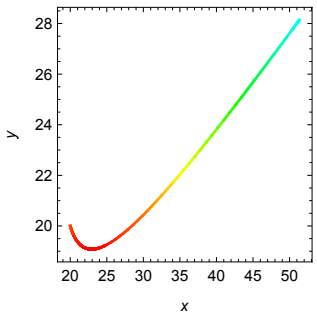

(a) $m_3 \ll m$ is repelled.

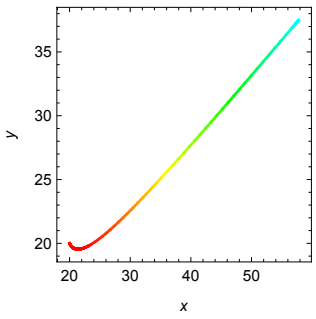

(b) $m_3 = 30m$ is still repelled.

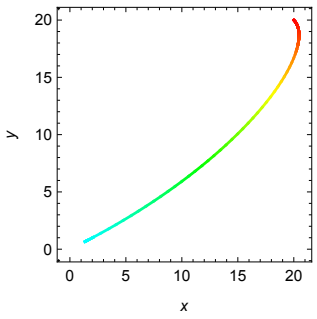

(c) $m_3 \gg m$ is attracted (and attracting, too).

Figure 4.10: Comparing evolution of the small, medium and large-mass black hole within $z = 0$ plane. System of two extremally charged mutually orbiting black holes $m_1 = m_2 = m$ is located in the vicinity of origin. Initial conditions: $\vec{x}_3(t_0) = (20, 20, 0)$, $\vec{v}_3(t_0) = (0.05, -0.05, 0)$. Based on z-axis motion, the results match our expectations.

Conclusion

Expecting similar outcomes grounded in physics, we studied motion of a smaller charged black hole and of a charged test particle on the background of an orbiting charged binary black hole. Restricting to slow-motion limit and extremally charged bodies, we aimed to compare their evolution.

In Chapter 1 we covered the basic properties of static spacetimes, namely the Majumdar-Papapetrou (MP) solution and its detailed derivation in Section 1.3.

In Chapter 2 we started with the general exact action and reproduced a tedious derivation of approximate action up to the order $\mathcal{O}(v^2)$. Our result contains exactly the right terms of the action of [5] but also several redundant terms, which seem difficult to get rid off. During further calculation we assumed that the paper [5] is correct and discarded the remaining terms.

As an aside, we showed that the ADM mass of a perturbed MP system is the same as that of a static one.

Then we solved the set of equations obtained by varying the action. The general form of perturbation was found in Chapter 3. Surprisingly, based on the symmetries of our rotating system, the perturbation vanished.

Afterwards, in Section 3.2, we compared motion of some selected test particles with a charge-to-mass ratio $\kappa = (-1, 0, 1)$ via equation of electro-geodesic.

We showed that the evolution of the test particles in the field of two extremally charged black holes orbiting each other obeys the laws of electrostatics in the leading order. The initially static position of $\kappa = 1$ was studied numerically and analytically via the electro-geodesic equation. Both approaches resulted in a fixed position of the test particle throughout its evolution. The particle with $\kappa = 1$ moving along the z-axis can pass through the origin and escape to infinity, according to symmetries, whilst $\kappa = (-1, 0)$ particles after passing the origin reach the turning point and harmonically oscillate.

In Chapter 4 we studied the motion of an extremally charged massive black hole. Starting with the general n-body Lagrangian, we first reproduced the two-body Lagrangian and its consequences for the evolution, describing our background. Calculation of the three-body Lagrangian required a new approximating technique based on separation of integration area into several parts, since most of the integrals were not analytically solvable.

The Lagrangian of the third black hole describes asymptotically free motion up to the second order (consistent with Newtonian mechanics). The second-order Lagrangian also allows the limit of the third black hole-mass much larger that those of its binary components, unlike the first order. This case results in the coalescence of the third black hole and the binary system.

The goal of the thesis was to compare the motion of the smaller black hole and of an extremally charged test particle. The static initial position in electro-geodesic equation provided us with a static solution.

We concluded, that the black hole evolves in a totally different way. The smaller black hole is repelled throughout its evolution and ultimately escapes.

Based on our calculations, the outcome is that, perhaps surprisingly, there is no straightforward analogy between the motion of the small black hole in the field of a massive binary, consisting of two extremally charged black holes, and

the motion of an extremally charged test-particle managed by the field of the massive black-hole binary. According to the recent observations of motions of heavy objects near the center of the Galaxy, where small-distance encounters and scattering seem to occur frequently, these results might be of interest. In our future work, we will attempt to drop some of the assumptions used here to investigate various cases not covered here.

Appendix A: Calculation of three-body Lagrangian

The three-body Lagrangian reads

$$\begin{aligned}\text{perturbation} \equiv -\frac{3}{8\pi}\int\Bigg(&\frac{2m_3\left(\frac{m_1}{r_1}+\frac{m_2}{r_2}+1\right)\left(\frac{m_1m_2\ \vec{r}_1\cdot\vec{r}_2|\vec{v}_1-\vec{v}_2|^2}{r_1^3r_2^3}\right)}{r_3}\\
&+\frac{m_3^2\left(\frac{m_1m_2\ \vec{r}_1\cdot\vec{r}_2|\vec{v}_1-\vec{v}_2|^2}{r_1^3r_2^3}\right)}{r_3^2}\\
&+\frac{\frac{m_1m_3\ \vec{r}_1\cdot\vec{r}_3|\vec{v}_1-\vec{v}_3|^2\left(\frac{m_1}{r_1}+\frac{m_2}{r_2}+1\right)^2}{r_1^3}+\frac{m_2m_3\ \vec{r}_2\cdot\vec{r}_3|\vec{v}_2-\vec{v}_3|^2\left(\frac{m_1}{r_1}+\frac{m_2}{r_2}+1\right)^2}{r_2^3}}{r_3^3}\\
&+\frac{\frac{2m_1m_3^2\ \vec{r}_1\cdot\vec{r}_3|\vec{v}_1-\vec{v}_3|^2\left(\frac{m_1}{r_1}+\frac{m_2}{r_2}+1\right)}{r_1^3}+\frac{2m_2m_3^2\ \vec{r}_2\cdot\vec{r}_3|\vec{v}_2-\vec{v}_3|^2\left(\frac{m_1}{r_1}+\frac{m_2}{r_2}+1\right)}{r_2^3}}{r_3^4}\\
&+\frac{\frac{m_1m_3^3\ \vec{r}_1\cdot\vec{r}_3|\vec{v}_1-\vec{v}_3|^2}{r_1^3}+\frac{m_2m_3^3\ \vec{r}_2\cdot\vec{r}_3|\vec{v}_2-\vec{v}_3|^2}{r_2^3}}{r_3^5}\Bigg)\mathrm{d}^3x.\end{aligned} \tag{28}$$

In Section 4.3 Three-body Lagrangian we sketched an example process which we follow in derivation of the Lagrangian, we also described the integration strategy in detail. The whole calculation proceeds in a similar manner. We will not reproduce the paragraph here, on the contrary, we will continue with calculation. Let us reproduce here Figure 4.3, depicting the splitting of integration domain.

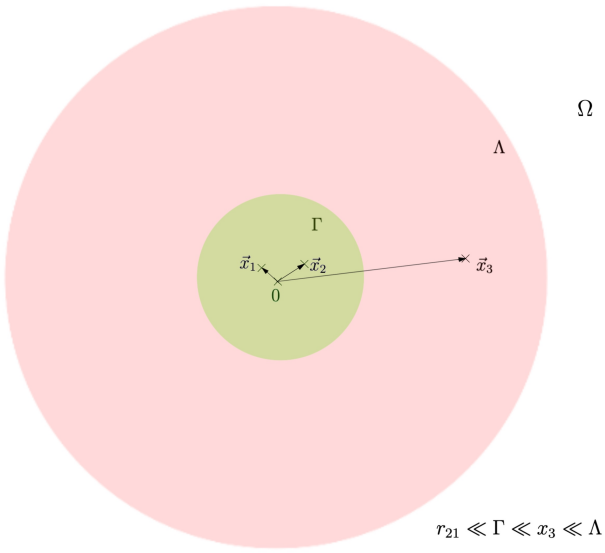

Figure 11: Separating integration domain into three parts, each of which either contributes significantly (Γ, Λ) or negligibly (Ω). The definition is $r_{21} \ll \Gamma \ll x_3 \ll \Lambda$. In each of these regions the particular integrals simplify significantly.

We also repeat the shift of coordinates, used, in variations, in most of the calculations.

$$\vec{r}_2 = \vec{x} - \vec{x}_2 = \vec{y}, \quad \vec{r}_1 = \vec{x} - \vec{x}_1 = \vec{y} + \vec{x}_2 - \vec{x}_1 \equiv \vec{y} - \vec{r}_{21} \tag{29}$$

We denote the i-th line of (28) as by "pert(i)" for better orientation during calculation, $\vec{r}_a = \vec{x} - \vec{x}_a$ is shifted Cartesian position of the a-th black hole, its velocity is (of course, independent of position) $\vec{v}_a = \frac{\mathrm{d}\vec{x}_a}{\mathrm{d}t}$. Moreover, Γ and Λ denote either the part of 3-dim integration domain, or, in locally spherical coordinates, the boundary of radius coordinate. We tried to avoid ambiguities, the meaning should be clear during evaluation.

1st line of perturbation

To summarize results from Section 4.3, the first line and integral associated with unity from the RHS parenthesis read

$$-\frac{8\pi}{3}\cdot \mathrm{pert}(1) = 2m_1m_2m_3\left|\vec{v}_1-\vec{v}_2\right|^2 \int \left(\frac{m_1}{r_1}+\frac{m_2}{r_2}+1\right)\frac{\vec{r}_1\cdot\vec{r}_2}{r_1^3r_2^3}\frac{1}{r_3}\,\mathrm{d}^3x. \tag{30}$$

$$I_1 = \int \frac{\vec{r}_1\cdot\vec{r}_2}{r_1^3r_2^3}\frac{1}{r_3}\,\mathrm{d}^3x = \frac{4\pi}{x_3 r_{12}} - \frac{2\pi}{x_3^2}.$$

Note, that the $|\vec{r}_{12}| = r_{12} = r_{21}$ is a fixed constant distance between two black holes rather than a free parameter. Its physical value is given uniquely by the mass ratio of the two extremally charge mutually orbiting black holes [19], for two equally massive holes it is [4]

$$r_{12} = \frac{\sqrt{3}-1}{2}.$$

Another contributing terms are associated with $\frac{m_1}{r_1}$, $\frac{m_2}{r_2}$ in the parenthesis on RHS of (30). It is enough to calculate one of the only, since both of these terms contribute in the same way (however with indices swapped $\vec{r}_{12} \leftrightarrow \vec{r}_{21}$). We denote them as I_2 and I_2'.

$$I_2 = \int \frac{m_1}{r_1}\frac{\vec{r}_1\cdot\vec{r}_2}{r_1^3r_2^3}\frac{1}{r_3}\mathrm{d}^3x = m_1\left(\int_\Gamma \frac{\vec{r}_1\cdot\vec{r}_2}{r_1^4r_2^3r_3}\mathrm{d}^3x + \int_\Lambda \frac{\vec{r}_1\cdot\vec{r}_2}{r_1^4r_2^3r_3}\mathrm{d}^3x\right) \equiv m_1\left(I_{2\Gamma}+I_{2\Lambda}\right)$$

$$I_2' = \int \frac{m_2}{r_2}\frac{\vec{r}_1\cdot\vec{r}_2}{r_1^3r_2^3}\frac{1}{r_3}\mathrm{d}^3x$$

In the following we split the integration domain as in Figure 11. In the vicinity of the two holes it holds

$$\forall \vec{x}\in\Gamma: \quad r_3 = |\vec{x}-\vec{x}_3| \approx |\vec{x}_3| = \mathrm{const.} \tag{31}$$

We introduce the shift of coordinates (29) and then transform into locally spherical coordinates.

$$\begin{aligned} I_{2\Gamma} &= \int_\Gamma \frac{\vec{r}_1\cdot\vec{r}_2}{r_1^4 r_2^3}\frac{1}{r_3}\mathrm{d}^3x \doteq \frac{1}{x_3}\int_\Gamma \frac{\vec{r}_1\cdot\vec{r}_2}{r_1^4 r_2^3}\mathrm{d}^3x = \frac{1}{x_3}\int_\Gamma \frac{(\vec{y}-\vec{r}_{21})\cdot\vec{y}}{|\vec{y}-\vec{r}_{21}|^4 y^3}\mathrm{d}^3y = \\ &= \frac{1}{x_3}\int_0^{2\pi}\mathrm{d}\phi\int_{-1}^{1}\mathrm{d}(\cos\theta)\left(\int_0^\Gamma \frac{y - r_{21}\cos\theta}{\sqrt{y^2+r_{21}^2-2yr_{21}\cos\theta}^4}\mathrm{d}y\right) \\ &= \frac{2\pi}{x_3}\left(-\frac{1}{2}\right)\int_{-1}^{1}\mathrm{d}(\cos\theta)\left[\frac{1}{y^2+r_{21}^2-2yr_{21}\cos\theta}\right]_{y=0}^{y=\Gamma} = \\ &= \frac{\pi}{x_3 r_{21}}\left(\frac{2}{r_{21}} - \frac{1}{\Gamma}\log\left|\frac{r_{21}+\Gamma}{r_{21}-\Gamma}\right|\right) \xrightarrow{\Gamma\gg r_{21}} \frac{2\pi}{x_3 r_{21}^2} \end{aligned} \tag{32}$$

The logarithmic term is, indeed, a consequence of finiteness of the integration region. However, in vanishes in the last step after performing the limit based on our choice $r_{21} \ll \Gamma$.

Now let us compute the contribution of Λ, i.e. we are far away from origin $x_1, x_2 \ll x$. Then we have

$$\forall \vec{x}\in\Lambda: \quad r_1 = |\vec{x}-\vec{x}_1| \approx |\vec{x}| \approx |\vec{x}-\vec{x}_2| = r_2. \tag{33}$$

We introduce locally spherical coordinates as in (4.20).

$$\begin{aligned} I_{2\Lambda} &= \int_\Lambda \frac{\vec{r}_1\cdot\vec{r}_2}{r_1^4 r_2^3}\frac{1}{r_3}\,\mathrm{d}^3x \doteq \int_\Lambda \frac{\vec{x}\cdot\vec{x}}{x^4 x^3}\frac{1}{|\vec{x}-\vec{x}_3|}\,\mathrm{d}^3x = \int_\Lambda \frac{\mathrm{d}^3x}{x^5|\vec{x}-\vec{x}_3|} = \\ &= \frac{2\pi}{x_3}\int_\Gamma^\Lambda \frac{|x+x_3|-|x-x_3|}{x^4}\mathrm{d}x = \frac{2\pi}{x_3}2\int_\Gamma^{x_3}\frac{1}{x^3}\mathrm{d}x + \frac{2\pi}{x_3}2x_3\int_{x_3}^\Lambda\frac{1}{x^4}\mathrm{d}x = \\ &= \frac{4\pi}{x_3}\left(\frac{-1}{2}\right)\left[\frac{1}{x^2}\right]_\Gamma^{x_3} + 4\pi\left(-\frac{1}{3}\right)\left[\frac{1}{x^3}\right]_{x_3}^\Lambda = \\ &= -\frac{2\pi}{x_3}\left[\frac{1}{x_3^2}-\frac{1}{\Gamma^2}\right] + \frac{4\pi}{3}\left[\frac{1}{x_3^3} - \cancelto{0}{\frac{1}{\Lambda^3}}\right] = \\ &= -\frac{2\pi}{3}\frac{1}{x_3^3} + \frac{2\pi}{x_3}\cancel{\frac{1}{\Gamma^2}} \end{aligned} \tag{34}$$

The "orange" term in (34) can be neglected with respect to the result of (32), according to $r_{21} \ll \Gamma$. All of the dangerous terms from pert(1) that could blow up, are now discarded. As discussed, we obtain I_2' from I_2 by the exchange of indices 1, 2 and arrive at

$$I_2 = m_1\left[\frac{2\pi}{x_3}\frac{1}{r_{21}^2} - \frac{2\pi}{3}\frac{1}{x_3^3}\right], \qquad I_2' = m_2\left[\frac{2\pi}{x_3}\frac{1}{r_{21}^2} - \frac{2\pi}{3}\frac{1}{x_3^3}\right].$$

To summarize this, we have

$$\begin{aligned}\mathrm{pert}(1) = -\frac{3}{2} m_1 m_2 m_3 \left|\vec{v}_1 - \vec{v}_2\right|^2 \left(\frac{2}{x_3}\frac{1}{r_{12}} + \frac{1}{x_3^2} + \right. \\ \left. + (m_1 + m_2)\left[\frac{1}{x_3}\frac{1}{r_{21}^2} - \frac{1}{x_3^3}\right]\right).\end{aligned} \tag{35}$$

Similarly we will proceed with the remaining integrals.

2nd line of the perturbation

Till now we introduced several ways how to integrate effectively the mixed terms, so we can have a look at terms of higher order in m_3. Concerning the second order, we work with pert(2) and pert(4).

$$\mathrm{pert}(2) = -\frac{3}{8\pi} m_3^2 m_1 m_2 |\vec{v}_1 - \vec{v}_2|^2 \underbrace{\int \frac{\vec{r}_1 \cdot \vec{r}_2}{r_1^3 r_2^3}\frac{1}{r_3^2}\mathrm{d}^3 x}_{K_1} \tag{36}$$

Due to the mixed denominator we have to split the integration domain to Γ and Λ, i.e.,

$$K_1 = K_{1\Gamma} + K_{1\Lambda}.$$

In the following lines we first use $x \ll x_3$ as (31) and then within the same procedure as in (4.19) we arrive at the result.

$$\begin{aligned}K_{1\Gamma} = \int_\Gamma \frac{\vec{r}_1 \cdot \vec{r}_2}{r_1^3 r_2^3}\frac{1}{r_3^2}\mathrm{d}^3 x = \int_\Gamma \frac{(\vec{x} - \vec{x}_1)\cdot(\vec{x} - \vec{x}_2)}{|\vec{x} - \vec{x}_1|^3\ |\vec{x} - \vec{x}_2|^3}\frac{1}{|\vec{x} - \vec{x}_3|^2}\mathrm{d}^3 x \doteq \\ \doteq \frac{1}{x_3^2}\int_\Gamma \frac{\vec{r}_1 \cdot \vec{r}_2}{r_1^3 r_2^3}\mathrm{d}^3 x = \frac{1}{x_3^2}\frac{4\pi}{r_{12}}\end{aligned} \tag{37}$$

In Λ we use (33) and the shift of coordinates $\vec{x} - \vec{x}_3 = \vec{y}$, then transform into locally spherical coordinates and finally some simple algebraic manipulations. Neglecting the terms which are associated with finiteness of the integration region always involves either the limit $\Lambda \gg x_3$ (occassionally $\Lambda \to \infty$) or $\Gamma \ll x_3$, we neglect

with respect to corresponding larger terms.

$$
\begin{aligned}
K_{1\Lambda} &= \int_\Lambda \frac{\vec{r}_1\cdot\vec{r}_2}{r_1^3 r_2^3}\frac{1}{r_3^2}\mathrm{d}^3x = \int_\Lambda \frac{(\vec{x}-\vec{x}_1)\cdot(\vec{x}-\vec{x}_2)}{|\vec{x}-\vec{x}_1|^3\ |\vec{x}-\vec{x}_2|^3}\frac{1}{|\vec{x}-\vec{x}_3|^2}\mathrm{d}^3x \doteq \\
&\doteq \int_\Lambda \frac{\vec{x}\cdot\vec{x}}{x^6}\frac{1}{|\vec{x}-\vec{x}_3|^2}\mathrm{d}^3x = \\
&= \int_0^{2\pi}\mathrm{d}\phi\int_{-1}^{1}\mathrm{d}(\cos\theta)\left(\int_\Gamma^\Lambda \mathrm{d}x\frac{\cancel{x^2}}{\cancel{x^2}\ x^2}\frac{1}{x^2+x_3^2-2xx_3\cos\theta}\right) \\
&= 2\pi\left[-\frac{1}{xx_3^2}+\frac{1}{4x^2x_3^3}\left(x^2-x_3^2\right)\left(\log(x+x_3)^2-\log(x-x_3)^2\right)\right]_{x=\Gamma}^{x=\Lambda} \\
&= 2\pi\left[-\frac{1}{xx_3^2}+\frac{1}{4x^2x_3^3}\left(x^2-x_3^2\right)\ 2\log\frac{|x+x_3|}{|x-x_3|}\right]_{x=\Gamma}^{x=\Lambda} \qquad (38)\\
&= 2\pi\Bigg(-\frac{1}{x_3^2}\frac{1}{\cancel{\Lambda}}+\frac{1}{x_3^2\Gamma}+\underbrace{\frac{1}{4\Lambda^2x_3^3}\left(\Lambda^2-x_3^2\right)\ 2\log\frac{|\Lambda+x_3|}{|\Lambda-x_3|}}_{\to 0} \\
&\qquad -\frac{1}{4\Gamma^2x_3^3}\left(\cancel{\Gamma}^2-x_3^2\right)\ 2\log\frac{|\Gamma+x_3|}{|\Gamma-x_3|}\Bigg) = \\
&= 2\pi\left(\frac{1}{x_3^2\Gamma}+\frac{1}{2x_3}\frac{1}{\Gamma^2}\log\frac{|\Gamma+x_3|}{|\Gamma-x_3|}\right) \\
&= \frac{4\pi}{x_3^2\ \Gamma}
\end{aligned}
$$

Moving to the very last last line we used a Taylor series of the function and

$$
\lim_{\frac{\Gamma}{x_3}\to 0}\left(\frac{1}{\frac{\Gamma^2}{x_3^2}}\frac{1}{x_3^2}\log\frac{|\frac{\Gamma}{x_3}+1|}{|\frac{\Gamma}{x_3}-1|}\right) = \frac{1}{x_3^2}\left(\frac{2x_3}{\Gamma}+\frac{2}{3}\frac{\cancel{\Gamma}^{0}}{\cancel{x_3}}+\underbrace{O\left(\frac{\Gamma}{x_3}\right)^3}_{\to 0}\right). \qquad (39)
$$

In (40) we use an obvious inequality based on our choice of parameters $\frac{1}{r_{21}} \gg \frac{1}{\Gamma}$

$$
\mathrm{pert}(2) = -\frac{3}{2}m_3^2m_1m_2|\vec{v}_1-\vec{v}_2|^2\left(\frac{1}{x_3^2}\frac{1}{r_{12}}-\frac{1}{x_3^2}\frac{1}{\cancel{\Gamma}}\right) \doteq -\frac{3}{2}m_3^2m_1m_2\frac{|\vec{v}_1-\vec{v}_2|^2}{x_3^2\ r_{12}}. \qquad (40)
$$

3rd line of the perturbation

The 3rd line reads

$$\begin{aligned}\mathrm{pert}(3) &= -\frac{3}{8\pi}\sum_{i=1}^{2} m_i m_3 \ |\vec{v}_i - \vec{v}_3|^2 \int \mathrm{d}^3x \frac{\vec{r}_i\cdot\vec{r}_3}{r_i^3 r_3^3}\left(\frac{m_1}{r_1}+\frac{m_2}{r_2}+1\right)^2 = \\ &= -\frac{3}{8\pi} m_1 m_3 \ |\vec{v}_1 - \vec{v}_3|^2 \int \mathrm{d}^3x \Bigg[\underbrace{\frac{\vec{r}_1\cdot\vec{r}_3}{r_1^3 r_3^3}}_{J_1} + 2m_1 \underbrace{\frac{\vec{r}_1\cdot\vec{r}_3}{r_1^4 r_3^3}}_{J_2} \\ &\quad + 2m_2 \underbrace{\frac{\vec{r}_1\cdot\vec{r}_3}{r_1^3 r_2 r_3^3}}_{J_3} + m_1^2 \underbrace{\frac{\vec{r}_1\cdot\vec{r}_3}{r_1^5 r_3^3}}_{J_4} + 2m_1 m_2 \underbrace{\frac{\vec{r}_1\cdot\vec{r}_3}{r_1^4 r_2 r_3^3}}_{J_5} + m_2^2 \underbrace{\frac{\vec{r}_1\cdot\vec{r}_3}{r_1^3 r_2^2 r_3^3}}_{J_6} \Bigg] \\ &\quad + \Big[\text{the same with swapped } \{1 \leftrightarrow 2\}\Big].\end{aligned} \tag{41}$$

We have six independent integrals, with of which we have to deal in quite a different manner. We already know, how to integrate J_1, J_2 and J_4 exactly from the section about Lagrangian of two black holes. First we introduce the shift of coordinates

$$\vec{x} - \vec{x}_1 = \vec{y}, \quad \vec{x} - \vec{x}_3 = \vec{y} - \vec{r}_{31}$$

and then transfer into spherical coordinates $\mathrm{d}^3y = y^2\mathrm{d}y\ \mathrm{d}(\cos\theta)\mathrm{d}\phi$, analogically for all of these three integrals.

$$\begin{aligned} J_1 &:= \int \frac{\vec{r}_1\cdot\vec{r}_3}{r_1^3 r_3^3}\mathrm{d}^3x = \int \frac{(\vec{x}-\vec{x}_1)\cdot(\vec{x}-\vec{x}_3)}{|\vec{x}-\vec{x}_1|^3|\vec{x}-\vec{x}_3|^3}\mathrm{d}^3x = \int \frac{\vec{y}\cdot(\vec{y}-\vec{r}_{31})}{y^3|\vec{y}-\vec{r}_{31}|^3}\mathrm{d}^3y = \\ &= 2\pi\int_{-1}^{1}\mathrm{d}(\cos\theta)\int_0^\infty \frac{y - r_{31}\cos\theta}{(y^2 + r_{31}^2 - 2yr_{31}\cos\theta)^{\frac{3}{2}}}\mathrm{d}y = \frac{4\pi}{r_{31}} \\ J_2 &:= \int \frac{\vec{r}_1\cdot\vec{r}_3}{r_1^4 r_3^3}\mathrm{d}^3x = \frac{2\pi}{r_{13}^2} \\ J_4 &:= \int \frac{\vec{r}_1\cdot\vec{r}_3}{r_1^5 r_3^3}\mathrm{d}^3x = \frac{4}{3}\frac{\pi}{r_{13}^3} \end{aligned} \tag{42}$$

The exact part of this job has already been done and now we shall have a look at the remaining integrals, compound of mixed terms, i.e. J_3, J_5 and J_6.

The denominator of J_3 is of the mixed form $r_1^m r_2^n r_3^o$ with nonzero exponents, hence we have to split the integration area to Γ & Λ regions,

$$J_3 = J_{3\Gamma} + J_{3\Lambda}.$$

In the area Γ we use the traditional feature $r_3 \approx x_3$. Then we introduce the shift of coordinates $\vec{x} - \vec{x}_1 = \vec{y}$, $\vec{x} - \vec{x}_2 = \vec{y} - \vec{r}_{21}$. We use the relationship of local spherical coordinates and cartesian coordinates, i.e., $y_x = |y|\sin\theta\cos\phi$, $y_y = |y|\sin\theta\sin\phi$, $y_z = |y|\cos\theta$, moreover we set z-axis parallel to $\vec{r}_{21}$, so that θ measures deviation of $\vec{y}$ and $\vec{r}_{21}$. We observe that due to $\int_0^{2\pi}\cos\phi\mathrm{d}\phi = \int_0^{2\pi}\sin\phi\mathrm{d}\phi = 0$ only the 3rd term $x_{3z}y_z$ from the dot product of numerator in the 3rd line is

nonzero. At the final step in (43) we perform the limit $\Gamma \gg r_{21}$, after which we obtain the result.

$$
\begin{aligned}
J_{3\Gamma} &:= \int \frac{\vec{r}_1 \cdot \vec{r}_3}{r_1^3 r_2 r_3^3}\, \mathrm{d}^3x = \int \frac{(\vec{x}-\vec{x}_1)\cdot(\vec{x}-\vec{x}_3)}{|\vec{x}-\vec{x}_1|^3|\vec{x}-\vec{x}_2||\vec{x}-\vec{x}_3|^3}\mathrm{d}^3x \doteq \\
&\doteq -\frac{\vec{x}_3}{x_3^3}\cdot\int \frac{\vec{x}-\vec{x}_1}{|\vec{x}-\vec{x}_1|^3|\vec{x}-\vec{x}_2|}\mathrm{d}^3x = -\frac{\vec{x}_3}{x_3^3}\cdot\int \frac{\vec{y}}{y^3|\vec{y}-\vec{r}_{21}|}\mathrm{d}^3y = \\
&= -\frac{1}{x_3^3}\int_0^{2\pi}\int_0^{\pi}\int_0^{\Gamma} y\frac{x_{3x}\sin\theta\cos\phi + x_{3y}\sin\theta\sin\phi + x_{3z}\cos\theta}{y^3\sqrt{y^2+r_{21}^2-2yr_{21}\cos\theta}}\times \\
&\qquad\qquad \times y^2\mathrm{d}y\sin\theta\mathrm{d}\theta\mathrm{d}\phi \\
&= -\frac{2\pi}{x_3^3}\int_0^{\Gamma}\int_{-1}^{1}\frac{x_{3z}\cos\theta}{\sqrt{y^2+r_{21}^2-2yr_{21}\cos\theta}}\mathrm{d}(\cos\theta)\mathrm{d}y = \\
&= -\frac{2\pi x_{3z}}{x_3^3}\int_0^{\Gamma}\frac{\sqrt{(r_{21}+y)^{\,2}}\,(y^2-r_{21}y+r_{21}^2)}{3r_{21}^2y^2} \\
&\qquad\qquad -\frac{\sqrt{(y-r_{21})^{\,2}}\,(y^2+r_{21}y+r_{21}^2)}{3r_{21}^2y^2}\mathrm{d}y \\
&= -\frac{2\pi x_{3z}}{x_3^3}\left[\frac{\frac{\sqrt{(r_{21}+y)^2}\left(y^3-2r_{21}^3\right)}{r_{21}+y} - \frac{\sqrt{(y-r_{21})^2}\left(2r_{21}^3+y^3\right)}{y-r_{21}}}{6r_{21}^2y}\right]_{y=0}^{y=\Gamma\gg r_{21}} = \\
&= 0
\end{aligned}
\tag{43}
$$

We proceed with Λ, in the following integral we first shift the coordinates and again use the salient feature of actual integration domain $r_1 \approx x \approx r_2$. During transition from the 3rd line from the end to the 2nd line from the end we use

$$
\begin{aligned}
&[x-x_3>0]...x\in[x_3,\Lambda] \to |x-x_3| = x-x_3 \\
&[x-x_3<0]...x\in[\Gamma,x_3] \to |x-x_3| = -x+x_3 \\
&[x+x_3>0]...\forall x\in[\Gamma,\Lambda], \qquad \frac{a}{|a|} = \mathrm{sign}(a),
\end{aligned}
\tag{44}
$$

$$
\begin{aligned}
J_{3\Lambda} &:= \int_\Lambda \frac{\vec{r}_1\cdot\vec{r}_3}{r_1^3 r_2 r_3^3}\mathrm{d}^3x \doteq \int_\Lambda \frac{\vec{x}\cdot(\vec{x}-\vec{x}_3)}{x^4\,|\vec{x}-\vec{x}_3|^3}\mathrm{d}^3x = \\
&= \int_0^{2\pi}\mathrm{d}\phi\int_{-1}^{1}\mathrm{d}(\cos\theta)\int_\Gamma^\Lambda \mathrm{d}x\frac{x^3\,(x-x_3\cos\theta)}{x^4\sqrt{x^2+x_3^3-2xx_3\cos\theta}^{\,3}} = \\
&= 2\pi\int_\Gamma^\Lambda \mathrm{d}x\left(\int_{-1}^{1}\mathrm{d}(\cos\theta)\frac{1}{x}\frac{(x-x_3\cos\theta)}{\sqrt{x^2+x_3^3-2xx_3\cos\theta}^{\,3}}\right) = \\
&= 2\pi\int_\Gamma^\Lambda \mathrm{d}x\left[\frac{x\cos\theta-x_3}{x^3\sqrt{x^2+x_3^2-2xx_3\cos\theta}}\right]_{\cos\theta=-1}^{\cos\theta=1} = \\
&= 2\pi\int_\Gamma^\Lambda \mathrm{d}x\left(\frac{x-x_3}{x^3\sqrt{x^2-2xx_3+x_3^2}}-\frac{-x-x_3}{x^3\sqrt{x^2+2xx_3+x_3^2}}\right) = \\
&= 2\pi\int_\Gamma^{x_3}\mathrm{d}x(-1)\frac{1\!\!\!/}{x\!\!\!/^3}+2\pi\int_{x_3}^\Lambda \mathrm{d}x\frac{1}{x^3}+2\pi\int_\Gamma^{x_3}\mathrm{d}x\frac{+1\!\!\!/}{x\!\!\!/^3}+2\pi\int_{x_3}^\Lambda \mathrm{d}x\frac{+1}{x^3} \\
&= 2\cdot 2\pi\int_{x_3}^\Lambda\frac{\mathrm{d}x}{x^3} = 4\pi\left(-\frac{1}{2}\right)\left(\frac{1\!\!\!/}{\Lambda\!\!\!/^2}-\frac{1}{x_3^2}\right)\doteq\frac{2\pi}{x_3^2}
\end{aligned}
\tag{45}
$$

During the computation of the integral $J_5 = J_{5\Gamma}+J_{5\Lambda}$ we will proceed similarly as in (43) and (45), so it is not necessary to describe it again in such a detail. We obtain zero after the integration.

$$
\begin{aligned}
J_{5\Gamma} &:= \int \frac{\vec{r}_1\cdot\vec{r}_3}{r_1^4 r_2 r_3^3}\,\mathrm{d}^3x = \int\frac{(\vec{x}-\vec{x}_1)\cdot(\vec{x}-\vec{x}_3)}{|\vec{x}-\vec{x}_1|^4|\vec{x}-\vec{x}_2||\vec{x}-\vec{x}_3|^3}\mathrm{d}^3x \doteq \\
&\doteq -\frac{\vec{x}_3}{x_3^3}\cdot\int\frac{\vec{x}-\vec{x}_1}{|\vec{x}-\vec{x}_1|^4|\vec{x}-\vec{x}_2|}\mathrm{d}^3x = -\frac{\vec{x}_3}{x_3^3}\cdot\int\frac{\vec{y}}{y^4|\vec{y}-\vec{r}_{21}|}\mathrm{d}^3y = \\
&= -\frac{2\pi}{x_3^3}\int_0^\Gamma\int_{-1}^{1}\frac{x_{3z}\cos\theta}{y\sqrt{y^2+r_{21}^2-2yr_{21}\cos\theta}}\mathrm{d}(\cos\theta)\mathrm{d}y = \\
&= 0
\end{aligned}
\tag{46}
$$

$$
\begin{aligned}
J_{5\Lambda} &:= \int_\Lambda \frac{\vec{r}_1\cdot\vec{r}_3}{r_1^4 r_2 r_3^3}\mathrm{d}^3x \doteq \int_\Lambda \frac{\vec{x}\cdot(\vec{x}-\vec{x}_3)}{x^5\ |\vec{x}-\vec{x}_3|^3}\mathrm{d}^3x = \\
&= \int_0^{2\pi}\mathrm{d}\phi\int_{-1}^{1}\mathrm{d}(\cos\theta)\int_\Gamma^\Lambda \mathrm{d}x \frac{x^3\ (x-x_3\cos\theta)}{x^5\sqrt{x^2+x_3^2-2xx_3\cos\theta}^5} = \\
&= 2\pi\int_\Gamma^\Lambda \mathrm{d}x\left(\int_{-1}^{1}\mathrm{d}(\cos\theta)\frac{1}{x}\frac{(x-x_3\cos\theta)}{\sqrt{x^2+x_3^2-2xx_3\cos\theta}^5}\right) = \\
&= 2\pi\int_\Gamma^\Lambda \mathrm{d}x\frac{1}{x^4}\left[\frac{x\cos\theta-x_3}{\sqrt{x^2+x_3^2-2xx_3\cos\theta}}\right]_{\cos\theta=-1}^{\cos\theta=1} = \\
&= 2\pi\int_\Gamma^\Lambda \mathrm{d}x\frac{1}{x^4}\left(\frac{x-x_3}{\sqrt{(x-x_3)^2}}-\frac{-x-x_3}{\sqrt{(x+x_3)^2}}\right) = \\
&= 2\pi\int_\Gamma^{x_3}\mathrm{d}x(-1)\frac{1}{\cancel{x^4}} + 2\pi\int_{x_3}^\Lambda \mathrm{d}x\frac{+1}{x^4} + 2\pi\int_\Gamma^{x_3}\mathrm{d}x\frac{1}{\cancel{x^4}} + 2\pi\int_{x_3}^\Lambda \mathrm{d}x\frac{+1}{x^4} \\
&\doteq -\frac{4\pi}{3}\left(\frac{1}{\cancel{\Lambda^3}}-\frac{1}{x_3^3}\right) \doteq \frac{4\pi}{3}\frac{1}{x_3^3}
\end{aligned}
\tag{47}
$$

The 6th integral we calculate as

$$J_6 = J_{6\Gamma} + J_{6\Lambda}$$

as per (43) and (45), however this time we do not obtain zero for J_6.

$$
\begin{aligned}
J_{6\Gamma} &:= \int \frac{\vec{r}_1\cdot\vec{r}_3}{r_1^3 r_2^2 r_3^3}\ \mathrm{d}^3x = \int \frac{(\vec{x}-\vec{x}_1)\cdot(\vec{x}-\vec{x}_3)}{|\vec{x}-\vec{x}_1|^3|\vec{x}-\vec{x}_2|^2|\vec{x}-\vec{x}_3|^3}\mathrm{d}^3x \doteq \\
&\doteq -\frac{\vec{x}_3}{x_3^3}\cdot\int\frac{\vec{x}-\vec{x}_1}{|\vec{x}-\vec{x}_1|^3|\vec{x}-\vec{x}_2|^2}\mathrm{d}^3x = -\frac{\vec{x}_3}{x_3^3}\cdot\int\frac{\vec{y}}{y^3|\vec{y}-\vec{r}_{21}|^2}\mathrm{d}^3y = \\
&= -\frac{2\pi}{x_3^3}\int_0^\Gamma\int_{-1}^{1}\frac{x_{3z}\cos\theta}{y^2+r_{21}^2-2yr_{21}\cos\theta}\mathrm{d}(\cos\theta)\mathrm{d}y = \\
&= -\frac{2\pi x_{3z}}{x_3^3}\underbrace{\int_{-1}^{1}\left[\frac{\cos\theta\tanh^{-1}\left(\frac{r_{21}\cos\theta-y}{r_{21}\sqrt{\cos^2\theta-1}}\right)}{r_{21}\sqrt{\cos^2\theta-1}}\right]_{y=0}^{y=\Gamma\gg r_{21}}\mathrm{d}(\cos\theta)}_{\frac{2}{r_{21}}} \\
&= -\frac{2\pi x_{3z}}{x_3^3}\frac{2}{r_{21}}
\end{aligned}
\tag{48}
$$

$$
J_{6\Lambda} := \int_\Lambda \frac{\vec{r}_1\cdot\vec{r}_3}{r_1^3 r_2^2 r_3^3}\mathrm{d}^3x \doteq \int_\Lambda \frac{\vec{x}\cdot(\vec{x}-\vec{x}_3)}{x^5\ |\vec{x}-\vec{x}_3|^3}\mathrm{d}^3x = J_{5\Lambda} = \frac{4\pi}{3}\frac{1}{x_3^3}
\tag{49}
$$

Till now we have covered half of the integrals of pert(3), i.e., we still have to work out the terms with exchanged indices (1 and 2). We just need to switch indices $1 \leftrightarrow 2$ in the original integrals, having trivial consequences regarding all of the results, except $J_{6\Gamma}$.

Note, that sign of the result $J_{6\Gamma}$ changes after we switch indices (1 and 2) in the integral. That is because x_{3z} is the projection of $\vec{x}_3$ onto the z-axis of the

system (in the locally spherical coordinate system). At first this z-axis is $\vec{r}_{21}$ and then, after the swap, it is $\vec{r}_{12} = -\vec{r}_{21}$. Written schematically,

$$x_{3z} \xrightarrow{1\leftrightarrow 2} -x_{3z}.$$

Other integrals with such a complicating property vanished. Let us summarise the results in the following table.

Original calculated terms		Switched $1 \leftrightarrow 2$
$J_1 = \int \frac{\vec{r}_1\cdot\vec{r}_3}{r_1^3 r_3^3}\mathrm{d}^3x = \frac{4\pi}{r_{31}}$	$\to$	$J_1' = \int \frac{\vec{r}_2\cdot\vec{r}_3}{r_2^3 r_3^3}\mathrm{d}^3x = \frac{4\pi}{r_{32}}$
$J_2 = \int \frac{\vec{r}_1\cdot\vec{r}_3}{r_1^4 r_3^3}\mathrm{d}^3x = \frac{2\pi}{r_{31}^2}$	$\to$	$J_2' = \int \frac{\vec{r}_2\cdot\vec{r}_3}{r_2^4 r_3^3}\mathrm{d}^3x = \frac{2\pi}{r_{32}^2}$
$J_3 = \int \frac{\vec{r}_1\cdot\vec{r}_3}{r_1^3 r_2 r_3^3}\mathrm{d}^3x = \frac{2\pi}{x_3^2}$	$\to$	$J_3' = \int \frac{\vec{r}_2\cdot\vec{r}_3}{r_2^3 r_1 r_3^3}\mathrm{d}^3x = \frac{2\pi}{x_3^2}$
$J_4 = \int \frac{\vec{r}_1\cdot\vec{r}_3}{r_1^5 r_3^3}\mathrm{d}^3x = \frac{4}{3}\frac{\pi}{r_{31}^3}$	$\to$	$J_4' = \int \frac{\vec{r}_2\cdot\vec{r}_3}{r_2^5 r_3^3}\mathrm{d}^3x = \frac{4}{3}\frac{\pi}{r_{32}^3}$
$J_5 = \int \frac{\vec{r}_1\cdot\vec{r}_3}{r_1^4 r_2 r_3^3}\mathrm{d}^3x = \frac{4}{3}\frac{\pi}{x_3^3}$	$\to$	$J_5' = \int \frac{\vec{r}_2\cdot\vec{r}_3}{r_2^4 r_1 r_3^3}\mathrm{d}^3x = \frac{4}{3}\frac{\pi}{x_3^3}$
$J_6 = \int \frac{\vec{r}_1\cdot\vec{r}_3}{r_1^3 r_2^2 r_3^3}\mathrm{d}^3x = -\frac{2\pi x_{3z}}{x_3^3}\frac{2}{r_{21}} + \frac{4}{3}\frac{\pi}{x_3^3}$	$\to$	$J_6' = \int \frac{\vec{r}_2\cdot\vec{r}_3}{r_2^3 r_1^2 r_3^3}\mathrm{d}^3x = +\frac{2\pi x_{3z}}{x_3^3}\frac{2}{r_{21}} + \frac{4}{3}\frac{\pi}{x_3^3}$

Table 1: Table of integrals of the 3rd line $\{1 \leftrightarrow 2\}$.

Summarising the lines above, the 3rd line reads

$$\begin{aligned}
&\mathrm{pert}(3) = \\
&= -\frac{3}{8\pi}\sum_{i=1}^{2} m_i m_3 \ |\vec{v}_i - \vec{v}_3|^2 \int \mathrm{d}^3x \frac{\vec{r}_i\cdot\vec{r}_3}{r_i^3 r_3^3}\times \\
&\quad\times\left(1 + 2\left(\frac{m_1}{r_1}+\frac{m_2}{r_2}\right) + \left(\frac{m_1}{r_1}\right)^2 + \frac{2m_2m_1}{r_2 r_1} + \left(\frac{m_2}{r_2}\right)^2\right) = \\
&= -\frac{3}{8\pi} m_1 m_3 |\vec{v}_1 - \vec{v}_3|^2 \left(1\cdot J_1 + 2m_1 J_2 + 2m_2 J_3 + m_1^2 J_4 + 2m_1 m_2 J_5 + m_2^2 J_6\right) \\
&\quad - \frac{3}{8\pi} m_2 m_3 |\vec{v}_2 - \vec{v}_3|^2 \left(1\cdot J_1' + 2m_1 J_3' + 2m_2 J_2' + m_1^2 J_6' + 2m_1 m_2 J_5' + m_2^2 J_4'\right) \\
&= -\frac{3}{8\pi} m_1 m_3 |\vec{v}_1 - \vec{v}_3|^2 \left(\frac{4\pi}{r_{31}} + 2m_1\frac{2\pi}{r_{31}^2} + 2m_2\frac{2\pi}{x_3^2} + m_1^2\frac{4}{3}\frac{\pi}{r_{31}^3} + 2m_1 m_2\frac{4}{3}\frac{\pi}{x_3^3}\right. \\
&\qquad\qquad \left. + m_2^2\left(-\frac{2\pi x_{3z}}{x_3^3}\frac{2}{r_{21}} + \frac{4}{3}\frac{\pi}{x_3^3}\right)\right) \\
&\quad - \frac{3}{8\pi} m_2 m_3 |\vec{v}_2 - \vec{v}_3|^2 \left(\frac{4\pi}{r_{32}} + 2m_1\frac{2\pi}{x_3^2} + 2m_2\frac{2\pi}{r_{32}^2} + m_1^2\left(\frac{+2\pi x_{3z}}{x_3^3}\frac{2}{r_{21}} + \frac{4}{3}\frac{\pi}{x_3^3}\right)\right. \\
&\qquad\qquad \left. + 2m_1 m_2\frac{4}{3}\frac{\pi}{x_3^3} + m_2^2\frac{4}{3}\frac{\pi}{r_{32}^3}\right).
\end{aligned} \tag{50}$$

After trivial algebraic manipulations the result reads

$$\begin{aligned}\mathrm{pert}(3) = &-\frac{3}{2}m_1m_3\,|\vec{v}_1-\vec{v}_3|^2\left(\frac{1}{r_{31}}+\frac{m_1}{r_{31}^2}+\frac{m_2}{x_3^2}+\frac{1}{3}\frac{m_1^2}{r_{31}^3}+\frac{2}{3}\frac{m_1m_2}{x_3^3}\right.\\ &\left.+m_2^2\left(-\frac{1}{r_{21}}\frac{x_{3z}}{x_3^3}+\frac{1}{3}\frac{1}{x_3^3}\right)\right)\\ &-\frac{3}{2}m_2m_3\,|\vec{v}_2-\vec{v}_3|^2\left(\frac{1}{r_{32}}+\frac{m_2}{r_{32}^2}+\frac{m_1}{x_3^2}+\frac{1}{3}\frac{m_2^2}{r_{32}^3}+\frac{2}{3}\frac{m_1m_2}{x_3^3}\right.\\ &\left.+m_1^2\left(+\frac{1}{r_{21}}\frac{x_{3z}}{x_3^3}+\frac{1}{3}\frac{1}{x_3^3}\right)\right).\end{aligned} \tag{51}$$

4th line of the perturbation

The other contributions $O(m_3^2)$ are produced by the fourth line of (28).

$$\begin{aligned}\mathrm{pert}(4) = &-\frac{3}{8\pi}2m_3^2m_1|\vec{v}_1-\vec{v}_3|^2\int\left(\frac{\overbrace{\vec{r}_1\cdot\vec{r}_3}^{M_1}}{r_1^3r_3^4}+m_1\frac{\overbrace{\vec{r}_1\cdot\vec{r}_3}^{M_2}}{r_1^4r_3^4}+m_2\frac{\overbrace{\vec{r}_1\cdot\vec{r}_3}^{M_3}}{r_1^3r_3^4}\frac{1}{r_2}\right)\mathrm{d}^3x\\ &-\frac{3}{8\pi}2m_3^2m_2|\vec{v}_2-\vec{v}_3|^2\int\left(\frac{\overbrace{\vec{r}_2\cdot\vec{r}_3}^{M_1'}}{r_2^3r_3^4}+m_2\frac{\overbrace{\vec{r}_2\cdot\vec{r}_3}^{M_2'}}{r_2^4r_3^4}+m_1\frac{\overbrace{\vec{r}_2\cdot\vec{r}_3}^{M_3'}}{r_2^3r_3^4}\frac{1}{r_1}\right)\mathrm{d}^3x\end{aligned} \tag{52}$$

We are already familiar with some of these. Namely we have already calculated M_1, M_1' exactly, looking at (4.7) and also $M_2,\ M_2'$ using the procedure and result of (4.9).

$$\begin{aligned}M_1 &= \int\frac{\vec{r}_1\cdot\vec{r}_3}{r_1^3r_3^4}\mathrm{d}^3x = \frac{2\pi}{r_{13}^2}\\ M_1' &= \int\frac{\vec{r}_2\cdot\vec{r}_3}{r_2^3r_3^4}\mathrm{d}^3x = \frac{2\pi}{r_{23}^2}\\ M_2 &= \int\frac{\vec{r}_1\cdot\vec{r}_3}{r_1^4r_3^4}\mathrm{d}^3x = 0\\ M_2' &= \int\frac{\vec{r}_2\cdot\vec{r}_3}{r_2^4r_3^4}\mathrm{d}^3x = 0\end{aligned} \tag{53}$$

Now we are left with $M_3,\ M_3'$ only. Since their denominators include mixed terms, we have to split the integration area again. We proceed in the same way, as in (43).

$$M_3 = \int\frac{\vec{r}_1\cdot\vec{r}_3}{r_1^3r_3^4}\frac{1}{r_2}\mathrm{d}^3x \equiv M_{3\Gamma}+M_{3\Lambda}.$$

$$
\begin{aligned}
M_{3\Gamma} &= \int_\Gamma \frac{(\vec{x}-\vec{x}_1)\cdot(\vec{x}-\vec{x}_3)}{|\vec{x}-\vec{x}_1|^3|\vec{x}-\vec{x}_3|^4|\vec{x}-\vec{x}_2|}\mathrm{d}^3x \doteq -\frac{\vec{x}_3}{x_3^4}\cdot\int_\Gamma \frac{\vec{x}-\vec{x}_1}{|\vec{x}-\vec{x}_1|^3|\vec{x}-\vec{x}_2|} = \\
&= -\frac{\vec{x}_3}{x_3^4}\cdot\int_\Gamma \frac{\vec{y}}{y^3|\vec{y}-\vec{r}_{21}|}\mathrm{d}^3x = -\frac{2\pi}{x_3^4}\int_0^\Gamma\int_{-1}^1 \frac{x_{3z}\cos\theta \;\; \mathrm{d}(\cos\theta)\mathrm{d}y}{\sqrt{y^2+r_{21}^2-2yr_{21}\cos\theta}} = \\
&= |\Gamma \gg r_{21}| = 0 \\
M_{3\Lambda} &= \int_\Lambda \frac{(\vec{x}-\vec{x}_1)\cdot(\vec{x}-\vec{x}_3)}{|\vec{x}-\vec{x}_1|^3|\vec{x}-\vec{x}_3|^4|\vec{x}-\vec{x}_2|}\mathrm{d}^3x \doteq \int_\Lambda \frac{\vec{x}\cdot(\vec{x}-\vec{x}_3)}{x^4\;|\vec{x}-\vec{x}_3|^4}\mathrm{d}^3x = \\
&= \int_0^{2\pi}\mathrm{d}\phi\int_\Gamma^\Lambda \mathrm{d}x\left(\int_{-1}^1 \mathrm{d}(\cos\theta)\frac{\cancel{x^3}}{\cancel{x^3}\;x}\frac{x-x_3\cos\theta}{\left(x^2+x_3^2-2xx_3\cos\theta\right)^2}\right) \\
&= 2\pi\int_\Gamma^\Lambda \mathrm{d}x\left(\frac{1}{x^2\left(x^2-x_3^2\right)}+\frac{1}{4x_3x^3}\left[\log(x+x_3)^2-\log(x-x_3)^2\right]\right) \\
&= \frac{2\pi}{x_3}\left(\frac{1}{2x_3x}-\frac{1}{2x_3^2}\log\frac{|x-x_3|}{|x+x_3|}+\frac{1}{4x_3^2}\log\frac{|x+x_3|}{|x-x_3|}\right. \\
&\qquad\left.+\frac{1}{8x^2}\log\frac{(x-x_3)^2}{(x+x_3)^2}\right)\Bigg|_{x=\Gamma}^{x=\Lambda} \\
&= \frac{2\pi}{x_3}\left(\frac{1}{2x_3}\frac{1}{\cancel{\Lambda}}-\frac{1}{2x_3\Gamma}-\frac{1}{4x_3^2}\underbrace{\log\frac{|\Lambda-x_3|}{|\Lambda+x_3|}}_{\to 0}+\frac{1}{4x_3^2}\underbrace{\log\frac{|\Gamma-x_3|}{|\Gamma+x_3|}}_{\to 0}\right. \\
&\qquad\left.+\frac{1}{8}\frac{1}{\Lambda^2}\underbrace{\log\frac{(\Lambda-x_3)^2}{(\Lambda+x_3)^2}}_{\to 0}-\frac{1}{8}\frac{1}{\Gamma^2}\log\frac{(\Gamma-x_3)^2}{(\Gamma+x_3)^2}\right) \\
&\doteq \frac{2\pi}{x_3}\left(-\frac{1}{2}\frac{1}{x_3\Gamma}+\frac{1}{4}\frac{1}{x_3\Gamma}\right) = -\frac{\pi}{2}\frac{1}{x_3^2\;\Gamma}
\end{aligned}
\tag{54}
$$

To obtain the very last line we used the familiar limit (39). In total the fourth row of perturbation reads

$$
\mathrm{pert}(4) = -\frac{3}{2}m_3^2\left(m_1|\vec{v}_1-\vec{v}_3|^2\left[\frac{1}{r_{13}^2}-\frac{1}{4}\frac{m_2}{x_3^2\Gamma}\right]+m_2|\vec{v}_2-\vec{v}_3|^2\left[\frac{1}{r_{23}^2}-\frac{1}{4}\frac{m_1}{x_3^2\Gamma}\right]\right). \tag{55}
$$

The terms containing Γ will be the source of limitation of applicability and validity of our Lagrangian.

5^{th} line of the perturbation

Here we have to integrate

$$\text{pert}(5) = -\frac{3}{8\pi}m_3^3\left(m_1|\vec{v}_1-\vec{v}_3|^2\underbrace{\int\frac{\vec{r}_1\cdot\vec{r}_3}{r_1^3r_3^5}\mathrm{d}^3x}_{N_1}+m_2|\vec{v}_2-\vec{v}_3|^2\underbrace{\int\frac{\vec{r}_2\cdot\vec{r}_3}{r_2^3r_3^5}\mathrm{d}^3x}_{N_1'}\right). \tag{56}$$

However, that is what we have already calculated exactly in (4.8), so we have

$$\begin{aligned} N_1 &= \int\frac{\vec{r}_1\cdot\vec{r}_3}{r_1^3r_3^5}\mathrm{d}^3x = \int\frac{\vec{y}\cdot(\vec{y}-\vec{r}_{31})}{y^3|\vec{y}-\vec{r}_{31}|^5}\mathrm{d}^3y = \frac{4\pi}{3}\frac{1}{r_{31}^3}, \\ N_1' &= \frac{4\pi}{3}\frac{1}{r_{32}^3}. \end{aligned} \tag{57}$$

Thus, we end up with

$$\text{pert}(5) = -\frac{m_3^3}{2}\left(\frac{m_1|\vec{v}_1-\vec{v}_3|^2}{r_{31}^3}+\frac{m_2|\vec{v}_2-\vec{v}_3|^2}{r_{32}^3}\right). \tag{58}$$

We can finally sum over all of the preceding results to get the whole perturbation.

Overall perturbation

Now, after this somewhat lengthy calculation we are competent to write the overall result. This Lagrangian controls the motion of the 3rd extremally charged black hole approaching from large distance towards two extremally charged black holes orbiting around origin on a common circular path.

$$
\begin{aligned}
&L_{BH3}(x_{3x}, x_{3y}, x_{3z}, v_{3x}, v_{3y}, v_{3z}) \equiv \text{perturbation} = \\
&\quad = \sum_{i=1}^{5} \text{pert(i)} = \\
&\quad = -\frac{3}{2} m_1 m_2 m_3 \left|\vec{v}_1 - \vec{v}_2\right|^2 \left(\frac{2}{x_3} \frac{1}{r_{12}} + \frac{1}{x_3^2} + \right. \\
&\qquad\qquad \left. + (m_1 + m_2) \left[\frac{1}{x_3} \frac{1}{r_{21}^2} - \frac{1}{x_3^3} \right] \right) \\
&\qquad - \frac{3}{2} m_3^2 m_1 m_2 |\vec{v}_1 - \vec{v}_2|^2 \left(\frac{1}{x_3^2} \frac{1}{r_{12}} \right) \\
&\qquad - \frac{3}{2} m_1 m_3 \left|\vec{v}_1 - \vec{v}_3\right|^2 \left(\frac{1}{r_{31}} + \frac{m_1}{r_{31}^2} + \frac{m_2}{x_3^2} + \frac{1}{3} \frac{m_1^2}{r_{31}^3} + \frac{2}{3} \frac{m_1 m_2}{x_3^3} \right. \\
&\qquad\qquad \left. + m_2^2 \left(-\frac{1}{r_{21}} \frac{x_{3z}}{x_3^3} + \frac{1}{3} \frac{1}{x_3^3} \right) \right) \\
&\qquad - \frac{3}{2} m_2 m_3 \left|\vec{v}_2 - \vec{v}_3\right|^2 \left(\frac{1}{r_{32}} + \frac{m_2}{r_{32}^2} + \frac{m_1}{x_3^2} + \frac{1}{3} \frac{m_2^2}{r_{32}^3} + \frac{2}{3} \frac{m_1 m_2}{x_3^3} \right. \\
&\qquad\qquad \left. + m_1^2 \left(+\frac{1}{r_{21}} \frac{x_{3z}}{x_3^3} + \frac{1}{3} \frac{1}{x_3^3} \right) \right) \\
&\qquad - \frac{3}{2} m_3^2 \left(\frac{m_1 |\vec{v}_1 - \vec{v}_3|^2}{r_{13}^2} + \frac{m_2 |\vec{v}_2 - \vec{v}_3|^2}{r_{23}^2} \right) \\
&\qquad - \frac{3}{2} m_3^2 m_1 m_2 \left(|\vec{v}_1 - \vec{v}_3|^2 + |\vec{v}_2 - \vec{v}_3|^2 \right) \cdot \left(\frac{-1}{4} \frac{1}{x_3^2 \Gamma} \right) \\
&\qquad - \frac{m_3^3}{2} \left(\frac{m_1 |\vec{v}_1 - \vec{v}_3|^2}{r_{31}^3} + \frac{m_2 |\vec{v}_2 - \vec{v}_3|^2}{r_{32}^3} \right)
\end{aligned}
\tag{59}
$$

Appendix B: Taylor expansion of geodesic equation

We analyse the geodesic equation (GE) with generally nonzero right hand side. Studying higher derivatives we determine overall proportionality of the Taylor expansion to $(1-\kappa)$.

$$\frac{Du^\mu}{\mathrm{d}\tau} = \dot{u}^\mu + \Gamma^\mu{}_{\alpha\beta} u^\alpha u^\beta = \kappa F^\mu{}_\alpha u^\alpha \tag{60}$$

The Maxwell tensor is

$$F^\mu{}_\nu = \begin{pmatrix} 0 & -\partial_x\psi & -\partial_y\psi & -\partial_z\psi \\ -\frac{\partial_x\psi}{\psi^4} & 0 & 0 & 0 \\ -\frac{\partial_y\psi}{\psi^4} & 0 & 0 & 0 \\ -\frac{\partial_z\psi}{\psi^4} & 0 & 0 & 0 \end{pmatrix}. \tag{61}$$

Let us take the spatial part, we choose x (one proceeds analogically for the other spatial coordinates). The nonzero Christoffel's symbols $\Gamma^x_{\mu\nu}$, defined in a traditional way, read

$$\Gamma^x{}_{tt} = -\frac{\partial_x\psi}{\psi^5},\ \Gamma^x{}_{\mu x} = \frac{\partial_\mu\psi}{\psi},\ \Gamma^x{}_{yy} = \Gamma^x{}_{zz} = -\frac{\partial_x\psi}{\psi}, \tag{62}$$

where the partial derivatives' indices are lower, indices $\{t,x,y,z\}$ denote the particular components. In the equation below we dropped the zero Christoffel symbols, occasional factor 2 appears due to symmetry $\Gamma^\alpha{}_{(\beta\gamma)}$.

$$\begin{aligned} \ddot{x} = -\Big(&\Gamma^x{}_{tt}(u^t)^2 + 2\Gamma^x{}_{tx}u^t u^x + 2\Gamma^x{}_{xy}u^x u^y + 2\Gamma^x{}_{xz}u^x u^z \\ &+ \Gamma^x{}_{xx}(u^x)^2 + \Gamma^x{}_{yy}(u^y)^2 + \Gamma^x{}_{zz}(u^z)^2\Big) + \kappa F^x{}_t u^t \end{aligned} \tag{63}$$

We can substitute (62) into the last equation and obtain

$$\begin{aligned} \ddot{x} =& \frac{\partial_x\psi}{\psi^5}(u^t)^2 - 2\frac{\partial_t\psi}{\psi}u^t u^x - 2\frac{\partial_y\psi}{\psi}u^x u^y - 2\frac{\partial_z\psi}{\psi}u^x u^z \\ &- \frac{\partial_x\psi}{\psi}(u^x)^2 + \frac{\partial_x\psi}{\psi}(u^y)^2 + \frac{\partial_x\psi}{\psi}(u^z)^2 - \kappa\frac{\partial_x\psi}{\psi^4}u^t. \end{aligned} \tag{64}$$

Considering again the initially static particle $\vec{x}(t_0) = (x_0, y_0, z_0),\ \vec{u}_0 = \dot{\vec{x}}(t_0) = 0$ we also drop the zero velocity terms and the equation at $t = 0$ becomes

$$\ddot{x}^\alpha + \Gamma^\alpha{}_{tt}u^t u^t = \kappa F^\alpha{}_t u^t. \tag{65}$$

From normalisation we already have

$$\dot{t} = u^t = \psi(t).$$

Hence the equations for the time and space are now at $t = 0$

$$\ddot{t} = \psi \partial_t \psi \tag{66}$$

and

$$\ddot{x}^i = \frac{g^{i\nu}\partial_\nu \psi}{\psi}(1-\kappa) = \frac{\partial_i \psi}{\psi^3}(1-\kappa). \tag{67}$$

Solution to the time-component equation is $t = \int \psi \mathrm{d}\tau$ and the space-component equations are trivial for $\kappa = 1$.

Let us have a look at higher order derivatives of geodesic equation. The initially static case at $t = 0$ is described by (we drop zero terms)

$$\dddot{x} = -\left(\dot{\Gamma}^x{}_{tt}(u^t)^2 + 2\Gamma^x{}_{tt}u^t\dot{u}^t + 2\Gamma^x{}_{tx}u^t\dot{u}^x\right) + \kappa\dot{F}^x{}_t u^t + \kappa F^x{}_t \dot{u}^t \tag{68}$$

which after substitution of particular values of Christoffel's symbols is

$$\dddot{x} = \left(\frac{\partial_x\psi}{\psi^5}\right)^{\cdot}\psi^2 + 2\left(\frac{\partial_x\psi}{\psi^5}\right)\psi\dot{\psi} - 2\frac{\partial_t\psi}{\psi}\psi\ddot{x} - \kappa\left(\frac{\partial_x\psi}{\psi^4}\right)^{\cdot}\psi - \kappa\frac{\partial_x\psi}{\psi^4}\dot{\psi} \tag{69}$$

and after substituting (67) into the last equation we get

$$\dddot{x} = \underline{\left(\frac{\partial_x\psi}{\psi^5}\right)^{\cdot}\psi^2} + \underline{2\left(\frac{\partial_x\psi}{\psi^5}\right)\psi\dot{\psi}} \underline{- 2\frac{\partial_t\psi}{\psi}\psi\frac{\partial_x\psi}{\psi^3}(1-\kappa)} \underline{- \kappa\left(\frac{\partial_x\psi}{\psi^4}\right)^{\cdot}\psi} \underline{- \kappa\frac{\partial_x\psi}{\psi^4}\dot{\psi}} \tag{70}$$

The third term of the last equation can be rewritten using time-component equation $\dot{\psi} = \psi\partial_t\psi$ as

$$\underline{-2\frac{\partial_t\psi}{\psi}\psi\frac{\partial_x\psi}{\psi^3}(1-\kappa)} = 2\dot{\psi}\frac{\partial_x\psi}{\psi^4}(\kappa-1)\,. \tag{71}$$

Combination of the first and one before the last term of the equation is

$$\underline{\left(\frac{\partial_x\psi}{\psi^5}\right)^{\cdot}\psi^2 - \kappa\left(\frac{\partial_x\psi}{\psi^4}\right)^{\cdot}\psi} = \frac{(\partial_x\psi)^{\cdot}}{\psi^3}(1-\kappa) + \partial_x\psi\frac{\dot{\psi}}{\psi^4}(-5+4\kappa) \tag{72}$$

and adding the second and the last term we obtain

$$\underline{2\left(\frac{\partial_x\psi}{\psi^5}\right)\psi\dot{\psi} - \kappa\frac{\partial_x\psi}{\psi^4}\dot{\psi}} = \frac{\partial_x\psi}{\psi^4}\dot{\psi}(2-\kappa)\,. \tag{73}$$

Substituting the last three results into (70) after somewhat easy algebraic manipulations we arrive at

$$\dddot{x} = \frac{(\partial_x\psi)^{\cdot}}{\psi^3}(1-\kappa) + \partial_x\psi\frac{\dot{\psi}}{\psi^4}[(-5+4\kappa) + (2-\kappa) + 2(\kappa-1)] \tag{74}$$

and using $\frac{\dot{\psi}}{\psi^4} = -\frac{1}{3}\left(\frac{1}{\psi^3}\right)^{\cdot}$ we obtain

$$\dddot{x} = (1-\kappa)\left(\frac{(\partial_x\psi)^{\cdot}}{\psi^3} + \frac{5}{3}\partial_x\psi\left(\frac{1}{\psi^3}\right)^{\cdot}\right) \tag{75}$$

This seems to contradict the few expectations we had on this matter, since we rewrite this as

$$\dddot{x} = \left(\frac{\partial_x \psi}{\psi^3}\right)^{\cdot} (1-\kappa) + \frac{2}{3}\partial_x \psi \left(\frac{1}{\psi^3}\right)^{\cdot} (1-\kappa) \tag{76}$$

and we obtain $\dddot{x} \propto (1-\kappa)$ at $t = 0$. Thus the acceleration and its derivative vanish for $\kappa = 1$.

Differentiating once more, one obtains on the RHS another function of lower derivatives of the original equation. Whenever derivatives appear, we substitute from the known equations, thus gradually expressing all the higher derivatives in terms of the first and second derivatives of x^μ. The former as well as the latter is proportional to $(1-\kappa)$ at $t = 0$. From these circumstances we may conclude, that the entire Taylor expansion is fully proportional to $(1-\kappa)$.

Appendix C: Magic of numerics

During numerical solution of our electro-geodesic equations for $\kappa = 1$ particle we ran into problems regarding numerics of small numbers. Numerical solutions of equations with static particle starting at different positions led to different initial velocities, some of them greater and the rest smaller than zero. However, this velocity was analytically proved to be exactly zero at $t = 0$, hence we decided to study numerics properly to eliminate as many numerical errors as possible. We bring a brief sketch of useful information below. We followed [21] in this section, equations were solved using *Wolfram Mathematica 13.0*, using the package *xAct*. Also we list some of our results and their interesting numerical subtleties.

Description of methods

ND Solve is the basic function to numerically solve given differential equations with corresponding number of initial conditions. *ND Solve* also allows user to specify the precision or accuracy of the result, the function makes the time step it takes smaller and smaller until our solution reaches either the *AccuracyGoal* (AG) or *PrecisionGoal* (PG).

AG determines the absolute error tolerance in the reached solution, while PG determines the relative error of any such solution. If values of the tracked solution come close to zero, one typically increases AG setting. AG and PG allow us to control the error locally at particular time step. Sometimes it may occur that this error accumulates and either precision of accuracy of the resulting solution at the end of the time step may be much less than expected form setting AG and PG. Letting $AG \to \infty$ asks *NDSolve* to use PG only.

WorkingPrecision is and option to specify how many digits of precision should *Mathematica* maintain in internal computations during various numerical operations. Specifying large values of AG and PG requires increasing *WorkingPrecision*. The default setting of both (AG, PG) is equal to half of the setting of *WorkingPrecision*.

NDSolve also allows the user to choose the preferred method of solving, it has several methods built in or one can also add his own additional method. With the default setting $Method \to Automatic$, $NDSolve$ will choose on its own, which is quite useful for a wide range of non-problematic problems. However, some of our equations appeared to be stiff during evaluation, remedy for which was the method $StiffnessSwitching$, which automatically switches between nonstiff and stiff solver, testing stiffness during calculation. This was useful namely for solution in range of affine parameter about $[0, \frac{1}{1000000}]$, when studying dynamics of the beginning of motions. Another very useful method is $EquationSimplification \to Residual$, which presolves a problem, i.e. converts equations, that were originally unable to be solved, into the form easier to manage for *NDSolve*. For lower PG, $AG \sim 4$ it is convenient to use four-step Runge-Kutta method $RK4$, while for larger values of PG, $AG \sim 20$, as in our case, one should stick to different methods, e.g. those mentioned above.

Numerical subtleties of our results

For $\kappa \neq 1$ the resulting numerical solutions obtained by different methods are the same, since the functions which *NDSolve* works with are well behaved and their magnitude is also reasonably large, compared with e.g. double precision machine epsilon $\epsilon = 2^{-52} \approx 2.22 \times 10^{-16}$.

As said before, equations for the case $\kappa = 1$ are extraordinary, considering that numbers and terms in question are all about the same magnitude but with opposite sign. At $t = 0$ the terms on RHS explicitly vanish, as we showed in Appendix B: Taylor expansion of geodesic equation. We speculated whether the RHS remains zero at $t > 0$ as per our analytic result or any motion appears.

For $\kappa = 1$ the method we choose to solve the system of equations is crucial. Not only determines the choice of method whether *NDSolve* can solve it, but also how precise the solution is. For us it was decisive whether the particle (which stands still at first) starts moving little by little or whether this apparent motion is just a numerical noise, entirely unaffected by physics.

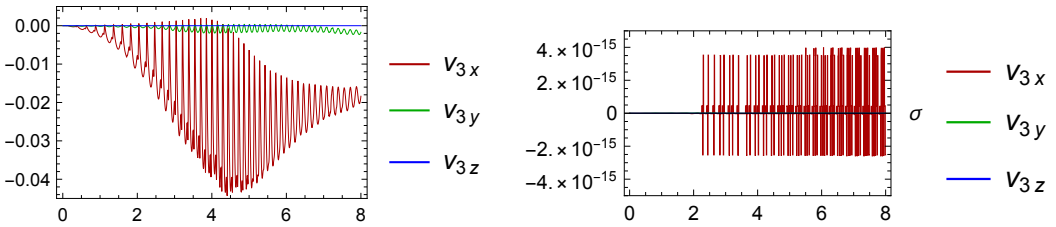

(a) **Low precision (*AG*=4, *PG*=5), method *EquationSimplification*→ *Residual***. Deviation from zero about 10^2 times larger than the desired precision.

(b) **High precision (*AG* = 20, *PG* = 19), method *StiffnessSwitching***. Accumulated error about 10^4 times larger than the desired precision, however yet 10^{13} times better precision than (a). The zero here is much stronger.

Figure 12: Comparision of methods and precision. Velocity calculated from numerical solution (positions). Particle's properties: $\kappa = 1$, $\vec{x}(t_0) = (0.2, 0, 0)$, $\dot{\vec{x}}(t_0) = 0$. The numerical error in (a) accumulates and one would erroneously conclude that particle leaves the initial position. Let us spill the beans and say it is only caused by numerics, since looking at calculation (b) where we increase precision and accuracy, the fluctuation around equilibrium, i.e. zero, is obvious.

Bibliography

[1] S. D. Majumdar. A Class of Exact Solutions of Einstein's Field Equations. *Physical Review*, 72(5):390–398, 1947. ISSN 0031-899X. URL https://link.aps.org/doi/10.1103/PhysRev.72.390.

[2] A. Papapetrou. A Static Solution of the Equations of the Gravitational Field for an Arbitary Charge-Distribution. *Proceedings of the Royal Irish Academy. Section A: Mathematical and Physical Sciences*, 51:191–204, 1945. ISSN 00358975. URL http://www.jstor.org/stable/20488481.

[3] J. B. Hartle and S. W. Hawking. Solutions of the Einstein-Maxwell Equations with Many Black Holes. *Commun. Math. Phys.*, 26:87–101, 01 1972. URL https://doi.org/10.1007/BF01645696.

[4] R. C. Ferrell and D. M. Eardley. Slow-motion scattering and coalescence of maximally charged black holes. *Phys. Rev. Lett.*, 59:1617–1620, Oct 1987. doi: 10.1103/PhysRevLett.59.1617. URL https://link.aps.org/doi/10.1103/PhysRevLett.59.1617.

[5] R. C. Ferrell and D. M. Eardley. *"Slowly moving maximally charged black holes" in "Frontiers in Numerical Relativity"*, pages 27–42. C. R. Evans, L. S. Finn, and D. W. Hobill, (eds.) Cambridge University Press, 1989.

[6] J. Ryzner and M. Žofka. Electrogeodesics in the di-hole Majumdar-Papapetrou spacetime. *Classical and Quantum Gravity*, 32(20):205010, October 2015. URL https://doi.org/10.1088%2F0264-9381%2F32%2F20%2F205010.

[7] K. Shiraishi. Moduli space metric for maximally-charged dilaton black holes. *Nuclear Physics B*, 402(1-2):399–410, 07 1993. doi: 10.1016/0550-3213(93)90648-9. URL https://doi.org/10.1016/0550-3213(93)90648-9.

[8] F. McCarthy, D. Kubizňák, and R. B. Mann. Dilatonic imprints on exact gravitational wave signatures. *Physical Review D*, 97(10), may 2018. doi: 10.1103/physrevd.97.104025. URL https://doi.org/10.1103%2Fphysrevd.97.104025.

[9] A. L. Myers. Natural system of units in general relativity (not-peer-reviewed). URL https://www.seas.upenn.edu/~amyers/NaturalUnits.pdf.

[10] J. Veselý. *Charged Particles in Spacetimes with an Electromagnetic Field*Master thesis, Charles University Prague, Institute of Theoretical Physics. 2017. URL https://dspace.cuni.cz/bitstream/handle/20.500.11956/90577/DPTX_2015_1_11320_0_484776_0_170034.pdf.

[11] D. Tong. General Relativity (lecture notes), University of Cambridge, 2019. URL https://www.damtp.cam.ac.uk/user/tong/gr/gr.pdf.

[12] V. E. Hubeny. The AdS/CFT correspondence. *Classical and Quantum Gravity*, 32(12):124010–124051, 2015. ISSN 0264-9381. URL https://doi.org/10.1088/0264-9381/32/12/124010.

[13] C. W. Misner, K. S. Thorne, and J. A. Wheeler. *Gravitation*. W.H.Freeman and company, New York, 1973 - 1973. ISBN 0-7167-0344-0.

[14] R. M. Wald. *General Relativity*. The University of Chicago Press, 1984. ISBN: 9780226870328.

[15] D. Lynden-Bell, J. Bičák, and J. Katz. On accelerated inertial frames in gravity and electromagnetism. *Annals of Physics*, 271(1):1–22, 1999. ISSN 0003-4916. URL https://www.sciencedirect.com/science/article/abs/pii/S0003491698958699?via%3Dihub.

[16] B. V. Ivanov. Static charged fluid spheres in general relativity, 2001. URL https://doi.org/10.48550/arXiv.gr-qc/0109010.

[17] J. L. Synge. *Relativity: The General Theory*. Amsterdam: North-Holland Publishing Company (Interscience), *Chapter VIII.*, 1960. ISBN 9780444102799.

[18] G. W. Gibbons and P. J. Ruback. Motion of Extreme Reissner-Nordstrom Black Holes in the Low-Velocity Limit. *Phys. Rev. Lett.*, 57:1492–1495, Sep 1986. doi: 10.1103/PhysRevLett.57.1492. URL https://doi.org/10.1103/PhysRevLett.57.1492.

[19] E. Klimešová. *Properties of Multi Black-hole Spacetimes*. Bachelor thesis, Charles University Prague, Institute of Theoretical Physics, 2021. 2021. URL https://dspace.cuni.cz/bitstream/handle/20.500.11956/149293/130315782.pdf?sequence=1&isAllowed=y.

[20] M. Blau. Lecture notes on general relativity, November 2022. URL http://www.blau.itp.unibe.ch/newlecturesGR.pdf.

[21] Introduction to Advanced Numerical Differential Equation Solving in the Wolfram Language, 06 2023. URL https://reference.wolfram.com/language/tutorial/NDSolveIntroductoryTutorial.html.